SAINT-PETERSBURG UNIVERSITY

Nerobelov Georgii Maksimovich

ESTIMATES OF CO_2 ANTHROPOGENIC EMISSIONS OF ST PETERSBURG MEGAPOLIS BY NUMERICAL MODELLING

Scientific specialty 1.6.18. Atmospheric and climate sciences

Thesis for the degree Candidate of Physical and Mathematical Sciences

Translation from Russian

Scientific supervisor:
Dr. of Phys.-Math. Sciences, Professor
Timofeyev Yurii Mikhailovich

St Petersburg
2023

Table of contents

Introduction

Changes in the content of greenhouse gases in the Earth's atmosphere affect the radiation balance of the planet, reducing thermal radiation escaping from the earth's surface and slowing down its cooling [1-3]. Over the past few decades, there has been an increase in the content of CO_2 and other greenhouse gases in the Earth's atmosphere, which is associated with human activity [4-6]. This in turn leads to a global increase in the temperature of the Earth's surface and the lower layer of the atmosphere [7-10]. An increase in the temperature of the Earth's surface has predominantly negative consequences for humans, leading to an increase in the number of adverse weather events [11].

CO_2 is called the main anthropogenic greenhouse gas due to its greatest influence on the Earth's outgoing radiation. This is due to the largest number of CO_2 molecules in the atmosphere and emissions compared to other greenhouse gases [12].

In order to monitor the implementation of accepted international agreements to reduce CO_2 emissions into the Earth's atmosphere [13, 14], high-quality and up-to-date information on the sources and sinks of CO_2 is needed. According to [15], CO_2 emissions from the territories of large cities contribute up to more than 70% of all anthropogenic CO_2 emissions. Therefore, first of all, qualitative assessments of gas emissions from urbanized areas of the planet are necessary.

Today there are two known approaches to assessing anthropogenic CO_2 emissions. The first is the inventory method. It is based on the assessment of emissions using data characterizing human activity that leads to anthropogenic emissions of CO_2 into the Earth's atmosphere (for example, the amount of fossil fuel burned over a period of time, the location of industrial enterprises, etc.) [16, 17]. Errors in anthropogenic CO_2 emissions according to country-scale inventories can reach only a few percent [18, 19]. However, on an urban scale, errors in the inventory approach can reach 100% or more [20].

In this regard, an independent approach of assessing anthropogenic CO_2 emissions at the city scale is being developed. It is based on measurements of the

spatiotemporal variation of CO_2 in the city's surroundings, a priori information and high spatial resolution numerical modeling of atmospheric transport. Estimation of anthropogenic CO_2 emissions using this method is an incorrect inverse problem in the classical sense and in some studies is called the inverse problem of atmospheric transfer.

Measurements of CO_2 in the vicinity of a city can be realized using a differential spectroscopic approach. It is based on parallel ground-based measurements of CO_2 total column (TC) using inter-calibrated spectrometers. At the same time, one of the instruments measures CO_2 content in the windward (unpolluted) part of the city, and the second - in the leeward (polluted) part. The difference between measurements under certain meteorological conditions should characterize the anthropogenic contribution of the city to the CO_2 environment. Such measurements are carefully planned and filtered for subsequent assessment of anthropogenic CO_2 emissions. Therefore, the method of determining anthropogenic CO_2 emissions of a city based on such measurements is called experimental - it is controlled by researchers.

Differential spectroscopic measurements have been carried out regularly and periodically for several years in some cities of the Earth as part of the COCCON measurement network [21-23]. St Petersburg is one of the largest industrial centers in Russia. Probably the territory of the city is a large anthropogenic source of CO_2 in Russia and on the planet. In 2019-2020 Scientists from St Petersburg State University and two German institutions (Karlsruhe Institute of Technology and University of Bremen) conducted a joint experiment (Emission Monitoring Mobile Experiment or EMME), the purpose of which was to assess anthropogenic emissions of the main greenhouse gases, including CO_2, from the territory of St Petersburg. As part of the EMME campaign, differential spectroscopic measurements of the total abundance of several gases were carried out in March and April 2019 using two mutually calibrated Fourier-transform infrared spectrometers. One of the instruments was located in the windward, and the second in the leeward parts of the city. Details of the experiment and the first estimates of specific anthropogenic CO_2 emissions in St Petersburg are given in [22].

Subsequently, a number of researchers assessed anthropogenic CO_2 emissions from the entire territory of St Petersburg for 2019 based on measurements from the EMME campaign, a priori information and numerical models of atmospheric transport [24-26]. Studies have shown that differences in the a priori information and atmospheric transport models used lead to differences in estimates of anthropogenic CO2 emissions in St Petersburg by ~30% and more. Differences in estimates are associated primarily with the use of models of CO_2 transfer in the atmosphere of different complexity, the quality of a priori information, and the amount of measurement data.

The aim of the study is to estimate anthropogenic CO_2 emissions from St Petersburg based on ground-based spectroscopic measurements obtained as part of the EMME campaign, various a priori information and atmospheric transport models.

To achieve the goal, the following **scientific tasks** were solved in the study:

- assessment of anthropogenic CO_2 emissions from the entire territory of St Petersburg using differential spectroscopic measurements of gas content in the atmosphere, a priori information and a one-dimensional box model of atmospheric transport, taking into account the spatial coverage of the measurements;
- assessment of the influence of absorption and release of CO_2 from the water surface of the Gulf of Finland on the gas content in the St Petersburg region and its contribution to estimates of anthropogenic CO_2 emissions;
- assessing the possibility of successfully using the numerical model of the chemical composition of the troposphere WRF-Chem to assess anthropogenic CO_2 emissions in St Petersburg by adapting the model to city conditions using measurements of CO_2 content in the atmosphere and its state;
- assessment of anthropogenic CO_2 emissions from the entire territory of St Petersburg using differential spectroscopic measurements of gas content in the atmosphere, a priori information and the WRF-Chem model;
- comparison of estimates of anthropogenic CO_2 emissions in St Petersburg based on the inventory approach and the method for solving the inverse problem of atmospheric transfer.

Methodology

The main method of this work is numerical modeling of atmospheric transport using as tools a one-dimensional box model, a three-dimensional particle dispersion model in the atmosphere STILT and a three-dimensional regional numerical weather prediction and tropospheric composition model WRF-Chem version 4.1.3.

Scientific novelty

The novelty of the work lies in the joint assessment of anthropogenic CO_2 emissions in St Petersburg based on differential spectroscopic measurements of total CO_2 content and atmospheric transport models of different complexity - a one-dimensional box model of atmospheric transport and a three-dimensional numerical model for forecasting weather and tropospheric composition WRF-Chem.

Unlike earlier studies where a box model was used to estimate emissions from St Petersburg, the current study uses a technique in which the spatial coverage of spectroscopic CO_2 measurements influences the box model estimate of anthropogenic CO_2 emissions.

The study analyzed the sensitivity of estimates of anthropogenic CO_2 emissions in St Petersburg by solving the inverse problem of atmospheric transport to the spatial coverage of measurement data, a priori information and the atmospheric transport model used.

In addition, for the first time, the WRF-Chem numerical model was adapted to the conditions of St Petersburg using comprehensive measurements of gas content in the atmosphere and its state to simulate CO_2 transport at the urban scale (2 km) over a period of more than a year.

Also, for the first time, the study collected and analyzed all currently available estimates of anthropogenic CO_2 emissions in St Petersburg for 2019, obtained by the inventory approach and the method of solving the inverse problem of atmospheric transfer.

Theoretical and practical significance of the work

The values of anthropogenic CO_2 emissions in St Petersburg obtained in the study support the conclusion that for a qualitative assessment of gas emissions from the

territories of large cities, in addition to the traditional inventory method, an independent approach should be used, based on data from parallel spectroscopic measurements of the total CO_2 content in the atmosphere and modeling of atmospheric transfer. This, in turn, indicates the need to establish regular measurements in the area of the study and improve modern models of atmospheric transport of high spatial resolution.

An analysis of the influence of the water surface of the Gulf of Finland on estimates of anthropogenic CO_2 emissions from St Petersburg indicates that the contribution of the water surface, even under extreme conditions, cannot be compared with the anthropogenic influence. Thus, when assessing anthropogenic CO_2 emissions in St Petersburg using the experimental method, the contribution of the water surface to the gas content in the atmosphere can be neglected.

The adaptation of the numerical model of weather prediction and tropospheric composition with high spatial resolution WRF-Chem to the conditions of St Petersburg and its surroundings, carried out in the study, makes it possible to use this model to assess anthropogenic CO_2 emissions from the city in the presence of high-precision spectroscopic measurements of the total CO_2 content in the city area.

Personal contribution

All numerical modeling results presented in this dissertation were obtained by the author independently. The author personally carried out all numerical experiments. Processing and analysis of the modeling results, as well as their comparison with measurement data, was carried out by the author personally or with his direct participation. The author by himself wrote scripts in Python and Bash for processing and analyzing modeling and measurement data.

Grants

- Grant of the Russian Foundation for Basic Research (RFBR) No 20-05-00627.
- St Petersburg State University "Laboratory for the study of the ozone layer and upper atmosphere"with the support of the Ministry of Science and Higher Education of the Russian Federation under the contract No 075-15-2021-583.
- State contract of the Ministry of Science and Higher Education of the Russian Federation No 13.2251.21.0005.

Author's publications on the topic of the dissertation

The main results on the topic of the dissertation are presented in publications indexed in the Web of Science and Scopus databases:

- Y. M. Timofeyev, G. M. **Nerobelov**, Ya. A. Virolainen, A. V. Poberovskii, S. C. Foka. Estimates of CO2 anthropogenic emission from the megacity St. Petersburg. *Dokl. Earth Sci*. 494(1): 753–756, 2020. https://doi.org/10.1134/S1028334X20090184
- **Nerobelov** G.M., Y. Timofeyev, S. Smyshlyaev, Y. Virolainen, M. Makarova, S. Foka. Comparison of CAMS Data on CO2 with Measurements in Peterhof. *Atmos Ocean Opt*, 34: 689–694, 2021. https://doi.org/10.1134/S102485602106018X
- **Nerobelov** G., Timofeyev Y., Smyshlyaev S., Foka S., Mammarella I., Virolainen Y. Validation of WRF-Chem Model and CAMS Performance in Estimating Near-Surface Atmospheric CO2 Mixing Ratio in the Area of Saint Petersburg (Russia). *Atmosphere*, 12(3): 387, 2021. https://doi.org/10.3390/atmos12030387
- Nikitenko A.A., G.M. **Nerobelov**, Yu.M. Timofeyev, A.V. Poberovskii. Analysis of ground-based spectroscopic measurements of CO2 in Peterhof. *Sovremennye problemy distantsionnogo zondirovaniya Zemli iz kosmosa*, 18(6): 265–272, 2021. (in Russian)
- Timofeyev, Y.M., **Nerobelov**, G.M., Poberovskii, A.V., Filippov N.N. Determining Both Tropospheric and Stratospheric CO2 Contents Using a Ground-Based IR Spectroscopic Method. *Izv. Atmos. Ocean. Phys*. 57: 286–296, 2021. https://doi.org/10.1134/S0001433821020110
- **Nerobelov**, G.M., Timofeyev, Y.M. Estimates of CO2 Emissions and Uptake by the Water Surface near St. Petersburg Megalopolis. *Atmos Ocean Opt.*, 34: 422–427, 2021. https://doi.org/10.1134/S1024856021050158
- Nikitenko, A.A., Timofeev, Y.M., Virolainen, Y.A., **Nerobelov** G.M., Poberovskii A.V. Comparison of Stratospheric CO2 Measurements by Ground- and Satellite-Based Methods. *Atmos Ocean Opt*. 35: 341–344, 2022. https://doi.org/10.1134/S1024856022040145

- Timofeyev, Y.M., **Nerobelov**, G.M., Poberovskii, A.V. Experimental Estimates of Integral Anthropogenic CO2 Emissions in the City of St. Petersburg. *Izv. Atmos. Ocean. Phys*. 58: 237–245, 2022. https://doi.org/10.1134/S0001433822030100
- **Nerobelov** G.M., Timofeyev Yu.M., Smyshlyaev S.P., Foka S.Ch., Imhasin H.H. Comparison of CO2 Content in the Atmosphere of St. Petersburg According to Numerical Modeling and Observations. *Izv. Atmos. Ocean. Phys*. 59: 275–286, 2023. https://doi.org/10.1134/S0001433823020056
- **Nerobelov** G., Timofeyev Y., Foka S., Smyshlyaev S., Poberovskiy A., Sedeeva M. Complex Validation of Weather Research and Forecasting—Chemistry Modelling of Atmospheric CO2 in the Coastal Cities of the Gulf of Finland. *Remote Sens*, 15: 1-30, 2023. https://doi.org/10.3390/rs15245757

Approbation of the work

The main results of the work were presented at the following international and Russian conferences:

- Yuri Timofeev, Georgy **Nerobelov**, Anatolii Poberovskii. Estimation of Anthropogenic CO2 Emissions of St. Petersburg Megacity by Different Methods. Oral presentation at the international conference AOGS2023, Singapore, 30 July – 4 August 2023.
- Georgy **Nerobelov**, Yuri Timofeev, Sergei Smyshlyaev, Stephany Foka. WRF-Chem Modelling of CO2 Transport in St. Petersburg Megacity. Oral presentation at the international conference AOGS2023, Singapore, 30 July – 4 August 2023.
- Timofeev Yu.M., **Nerobelov G.M.**, Poberovsky A.V. Anthropogenic CO2 emissions of St. Petersburg megacity by different methods. Oral presentation at the international conference ISARD-2023, St Petersburg, Russia, June 21-23 2023.
- **Nerobelov G.M.,** Timofeev Yu.M., Smyshlyaev S.P., Foka S.Ch. Validation of WRF-Chem modelling of CO2 transport in St Petersburg and Helsinki. Oral presentation at the international conference ISARD-2023, St Petersburg, Russia, June 21-23 2023.

- **Nerobelov G.**, Timofeyev Yu., Smyshlyaev S., Foka S., Hatakka J., Virolainen Ya. Validation of WRF-Chem modelling of Saint-Petersburg anthropogenic contribution to CO2 content Presentation at 19th Russian open international conference «Sovremennye problemy distantsionnogo zondirovaniya Zemli iz kosmosa». Moscow, Space Research Institute of the Russian Academy of Sciences. DOI 10.21046/19DZZconf-2021a, 2021
- Timofeyev Yu., **Nerobelov G.**, Virolainen Ya., Poberovskii A., Polyakov A. Analysis of robustness of differential spectroscopic IR method to estimate anthropogenic CO2 emission (with focus on Saint-Petersburg) Presentation at 19th Russian open international conference «Sovremennye problemy distantsionnogo zondirovaniya Zemli iz kosmosa». Moscow, Space Research Institute of the Russian Academy of Sciences. DOI 10.21046/19DZZconf-2021a, 2021
- **Nerobelov G.**, Timofeyev Y., Smyshlyaev S., Foka S., Mammarella I., Virolainen Y. (2021): Validation of the capability of WRF-Chem model and CAMS to simulate near surface atmospheric CO_2 mixing ratio for the territory of Saint-Petersburg. European Geosciences Union (EGU) General Assembly, 19-30 April 2021, Viena, Austria (virtual meeting); Geophysical Research Abstracts, Oral presentation, EGU21-1497, https://doi.org/10.5194/egusphere-egu21-1497
- Timofeyev Y., **Nerobelov G.**, Poberovskii A., Filippov N. (**2021**): Estimation of the tropospheric and stratospheric CO2 content by ground-based IR technique. European Geosciences Union (EGU) General Assembly, 19-30 April 2021, Viena, Austria (virtual meeting); Geophysical Research Abstracts, Oral presentation, EGU21-1477, https://doi.org/10.5194/egusphere-egu21-1477
- Timofeev Yu.M., **Nerobelov G.M.**, Virolainen Ya.A., Poberovskii A.V., Foka S.C. (2020) Comparison of different estimates of CO_2 anthropogenic emissions from Saint-Petersburg metropolis. Published in the report of a conference “Modern Problems of Hydrometeorology and Environment Monitoring on the Territory of CIS”. ISBN: 978-5-86813-508-8, p. 794.

- **Nerobelov G.M.**, Timofeev Yu.M., Smyshlyaev S.P., Virolainen Ya.A., Makarova M.V., Foka S.C. (2020) Validation of CAMS database and WRF-Chem 3D modelling of CO_2 content near Saint-Petersburg. Published in the report of a conference “Modern Problems of Hydrometeorology and Environment Monitoring on the Territory of CIS”. ISBN: 978-5-86813-508-8, p. 794.
- Timofeyev Y., **G. Nerobelov**, S. Smyshlyaev, I. Berezin, Ya. Virolainen, M. Makarova, A. Poberovsky, A. Polyakov, S. Foka (2020): Estimates of anthropogenic CO2 emissions from satellite and ground based measurements. European Geosciences Union General Assembly, 4-8 May 2020, Vienna, Austria; Geophysical Research Abstracts, Oral presentation, EGU2020-2580

Main scientific results

1. Adaptation of the WRF-Chem numerical model to the conditions of St Petersburg makes it possible to describe changes in CO_2 content in the atmosphere over a year with a high spatial resolution (2-3 km) with an average discrepancy from measurements of less than 0.6%. At the same time, the WRF-Chem model describes the spatiotemporal change in CO_2 content in the St Petersburg region than the available modeling data on the global scale CAMS and CarbonTracker. The adapted WRF-Chem model can be used to assess anthropogenic CO_2 emissions from the territory of St Petersburg.

   The result is presented on page 284 of the publication **Nerobelov** G.M., Timofeyev Yu.M., Smyshlyaev S.P., Foka S.Ch., Imhasin H.H. Comparison of CO2 Content in the Atmosphere of St. Petersburg According to Numerical Modeling and Observations. *Izv. Atmos. Ocean. Phys.* 59: 275–286, 2023. https://doi.org/10.1134/S0001433823020056; on pages 23-24 of the publication **Nerobelov** G., Timofeyev Y., Foka S., Smyshlyaev S., Poberovskiy A., Sedeeva M. Complex Validation of Weather Research and Forecasting—Chemistry Modelling of Atmospheric CO2 in the Coastal Cities of the Gulf of Finland. *Remote Sens*, 15: 1-30, 2023. https://doi.org/10.3390/rs15245757; on pages 267-268 of the publication Nikitenko A.A., G.M. **Nerobelov**, Yu.M. Timofeyev, A.V. Poberovskii. Analysis of ground-based spectroscopic measurements of CO2

in Peterhof. *Sovremennye problemy distantsionnogo zondirovaniya Zemli iz kosmosa*, 18(6): 265–272, 2021. (in Russian); on pages 294-295 of the publication Timofeyev, Y.M., **Nerobelov**, G.M., Poberovskii, A.V., Filippov N.N. Determining Both Tropospheric and Stratospheric CO2 Contents Using a Ground-Based IR Spectroscopic Method. *Izv. Atmos. Ocean. Phys*. 57: 286–296, 2021. https://doi.org/10.1134/S0001433821020110; on page 343 of the publication Nikitenko, A.A., Timofeev, Y.M., Virolainen, Y.A., **Nerobelov** G.M., Poberovskii A.V. Comparison of Stratospheric CO2 Measurements by Ground- and Satellite-Based Methods. *Atmos Ocean Opt*. 35: 341–344, 2022. https://doi.org/10.1134/S1024856022040145; on page 693 of the publication **Nerobelov** G.M., Y. Timofeyev, S. Smyshlyaev, Y. Virolainen, M. Makarova, S. Foka. Comparison of CAMS Data on CO2 with Measurements in Peterhof. *Atmos Ocean Opt*, 34: 689–694, 2021. https://doi.org/10.1134/S102485602106018X; and on pages 19-20 of the publication **Nerobelov** G., Timofeyev Y., Smyshlyaev S., Foka S., Mammarella I., Virolainen Y. Validation of WRF-Chem Model and CAMS Performance in Estimating Near-Surface Atmospheric CO2 Mixing Ratio in the Area of Saint Petersburg (Russia). *Atmosphere*, 12(3): 387, 2021. https://doi.org/10.3390/atmos12030387.

The personal contribution of the applicant is to adapt the WRF-Chem numerical model to the conditions of St Petersburg and carry out a numerical experiment of the transport of CO_2 in the atmosphere in the St Petersburg region for a period of more than a year; to validate the WRF-Chem model using complex measurements; to compare data WRF-Chem simulations with global CAMS and CarbonTracker simulation data.

2. The range of values of anthropogenic CO_2 emissions in St Petersburg for 2019, obtained by solving the inverse problem of atmospheric transfer using differential spectroscopic measurements and a one-dimensional model of atmospheric transport, taking into account the spatial coverage of the city territory by measurements, is 76–105 Mt/year with an average estimate of 91±19 Mt g^{-1}. Taking into account the limited spatial coverage of paired spectroscopic

measurements of CO_2 content in the atmosphere leads to a decrease in estimates of anthropogenic emissions of St Petersburg by ~22-55%.

The result is presented on page 755 of the publication Y. M. Timofeyev, G. M. **Nerobelov**, Ya. A. Virolainen, A. V. Poberovskii, S. C. Foka. Estimates of CO2 anthropogenic emission from the megacity St. Petersburg. *Dokl. Earth Sci*. 494(1): 753–756, 2020. https://doi.org/10.1134/S1028334X20090184; and on 243 of the publication Timofeyev, Y.M., **Nerobelov**, G.M., Poberovskii, A.V. Experimental Estimates of Integral Anthropogenic CO2 Emissions in the City of St. Petersburg. *Izv. Atmos. Ocean. Phys*. 58: 237–245, 2022. https://doi.org/10.1134/S0001433822030100.

The personal contribution of the applicant is to assess anthropogenic CO_2 emissions of St Petersburg by solving the inverse problem of atmospheric transport using differential spectroscopic measurements and a one-dimensional atmospheric transport model taking into account the spatial coverage of the city territory.

3. The contribution of the surface of the Gulf of Finland to the CO_2 content in the St Petersburg area is less than 1% of the anthropogenic contribution of the city and may not be taken into account when numerically modeling the transfer of CO_2 in the atmosphere in the city.

   The result is presented on page 426 of the publication **Nerobelov**, G.M., Timofeyev, Y.M. Estimates of CO2 Emissions and Uptake by the Water Surface near St. Petersburg Megalopolis. *Atmos Ocean Opt.*, 34: 422–427, 2021. https://doi.org/10.1134/S1024856021050158.

   The personal contribution of the applicant is to assess the absorption and emissions of CO_2 from the surface of the Gulf of Finland based on ship measurements; and to assess the contribution of the surface of the Gulf of Finland to the CO_2 content in the St Petersburg area in comparison with the anthropogenic contribution.

Provisions for defense

- The contribution of taking into account the spatial coverage of paired spectroscopic measurements when assessing anthropogenic CO_2 emissions in St Petersburg for 2019 using a one-dimensional box model reaches ~40%.
- Adaptation of the WRF-Chem numerical model to the conditions of St Petersburg allows the model to be used to solve the inverse problem of estimating anthropogenic CO_2 emissions of the city (modeling error ~0.2%) in ~60% of cases.
- The use of different sets of measurements, a priori information and atmospheric transport models lead to a range of values of anthropogenic CO_2 emissions in St Petersburg from ~62 to more than 90 Mt y^{-1}.
- The average anthropogenic CO_2 emission of St Petersburg in 2019 based on the method of solving the inverse problem of atmospheric transfer is 73±13 Mt y^{-1}.

Chapter 1. Greenhouse gas CO_2 and methods for its monitoring in the atmosphere

1.1 Earth's climate change - causes and current conditions

In this chapter, we will review the role of carbon dioxide (CO_2) in the Earth's climate change and the ways of monitoring the spatiotemporal variation of this gas.

The climate of the Earth can be called the average long-term state of its surface and atmosphere, which is described by such characteristics as the temperature of the air and the surface of the planet, the amount of precipitation, the height of the ocean surface, cloudiness, atmospheric composition, etc. Since the formation of the Earth's atmosphere, its average state has changed very much and continues to change as a result of interaction with the remaining shells of the Earth (hydrosphere, biosphere, cryosphere, lithosphere), as well as with external factors (changes in incoming solar radiation, variations in the gas and aerosol composition of the atmosphere as a result volcanic eruptions and anthropogenic activity) [1].

Analysis of long-term changes in the Earth's climatic characteristics, as well as studies of the atmospheres of other planets in the Solar System, indicate the importance of the composition of the atmosphere, namely the content of greenhouse gases, in forming the planet's climate. Greenhouse gases are chemical compounds whose molecules are capable of absorbing and re-emitting electromagnetic (EM) radiation in the infrared wavelength range (IR or thermal). The Earth's atmosphere contains many greenhouse gases (H_2O, CO_2, CH_4, N_2O, O_3, etc.), which are of both natural and anthropogenic origin. Most greenhouse gases are almost chemically inactive (for example, CO_2, CH_4, N_2O), which contributes to their long lifetime in the atmosphere (from several to hundreds and thousands of years [1, 2]). The presence of some greenhouse gases in the Earth's atmosphere with maximum content in its lower layer disrupts the planet's radiation balance, reducing the carrying capacity of the atmosphere for thermal radiation escaping from the earth's surface and slowing down the cooling of the surface. This phenomenon is called the greenhouse effect. It leads to heating of the

lower troposphere and provides suitable conditions for a comfortable life for humans and other living organisms on Earth [3].

The long-term accumulation of greenhouse gases in the atmosphere observed globally since the middle of the last century [4, 5] is associated with human (or anthropogenic) activity. This is evidenced by such facts as (1) a decrease in the concentration of molecular oxygen (O_2) at a rate proportional to anthropogenic CO_2 emissions; (2) a decrease in the relative content of the carbon isotope ^{14}C in the air, which is absent in fossil fuels; (3) the increase in CO_2 content is faster in the Northern Hemisphere, where there are many more anthropogenic sources of gas, compared to the Southern Hemisphere [6].

Today there is increasing confidence that anthropogenic activity is contributing to the observed gradual increase in the average global temperature of surface air and the earth's surface and, as a consequence, changes in other characteristics of the Earth's climate. According to the reports of the IPCC (Intergovernmental Panel on Climate Change, https://www.ipcc.ch/) [7, 8], the anomaly of the average global air temperature at the Earth’s surface in the period 2010-2019 in relation to 1850-1900 is in the range from +0.8 to 1.3 °C. At the same time, with a high probability, the main cause of global warming and related climate changes is the increase in the content of greenhouse gases in the atmosphere from anthropogenic emissions [9, 10]. The results of modeling the past states of the Earth's climate, as well as an analysis of long-term measurements, indicate a correlation between global climate change and an increase in the content of greenhouse gases in the atmosphere, which has been actively growing since approximately the beginning of the industrial revolution, i.e. from the mid-18th century [7]. The observed global climate changes due to the increasing average temperature of the Earth's surface and air in the lower troposphere have predominantly negative consequences for humans. The most significant consequences are caused by an increase in the number and intensity of annual adverse weather events. These include extreme air temperatures, heavy precipitation, flooding, drought, and others [11].

Climate changes are also noticeable on a regional scale. For example, the report [27] indicates that the average air and surface temperatures continue to increase at the

highest speed in the high latitudes of northern Europe (from Belarus to Finland according to the IPCC region classification). For the period 2002-2011 the temperature increase in this part of the Earth is ~1.3±0.11°C relative to the period 1850-1899. In addition, since 1950, precipitation has increased in northern Europe (by about 70 mm per decade) and decreased in southern Europe. According to the report [28], the average temperature of the Earth's surface in the Arctic part of Canada is increasing at a rate approximately 3 times higher than the average on Earth. This may be caused by a series of feedbacks. Analysis of climate change in Russia based on observational data [29] indicates a pronounced gradual increase in the average temperature of the Earth's surface. Thus, by 2014, the average temperature increased by ~1.5°C relative to the average temperature for the period 1961-1990 (the base period accepted by the WMO) with the highest rate in northern latitudes. At the same time, the rate of increase in temperature of the Earth's surface for the period 1976-2012 in Russia, turned out to be more than twice as high as the world average (0.45 versus 0.17°C over 10 years). Trend of changes in precipitation amounts for 1976-2010 is also positive and amounts to ~0.3 mm over 10 years. During the period from 1996 to 2012, the number of cases of adverse weather events causing damage to the economy and public health increased in Russia.

According to the report [30], the consequences of global warming are noticeable in the territory of the large Russian city of St Petersburg (Leningrad region). Thus, over the 30 years from 1988 to 2017, the average air temperature in the city increased by 1.3°C relative to the average temperature for the period 1961-1990. From 1881 to 2017, an increase in precipitation was observed from ~500 to 700 mm per year.

1.2 The role of CO_2 in climate change

Despite the fact that many greenhouse gases are of natural origin, the predominant contribution to the continuing increase in the content of these gases in the Earth's atmosphere is made by increasing anthropogenic activity. The increase in anthropogenic activity is associated with the growth of the planet's population and economic development, i.e. with the expansion of production and urbanization of new

territories [31, 32]. The main source of anthropogenic greenhouse gases is the combustion of fossil fuels (energy, transport, industry, etc.). According to the report [29], the main sources of greenhouse gases in Russia are energy, industry, agriculture and waste processing.

The main anthropogenic greenhouse gases in terms of their impact on the Earth's climate include carbon dioxide (CO_2), methane (CH_4) and nitrous oxide (N_2O). The predominance of the listed greenhouse gases over others is due to their highest concentration in the atmosphere. According to the sixth IPCC report of 2021 [33], due to the development of anthropogenic activity after the industrial revolution and, as a consequence, the increase in the quantity and power of anthropogenic sources of greenhouse gases, in the period from 1750 to 2019, the content of CO_2, CH_4 and N_2O in the atmosphere increased by ~47, 158 and 23%, respectively. Despite international agreements on reducing emissions of major greenhouse gases adopted by many developed countries (Kyoto Protocol [13], Paris Agreement [14], Montreal Protocol [34], Kigali Amendment [35] and others), their content continues to increase quite rapidly. For example, if in the 60-70s of the last century the growth rate of global CO_2 content was in the range of ~0.5-1.5 ppm/year, today it is more than ~2 ppm/year, and will probably continue to grow [36, 37].

Despite humanity’s desire to transition to an almost emission-free type of energy, according to one of the scenarios [38], the transition to energy production that is clean, from the point of view of the impact on the Earth’s climate, by 2050 requires spending ~$4*10^{12}$ USD per year, which is about 4% of the world's gross domestic product (GDP) in 2021 (about $96*10^{12}$ USD) and is a colossal cost. For example, the estimated annual spending on clean energy is approximately equal to the GDP of Germany in 2021 ($4.2 * 10^{12}$ USD) and more than the GDP of Russia ($1.78 * 10^{12}$ USD), Great Britain ($3.19 * 10^{12}$ USD), France ($2.94 * 10^{12}$ USD), Italy ($2.1*10^{12}$ USD) and many other countries [39]. However, it is predicted that following this scenario, by 2050, only less than 50% of all energy consumption could come from clean production [38]. It is therefore clear that in the coming decades we will continue to record an increase in greenhouse gases in the atmosphere from human activity.

CO_2 is called the main anthropogenic greenhouse gas, the increase in its content has the greatest impact on the increase in global surface temperature of the Earth. According to [12], radiation forcing of CO_2 (i.e., the effect on changes in the Earth's radiation balance) is approximately 4 times more than methane forcing, 6-7 times more than chlorofluorocarbons and 8-10 times more than nitrous oxide. This is due to the highest level of CO_2 molecules in the Earth's atmosphere, which is caused by a greater number of anthropogenic sources and the magnitude of their emissions. Thus, on average, the content of CO_2 in the atmosphere is ~200 times higher than CH_4 and ~1000 times higher than N_2O. As for the amount of substance emitted into the atmosphere, CO_2 emissions are ~3 times greater than CH_4 emissions and ~10 times greater than N_2O emissions.

1.3 Main sources and sinks of CO_2

The Earth's atmosphere is one of four reservoirs of carbon (mainly in the form of CO_2), in which the content of the substance constantly changes due to interaction with three other reservoirs - biota (particularly plants), the ocean and fossil fuel deposits in the bowels of the Earth. The type and rate of interactions between the atmosphere and the other three reservoirs determines the variety of CO_2 sources and sinks and the degree of their impact on the gas content in the atmosphere [40].

The Earth's interior is the largest reservoir of carbon, where it accumulates in the form of fossil fuels (coal, natural gas, oil), as well as in the form of sedimentary rocks, which accounts for the largest portion. For example, carbon reserves in the form of sedimentary rocks in the Earth's interior are about 100 t m^{-2} (~60 thousand times more than in the atmosphere), and in the form of fossil fuels - 0.01 t m^{-2} (average over the Earth's surface area). Despite the size of this reservoir, most of the accumulated carbon has a very low rate of exchange with the atmosphere, which takes hundreds of thousands and millions of years [2]. Due to the large size of the occupied territory and the high rate of exchange, the ocean is called the main natural source and sink of CO_2 in the atmosphere on a global scale over time periods ranging from tens of years to

millennia. In terms of carbon reserves, this reservoir is in second place, containing approximately 60 times more matter than the atmosphere [41]. Biota is a natural factor that is more significant for the dynamics of CO_2 in the atmosphere over time periods from days to months. In this case, the main contribution is made by the process of photosynthesis in plants, which has a pronounced seasonal nature [2, 6, 41-43].

Anthropogenic activity leads primarily to an increase in CO_2 content in the atmosphere, since it does not have such large and strong gas sinks as the ocean surface and biota. The main anthropogenic source of CO_2 is the combustion of fossil fuels, as a result of which carbon from the largest reservoir, the interior of the Earth, moves into the atmospheric reservoir, where it can linger for hundreds and thousands of years [6, 43].

From this we can conclude that the main sources of atmospheric CO_2 determine the gas content primarily in the lower layer of the atmosphere. Thus, in [44] it is shown that the CO_2 content in the layer up to 12 km is, firstly, higher than in the overlying layer, and secondly, it is subject to greater seasonal changes. The second conclusion was confirmed in the study [45].

The total contribution of the biosphere and the ocean surface leads to a constant absorption of ~50% of CO_2 from anthropogenic sources. According to the results of the study [46], for 2010-2019, the probable increase in CO_2 in the atmosphere was 5.1±0.02 GtC y^{-1}, which was facilitated by anthropogenic CO_2 emissions as a result of the combustion of fossil fuels (9.6±0.5 GtC y^{-1}), changes in land use (mainly deforestation forests, 1.6±0.7 GtC y^{-1}), natural absorption of gas by the ocean surface (2.5±0.6 GtC y^{-1}) and biota or biosphere (3.4±0.9 GtC y^{-1}). At the same time, the constant cycling of much larger amounts of carbon between the atmosphere-ocean (about 90 GtC y^{-1}) and atmosphere-biosphere (about 120 GtC y^{-1}) reservoirs does not make a significant contribution to climate change [46].

1.4 Modern methods for monitoring spatiotemporal variations of CO_2 content

Because of the importance of carbon dioxide in changing the Earth's climate, scientists from all over the world have been creating and developing systems for

monitoring this gas in the atmosphere for decades. Monitoring variation in the content of CO_2 and other greenhouse gases in the Earth's atmosphere began in the middle of the last century with the work of the American scientist Charles Keeling [4]. Today, monitoring and analysis of the information received is carried out regularly by scientists from all over the world; it involves all kinds of measurements (ground-based local and remote, satellite, aircraft, etc.) and numerical models of atmospheric composition [47-51].

Note that modern monitoring of the dynamics of carbon dioxide in the Earth's atmosphere consists not only of assessing the gas content, but also of analyzing sources and sinks. If the CO_2 content in the atmosphere can be used to judge the current climate impact of the gas, then information about sources and sinks makes it clear what makes the most significant contribution to the content. For example, as mentioned, today the greatest contribution to the increase in CO_2 content globally comes from gas emissions from anthropogenic sources, ~50% of which annually remains in the atmosphere, and the other half is predominantly absorbed by the ocean surface and vegetation. However, some studies [52] indicate that in the future, at the current or increased emission rate, the share of CO_2 from anthropogenic sources leaving the atmosphere in natural sinks will decrease. This should lead to an increase in the rate of growth of CO_2 content in the atmosphere and, as a consequence, to an acceleration in the increase in temperature of the Earth's surface. Therefore, at the moment, correct information about the sources and sinks of CO_2 at various spatial scales is valuable. Such information will make it possible to obtain a prediction of Earth's climate change according to the most plausible scenario, as well as monitor the contribution of countries, regions, cities and individual objects (thermal power plants, industrial enterprises, etc.) to the increase in CO_2 content in the Earth's atmosphere.

Information on variations in CO_2 content in the atmosphere obtained by various methods has its advantages and disadvantages. A fairly detailed review of modern measuring methods and instruments for monitoring CO_2 in the atmosphere is given in the report [16]. Below we briefly describe the main modern measuring systems and

numerical models for monitoring carbon dioxide in the atmosphere, as well as methods for assessing the sources and sinks of CO_2.

Today, two types of CO_2 measurements are carried out on a regular basis globally - local, characterizing a small volume of air (for example, in the vicinity of a measuring station near the Earth's surface), and remote, providing information mainly on the integral gas content in the entire atmosphere and in its selected layers (for example, in the troposphere and stratosphere).

Among the global networks of local measurements of surface CO_2 content, we can highlight the WMO GAW (The Global Atmosphere Watch) program [53]. Within the framework of this program, since 1989, global measurements of atmospheric composition have been carried out using ground-based, mast-based, radiosonde, aircraft, satellite and other measurements. As part of the program, surface CO_2 concentrations are measured at many ground stations [54]. In addition to this program, there is a global measurement network, the Global Greenhouse Gas Reference Network [55], which is part of the American research center National Oceanic and Atmospheric Administration, Earth System Research Laboratories (NOAA ESRL) [56] and is aimed at studying the atmospheric content of the three main greenhouse gases - CO_2, CH_4 and N_2O. The network carries out measurements of local CO_2 content at the Earth's surface layer and at specific altitudes (aircraft, mast and radiosonde measurements).

Regular local measurements of CO_2 at the Earth’s surface, as well as on masts, are carried out at the Finnish measuring stations SMEAR (Station for Measuring Ecosystem-Atmosphere Relations) [57]. We also note the European measuring network ICOS (Integrated Carbon Observation System, https://icos-atc.lsce.ipsl.fr/), the purpose of which is to study the sources of the main greenhouse gases, including CO_2, in the Earth’s atmosphere. Within the ICOS network, since 2009, regular ground-based measurements of the local content of greenhouse gases have been carried out at approximately 40 stations [58].

There is not a wide national network of regular greenhouse gas measurements in Russia. Regular CO_2 measurements in Russia are carried out under the leadership of Roshydromet and maintained by employees of the Voeikovo Main Geophysical

Observatory (St Petersburg) at three stations - the Teriberka (Kola Peninsula, since 1988), New Port (Yamal Peninsula, since 2002) and Tiksi (north of the Republic of Sakha (Yakutia), since 2011). All three stations are remote from large anthropogenic sources and are located in the Arctic part of Russia. Previously, under the leadership of Roshydromet, measurements were also carried out at two island stations - Bering Island (1986-1994) and Kotelny Island (1983-1993) [59].

Since 2004, within the framework of the Japan–Russia Siberian Tall Tower Inland Observation Network (JR-STATION) program, scientists from the Zuev Institute of Atmospheric Optics SB RAS (Tomsk, Russia) together with colleagues from Japan (National Institute for Environmental Studies, Tsukuba and Center for Environmental Remote Sensing, Chiba University, Chiba) organized a monitoring network for the measurements of local concentrations of carbon dioxide and methane, currently consisting of 9 observation posts [60, 61]. Most stations are located far from large anthropogenic sources of CO_2, which also makes it possible to study the natural influence on the content of carbon dioxide in the atmosphere. Measurements are carried out at the Earth's surface and at heights from masts and aircraft flights.

Since 2013, at the Faculty of Physics of St Petersburg State University in Peterhof (St Petersburg), episodic measurements of ground-level CO_2 content have been carried out using the Los Gatos Research Greenhouse Gas Analyzer (GGA-24r-EP) [62-64].

Regular measurements of CO2 content are also carried out in Central Russia. At the Obninsk research station, under the guidance of scientists from the Federal State Budgetary Institution “Research and Production Association Typhoon” (Obninsk, Central Russia), since 1998, measurements of the CO_2 and CH_4 content in a surface layer have been carried out by Fourier spectroscopy [65].

Using such measurements, it is possible to characterize local features of variations in CO_2 content, which are applicable to limited volumes of air (for example, the surface layer of the atmosphere), territory (for example, a metropolitan area, suburbs, forest, etc.) and time period (day, night, winter, summer). Despite their limitations, local measurements clearly reflect seasonal and annual changes in atmospheric CO_2 content [62].

Unlike measurements of surface layer CO_2 content, the gas content in the entire atmosphere is less sensitive to dynamic processes in the Earth's boundary layer. Measurements of CO_2 content in the entire dry atmosphere (hereinafter referred to as total column or TC) characterize the dynamics of gas in the atmosphere under the influence of sources and sinks of various kinds. Often, to describe the TC, the XCO_2 value is used, which characterizes the average ratio of the number of CO_2 molecules to the number of dry air molecules in the entire atmosphere or in its particular layer. This value is expressed in ppm (parts per million, millionths of mass or volume).

Measurements of total CO_2 and other greenhouse gases are regularly carried out on the global measurement networks TCCON (Total Carbon Column Observing Network) and COCCON (Collaborative Carbon Column Observing Network). Measurements on the TCCON network [66] have been carried out since 2004 using FTIR spectrometers from Bruker Optics GmbH at more than 20 stations. The requirements for measurement accuracy are 0.25%, but researchers on the network are not limited to this value, trying to achieve the smallest error in retrievals of CO_2 TC [67]. One of the most reliable and widespread devices on the TCCON network, Bruker 125RH, measures the spectra of incoming solar radiation in the IR range with a spectral resolution of about 0.02-0.002 cm^{-2}. To retrieve the TC of CO_2 and other gases, the inverse problem of atmospheric optics is solved, in which the measured spectra are interpreted using a priori information (the state of the atmosphere, the vertical profile of the gas under study and interfering gases) and special programs (for example, PROFFIT [68] and GFIT [69]) .

Measurements on the COCCON network [21] began in 2016, in which about 18 scientific groups from around the world are currently involved. Unlike TCCON, the main instrument of this network is the Bruker EM27/SUN FTIR spectrometer. This spectrometer has a coarser spectral resolution of 0.5 cm^{-1}, which, however, measures IR spectra also with small errors due to careful inter-calibration of instruments [70, 71]. In addition, the Bruker EM27/SUN spectrometer is mobile and can be used not only in stationary, but also in field measurements [72, 22, 24]. The random error of XCO_2

measurements using Bruker EM27/SUN instruments is approximately an order of magnitude lower than that of the Bruker 125HR and constitutes 0.03-0.08% [70, 22].

We also note the NDACC (Network for the Detection of Atmospheric Composition Change, https://www-air.larc.nasa.gov/missions/ndacc/) measurement network [73], which includes measurements of incoming IR radiation by Fourier spectrometers from the end 20th century to the present, which can be interpreted to retrieve the TC of CO2. However, the main objectives of this network do not officially include the retrieval of CO_2 TC. Therefore the retrieval of the content of this gas is carried out on the NDACC network in private research (see, for example, [74-77]).

In Russia, measurements of total CO_2 content are carried out by individual scientific institutes. For example, at the station in Peterhof, St Petersburg, since 2009, measurements of a series of environmentally and climatically important gases (including CO_2) have been carried out using a Bruker 125HR Fourier spectrometer [75-77, 44]. At the same time, since 2012, measurements of a series of gases at the station in Peterhof have been included in the international NDACC measurement network described above.

The results of ground-based measurements of CO_2 TC are valuable as reference data for the validation and calibration of satellite measurements, since they are more accurate [78]. At the same time, ground-based remote measurements are irregular in space (distances between nearest stations can reach thousands of kilometers) and have small territorial coverage.

The main advantage of satellite measurements is global coverage. Satellite measurements of CO_2 are based on recording reflected and scattered, as well as the Earth's own radiation in the IR wavelength range [16]. The possibility of the retrieval of CO_2 content from satellite measurements appeared in 1979 with the launch of the American TOVS instrument (Television Infrared Observation Satellite Operational Vertical Sounder, NOAA series satellites) to an Earth orbit [79]. The device measured infrared radiation leaving the Earth in the range of 4.3-15 microns in approximately 20 spectral channels and was created to reconstruct the profile of temperature, humidity and other atmospheric parameters. The spatial resolution of IR radiation measurements

was about 20 km. It has been shown that the retrieval of CO_2 TC based on TOVS measurements with a resolution of 15° has errors of the order of 2 ppm (less than 1%).

The first satellite measurements aimed at studying greenhouse gases, including CO_2, were started by scientists from Japan in 1996 with the launch of the IMG (Interferometric Monitor for Greenhouse gases) instrument [80]. The device had a spectral resolution of 0.1 cm^{-1} and measured IR outgoing Earth's radiation in the range of 3.3-14 μm with a spatial resolution of 8 km [81].

To date, space agencies from around the world have put into operation more than ten satellite instruments, which, based on measurements of the Earth's re-emitted and reflected IR radiation, make it possible to obtain information about the content of CO_2 and other gases both in the entire dry atmosphere and in particular layers. These are GOSAT, GOSAT2 (Japan), SCIAMACHY, IASI (EU), OCO-2, OCO-3, AIRS, TES (USA), IKFS-2 (Russia), TanSat (China) and others instruments [47, 82-87]. Modern satellite measuring systems make it possible to obtain information about CO_2 with a spatial resolution of up to 2-3 km (for example, TanSat and OCO-2/OCO-3) and with systematic random errors of up to about 0.4 ppm (0.1%) and 0.7-1.4 ppm (0.2-0.3%), respectively [88].

Thanks to the progress achieved in understanding atmospheric physical processes and spatiotemporal variations in CO_2 sources and sinks, modern numerical models of the dynamics of gas and aerosol composition in the atmosphere have been actively used over the past few decades to monitor carbon dioxide in conjunction with complex measurements [89-93]. Unlike measurements, modeling data have the required time periodicity and spatial coverage, are fully controlled by the researcher, and are often much cheaper than organizing regular stationary or field measurements [93]. However, even the most developed models have limitations in information about the main influencing factors - atmospheric transport, distribution of CO_2 sources and sinks, CO_2 emissions, daily and seasonal variations in gas emissions, etc., which affect modeling errors.

Numerical models of atmospheric transport and atmospheric composition are widely used in monitoring atmospheric CO_2. They are used to (1) determine the factors

influencing the variation of CO_2 in the atmosphere [94, 95]; (2) assess of gas sources and sinks [96, 97]; (3) predict possible climate changes on Earth under various scenarios of future CO2 emissions [98-100], as well as for other tasks.

Nowadays, there is no universal numerical model of the atmospheric composition that would be suitable for all kinds of objectives. We can say that for certain areas of application (for example, one of the three listed above), spaces and time intervals, there is its own class of numerical models. Models used to predict possible climate changes from the effects of increasing CO_2 levels in the atmosphere generally cover the entire Earth's surface and most of the atmospheric layer (usually up to hundreds of kilometers). Such models are among the most complex, since they must take into account the entire range of physical and chemical processes (including feedback) occurring both in the atmosphere and in the rest of the shells of the entire Earth. An example of such a model is SOCOL (SOlar Climate Ozone Links) [101]. The latest version of this model, SOCOL v4.0 [101], consists of three main parts - a model of interaction between the Earth's shells (MPI-ESM1.2 [102]), a chemical model representing reactions with gases and aerosols (MEZON [103]) and a model microphysics of sulfur-containing aerosols AER [104]. The horizontal spatial resolution of the model is 1.9°x1.9° (i.e., on average ~200x200 km2) with a vertical distribution at 47 hybrid levels from the Earth's surface to approximately 0.01 hPa. However, in this version of the model, the spatiotemporal change in CO_2 is not calculated, but is set in advance from the results of other global models or, for example, reanalysis data. Predefined information about the CO_2 content is associated with parameterization schemes for short- and long-wave electromagnetic radiation coming to and leaving the Earth, which makes it possible to take into account the influence of gas variations in the atmosphere on changes in the temperature of the Earth's surface and other characteristics of the atmosphere.

Another type is numerical models of weather prediction and atmospheric composition with high spatial resolution over a limited area. They are used, for example, to study the dynamics of CO_2 content in regions or cities with a spatial resolution of up to 1 km or less. Such models take into account local meteorological

conditions, complex terrain, heterogeneous distribution of CO_2 sources and sinks in urban areas and other features that cannot yet be fully taken into account in global models.

An example of a model of this class, which is actively used in the scientific communities of many countries for monitoring CO_2 and assessing anthropogenic emissions of this gas, is WRF-Chem (Weather Research and Forecasting - Chemistry [105-107]). Like the global SOCOL model, WRF-Chem consists of a dynamic and a chemical part. However, limiting the study area, specifying geophysical properties (relief, albedo, temperature, type of underlying surface, etc.) with a spatial resolution of up to several meters and describing atmospheric processes with a resolution of up to 1 km or less allow the use of the WRF-Chem model for analyzing processes and phenomena with time scales up to minutes (for example, local short-period changes in surface CO_2 concentration).

1.5 Modern methods for determining CO_2 emissions, their advantages and disadvantages

The third component of modern monitoring of CO_2 in the atmosphere is the assessment of emissions from gas sources and sinks. There are two methods for estimating emissions. The first and widely used is the inventory approach. It is based on the assessment of anthropogenic CO_2 emissions using information characterizing human activity [16, 17]. Examples of such information are the amount of fossil fuel consumed in the energy sector, industry, transport, etc., land use data, the location of combined heat and power plants (CHP) and industries (for example, metallurgy), night illumination of urban areas and much more. Some of such data characterizes the magnitude of CO_2 emissions, while the other characterizes the spatiotemporal distribution of sources and sinks, which is important when distributing integral emissions, for example, of the entire country across regions, cities, and even individual city districts. For example, one of the global databases of anthropogenic CO_2 emissions ODIAC (The Open-source Data Inventory for Anthropogenic CO_2) [108] has a spatial

resolution of ~1 km on average, which was obtained due to the spatial distribution of total emissions of individual countries by known point sources and by night satellite imagery. At the national level, databases of anthropogenic CO_2 emissions with high spatial resolution also exist (for example, for China [109]). Errors in anthropogenic CO_2 emissions based on the inventory approach at the national level (i.e. from the territories of countries) can reach only a few percent [18, 19]. However, when moving to the city scale and above, the errors in emission estimates can exceed 100% [20]. For example, works [110] and [111] present estimates of CO_2 emissions from the territories of Chinese cities for 2010 and 2012. The differences in estimates for some cities reach almost 80%.

Probably, to monitor the national contribution of most developed countries to the increase in CO_2 content in the Earth's atmosphere, it is sufficient to use existing inventory approach methods. However, firstly, not all countries provide information on the basis of which it is possible to estimate anthropogenic CO_2 emissions of equal quality and with uniform regularity [112]. Secondly, for monitoring and controlling the contribution of the country's subjects up to the analysis of individual cities and sources on their territories, the errors of the inventory approach, as already mentioned, can reach 100% or more [20, 113]. Thirdly, according to estimates, from ~35% [114] to more than 70% [15] of anthropogenic CO_2 emissions occur in urban areas. Accordingly, high-quality and comprehensive monitoring of anthropogenic emissions of CO_2 and other greenhouse gases from the territories of large cities is required to monitor accepted obligations to limit emissions.

These and other reasons led to the development of an independent method for assessing anthropogenic emissions of CO_2 and other greenhouse gases. It is based on high-quality measurements of spatiotemporal gas variation, a priori information, and numerical modeling of atmospheric transport.

The main idea of the method is to correlate the measured increase in CO_2 content with the source using information about the state of the atmosphere over the past period of time. Information about the past state of the atmosphere can be obtained using numerical models of the dynamics of gas composition of varying complexity. This

approach often uses CO_2 measurements either at the Earth's surface or in the entire atmosphere, derived from ground, tower, aircraft and satellite measurements [22, 24, 96, 115, 116]. Among the disadvantages of the method, one can highlight the high cost of measuring equipment and its dependence on weather conditions, which can significantly affect the number of quality measurements during the year. In addition, as will be shown below, the disadvantage of the method is the complexity of numerical models of atmospheric transport, which, for example, complicates the assessment of the error of the method.

Chapter 2. Estimation of anthropogenic CO_2 emissions in St Petersburg using a box model

2.1 Experimental estimate of CO_2 emissions as a sequence of solving inverse problems of atmospheric optics and atmospheric transport

Estimation of anthropogenic CO_2 emissions using data from measurements of gas content in the atmosphere, a priori information and an atmospheric transport model is an inverse problem that is ill-posed in the classical sense and in some studies is called the inverse atmospheric transport problem [117, 25, 118]. In addition, the inverse problem of atmospheric transfer is preceded by an ill-posed inverse problem of atmospheric optics, with the help of which the CO_2 content in the atmosphere is restored.

In a classical sense ill-posed problems are those which do not satisfy three conditions for a well-posed problem suggested by Hadamard. According to [119] these conditions can be formulated as follows:

1. every function f from the set F has a solution φ from the set Φ;
2. the solution φ is unique;
3. small changes of the function f correspond to small changes of the solution φ, i.e. the problem is stable.

Previously, it was believed that problems that did not fall under the Hadamard conditions of a well-posed problem could not be solved. However, in the 60s, the Soviet mathematician and geophysicist Andrei Nikolaevich Tikhonov formulated new conditions of well-posed problems, which made it possible to approximately solve inverse problems that are incorrect in the classical sense [120]. Conditions of well-posed problems according to Tikhonov can be formulated as in [119]:

1. it is a priori known that some functions f from the set F have solutions φ from the limited part of the Φ set (let's call it a subset M);
2. the solution φ is unique, but on the subset M;
3. small changes of the function f, which do not take the solution φ outside of the subset M, correspond to small changes of the solution φ.

With the advent of new non-classical Tikhonov conditions for well-posed problems, opportunities have emerged for solving a wide class of atmospheric optics problems and, as a consequence, atmospheric transport problems. Figure 1 presents a general diagram describing the main stages of solving inverse problems of atmospheric optics and atmospheric transport, which ultimately lead to the estimation of CO_2 emissions. This scheme combines the main stages of solving two inverse problems, which are described in many studies [24, 96, 112, 25, 121, 26]. Although we will focus on the inverse problem of atmospheric transport in what follows, a diagram of the inverse problem of atmospheric optics is presented to demonstrate the complexity of the procedure for determining CO_2 emissions from measurements.

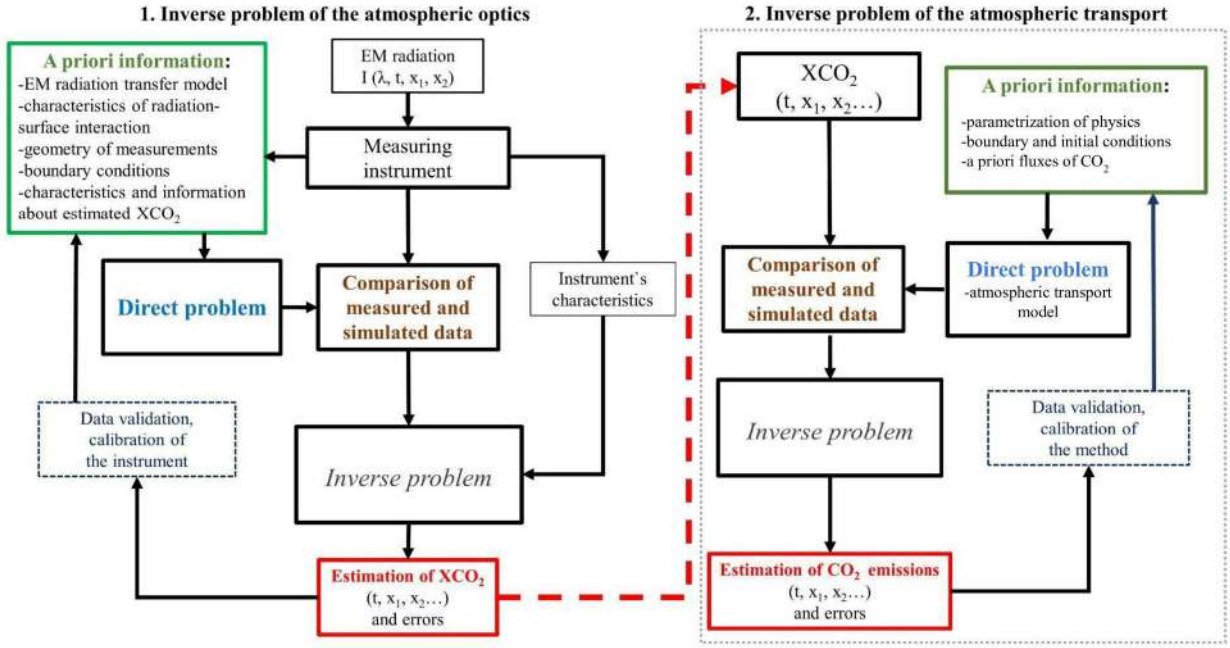

Figure 1: Scheme of inverse problems of atmospheric optics and atmospheric transport

Despite the fact that determining CO_2 emissions based on measured gas content and direct modeling of CO_2 transfer from sources is an inverse problem, today there is no general theory that would be used to solve it. Scientists use different mathematical algorithms, the main task of which is to minimize the difference between measured and simulated data constraining by a priori information (for example, the Bayesian approach described in [122]).

As can be noted from Figure 1, the method for determining anthropogenic CO_2 emissions by solving the inverse problem of atmospheric transfer is used not separately,

but together with the inventory approach. From an inverse problem perspective, inventory-based emissions data are a priori information that is often available with global coverage, high spatial resolution, and temporal variability (from interannual to daily). Using a priori information and a forward operator, which is a well-validated atmospheric transport model, one can transfer from CO_2 emissions to the spatiotemporal distribution of gas content in the atmosphere. By comparing model results with high-quality CO_2 measurements, a priori emissions are adjusted until differences between model results and measurements are minimized. Corrected emissions when the minimization condition is achieved are a solution to the inverse problem of atmospheric transfer. A priori information allows, firstly, to limit possible solutions, and secondly, it speeds up the process of finding a single solution. The method used is a relatively simple representation of the solution to the inverse problem, since, in addition, it is necessary to take into account the errors of modeling, a priori information and measurements, on which the errors of the estimated emissions depend.

Errors in solutions of classically ill-posed inverse problems strongly depend on the quality of the a priori information and direct operator used. The direct operator of the inverse problem of atmospheric optics is a well-studied and validated model of radiation transfer in the atmosphere. In turn, the direct operator of the inverse problem of atmospheric transfer is a model of the dynamics of the gas composition of the atmosphere (for example, the previously mentioned WRF-Chem). Such models are very complex, as they simulate many dynamic and chemical atmospheric processes that interact with each other.

Work [115] presents estimates of total CO_2 emissions from natural and anthropogenic sources for the entire Earth's surface for 2004-2006 in comparison with independent estimates based on the method of solving the inverse problem of atmospheric transfer. According to the study, estimates range from 12,000 to 13,000 Mt C y^{-1}, i.e. up to approximately 8% relative to the minimum estimate (random error). However, estimates of natural CO_2 emissions from solid surfaces differ from a priori ones in some cases by more than 100%. Work [121] shows that, depending on the choice of a priori natural CO_2 emissions, the random error in estimates can reach about

10% for the entire Earth's surface. Moreover, the obtained estimates for individual regions exceed the a priori ones by up to ~100% (for example, for the territory of Russia).

The Russian megapolis of St Petersburg is one of the largest industrial centers in the country. The city's population is more than 5 million people, and its area is ~1400 km^2. There are about ten combined thermal and power plants, many industrial enterprises in the city, and there is also high transport activity. It is obvious that St Petersburg is a major anthropogenic source of CO_2 in Russia and on the planet as a whole. A qualitative assessment of anthropogenic emissions from large cities is an important task, for example, to determine the total and regional annual contributions of Russia to CO_2 content, i.e. contributions to changes in radiative forcing of this gas.

Studies [24, 26] determine the total anthropogenic CO_2 emissions from the territory of St Petersburg based on spectroscopic measurements of the total gas content. It is shown that the atmospheric transport models used in these works lead to estimates of CO_2 emissions that differ by ~30% and more. According to [123, 124], differences in numerical models of atmospheric composition lead to even more significant differences in estimates of anthropogenic and natural CO_2 emissions, which reach ~50% and more.

The purpose of the current chapter is to estimate anthropogenic CO_2 emissions from St Petersburg based on solving the inverse problem of atmospheric transport using measurements of CO_2 total column (TC) and modeling atmospheric transport using a box model. The difference from the already carried out estimates of CO_2 emissions of St Petersburg in [22, 24, 26] is that current estimates will be given for the city area covered by the measurements of CO_2 TC.

2.2 Concept of the balance approach for estimating anthropogenic CO_2 emissions

The assessment of CO_2 emissions based on the balance approach is based on the condition that the number of gas molecules entering and leaving a certain volume must be equal, provided that there are no sources or sinks of CO_2 within this volume [125]. Thus, the non-zero difference between the number of CO_2 molecules entering and

leaving the volume will determine the presence and size of sources or sinks inside the volume.

The simplest use of the balance approach to estimate anthropogenic CO_2 emissions can be implemented using a box model of atmospheric transport and measurements of gas content in the atmosphere (Figure 2) [125]. Within the box model, a certain volume of the atmosphere with a fixed size is allocated. At the boundaries and inside the selected volume X, input parameters are set that describe the transport of air through the volume (for example, wind speed) and its change inside (the amount of solar radiation, sources and sinks of gases, gas and aerosol composition, etc.).

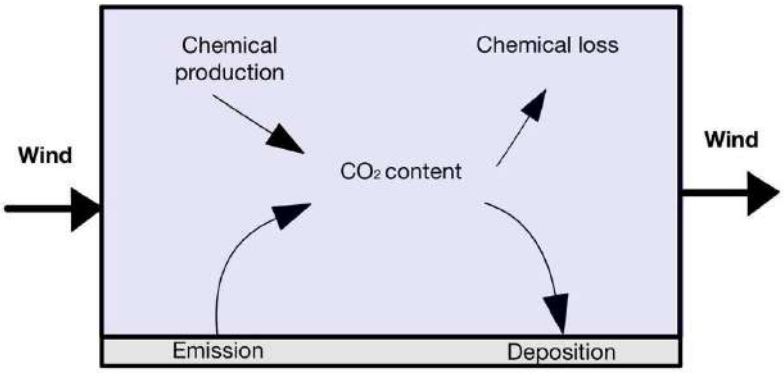

Figure 2: Schematic representation of the simplest box model of atmospheric transport in Euler form (image adapted from [125])

When considering the change within a given volume of a gas such as CO_2, several assumptions can be made to simplify the modeling of gas transport. Firstly, CO_2 is almost inert gas and usually when modeling changes in its content in the atmosphere, chemical reactions are not taken into account. In addition, the main sink of CO_2 at the city scale is vegetation during the growing season (approximately from mid-spring to mid-autumn) [126]. Accordingly, considering the dynamics of CO_2 content in months with weak plant activity, from the point of view of CO2 release and absorption, for the northern regions of Russia it can be assumed that vegetation makes almost no contribution to the gas content. Thus, to some approximation, we can assume that only anthropogenic activity is the source of CO_2 when a volume of air is transferred over a certain territory in a short period of time (several hours).

2.3 Data and methods

2.3.1 Differential spectroscopic method for determining anthropogenic CO_2 emissions

In recent years, a balance approach based on a box model has been implemented to estimate anthropogenic CO_2 emissions using remote spectroscopic measurements of electromagnetic radiation in the atmosphere. Using such measurements, it is possible to obtain information about the total (or total) content of CO_2 and other gases in the entire atmosphere. The main advantage of measurements of total CO_2 content (TC) in the atmosphere over local measurements is that they characterize the contribution of factors to the atmospheric CO_2 content at different altitudes [72].

It can be assumed that the study of CO_2 TC will lead to greater uncertainty in assessing the city's anthropogenic contribution to CO_2 content. However, in the last decade, the differential spectroscopic (hereinafter referred to as DS) method for assessing anthropogenic emissions of CO_2 and other greenhouse gases has been actively developing [72, 22, 24, 95, 26, 127, 128].

The essence of the DS method is based on simultaneous measurements of CO_2 in the windward and leeward parts of the city using inter-calibrated mobile spectrometers. Since ground-based spectroscopic measurements of TC characterize the volume of air covering the layers of the troposphere and stratosphere, then, in the case of CO_2, these measurements reflect the total influence of all main factors. These include atmospheric transport, biogenic impact, anthropogenic contribution, absorption of CO_2 by the water surface, biomass combustion, volcanic eruptions, etc. Accordingly, the difference between the CO_2 measurements of two mutually calibrated instruments in the windward and leeward parts of the city, under certain conditions, should highlight the influence of the city (anthropogenic contribution), reducing the influence of factors outside it. "Certain conditions" can be, for example, the state of the atmosphere with a slightly changing wind direction, high wind speed [127], as well as a relatively large sample of CO_2 measurements in the windward and leeward parts of the city. The first condition, if

we mentally remove the anthropogenic impact of the city, will ensure the transfer of background air mass similar in properties to the measurement points in the windward and leeward parts of the city. The second condition should reduce the residence time of the air mass in the city and reduce the degree of change in its physical properties under the influence of local features (for example, under the influence of the urban “heat island”). Finally, the third condition will ensure the reliability of conclusions about the measured contribution of the city to CO_2.

The advantages of this method are the high accuracy of CO_2 TC measurements, which is achieved through mutual calibration of instruments before measurements. Disadvantages include the limitation of measurements to daytime and cloudiness (when using solar radiation), as well as the relatively high cost of mobile spectrometers. Nevertheless, the differential method of emission estimation can be considered as a promising ground-based method for validating inventory and satellite methods for determining anthropogenic CO_2 emissions. For example, in Munich, a system for operational control of anthropogenic emissions was created, based on the DS method [129].

2.3.2 CO_2 TC measurements as part of the EMME campaign

In the period 2019-2020, in the large Russian megapolis of St Petersburg, scientists from St Petersburg State University and two German institutes - Karlsruhe Institute of Technology (Karlsruhe, Germany) and University of Bremen (Bremen, Germany) - conducted a joint project Emission Monitoring Mobile Experiment (EMME). One of the main goals of the project was to assess greenhouse gas emissions based on the DS method from the territory of St Petersburg. For this purpose, a pair of inter-calibrated IR Fourier spectrometers from Bruker model EM27/SUN was used. In the period from March to April 2019, parallel measurements of CO_2 and other greenhouse gases were carried out over 11 days in the windward (background) and leeward (polluted) parts of the city. To do this, the scientists of EMME campaign selected each day carefully using meteorological measurements, forecasts and

calculations of the numerical model of particle dispersion in the atmosphere HYSPLIT. Of the 11, only 9 days were selected by the EMME campaign participants for analysis, of which 4 were also selected as the best days for assessing anthropogenic CO_2 emissions. A description of the measurements performed, as well as measuring instruments, are presented in detail in [22]. The measurement results of the EMME campaign are presented on the website https://www.imk-asf.kit.edu/english/3884.php [last access 05.07.2023].

Subsequently, the resulting paired measurements were used to determine the anthropogenic contribution of St Petersburg to the CO_2 content (Δc) on a specific day. By solving the inverse problem, using a box model and Δc obtained as the difference between parallel measurements of CO_2, the authors of [22] estimated specific anthropogenic CO_2 emissions from the territory of St Petersburg and estimated errors. Thus, anthropogenic CO_2 emissions from a unit area of St Petersburg based on EMME measurements in 2019 are 89 kt km^{-2} y^{-1} with a variability of 28 kt km^{-2} y^{-1} based on nine days and 85 kt km^{-2} y^{-1} with a variability of 12 kt km^{-2} y^{-1} based on the 4 best days of measurements. Systematic and random errors are about 14 and 40%, respectively.

In [26], EMME measurements were used in conjunction with a one-dimensional box model of atmospheric transport to estimate the total anthropogenic CO_2 emissions of St Petersburg for 2019. According to the study, anthropogenic CO_2 emissions of St Petersburg in 2019 were ~65 Mt g^{-1} with an error of 20-40%.

The results of a more detailed study to assess the total CO_2 emissions of St Petersburg in 2019 and 2020 based on EMME measurements are presented in [24]. In contrast to [22, 26], the study [24] uses the HYSPLIT model of particle dispersion in the atmosphere. According to the study, the total emissions of St Petersburg in 2019 and 2020 are approximately 75.8 and 68.4 Mt y^{-1} with variability of 5.4 and 7.1 Mt y^{-1}, respectively. The authors point out that the estimates obtained more than double the emissions of the inventory databases for the territory of St Petersburg. In addition, the study provides an assessment of the total anthropogenic CO_2 emissions of St Petersburg based on measurements of the near-surface gas content. The resulting estimate is approximately 30% less than that based on the DS IR method. This finding supports

claims about the possible uncertainty in estimating CO_2 emissions based on local gas measurements.

As part of the EMME program in 2019, a pair of inter-calibrated Bruker EM27/SUN IR Fourier spectrometers was used [70, 130]. The devices measure the spectra of direct solar radiation in the IR wavelength range of 4000–12000 cm^{-1} with a spectral resolution of 0.5 cm^{-1}. Based on the measured solar spectra and the algorithm described in [70], the CO2 TC in a dry atmosphere was reconstructed. According to [70, 130, 71], the systematic and random errors of the reconstructed CO_2 content values based on Bruker EM27/SUN measurements reach ~0.5% and 0.025-0.075%, respectively. However, due to preliminary intercalibration between the two spectrometers and the use of the difference between them, the systematic differences are significantly reduced (on the order of 0.02%).

2.3.3 Box model of atmospheric transport

Let us write the equation of the box model in Lagrangian form (1). Unlike the Eulerian form, the Lagrangian approach considers the movement in space and time of a selected volume of air. According to (1), the concentration of CO_2 in a small volume transported over a certain territory depends only on emissions from the surface of this territory

$$E = u \times \frac{H^* \Delta c}{\Delta x} \qquad (1)$$

Here Δc - the total contribution of the territory over which a volume of air passes to the CO_2 concentration of a given volume; Δx - one of the horizontal dimensions of the allocated space along which the allocated volume of air moves; u - average wind speed (taken as a constant inside the volume); H - the height of an air volume.

Δc in the equation (1) can characterize the contribution of a city, for example St Petersburg, to the CO_2 content in a volume of air at height H. The height H may be, for example, the height of the Earth's boundary layer. Taking H into account in equation (1) is due to the fact that, in addition to ground sources, gas is transferred to the study area

from remote areas at different altitudes. In its simplest form, having only measurements of CO_2 content in a small volume of air (for example, obtained using a gas analyzer), when estimating emissions using a box model, it is assumed that the vertical distribution of gas content is the same within H. Accordingly, under conditions of highly heterogeneous CO_2 distribution altitude, emission estimates based on equation (1) and local measurements of gas content may have additional errors.

Having information about Δc and wind speed based on measurements, using equation (1) it is possible to estimate CO_2 emissions from the city. The balance approach, implemented using a box model in various approximations, has been used by scientists for several decades to estimate emissions of CO_2, as well as other climate- and environmentally important gases and aerosols. For example, [131] uses a simple box model together with paired measurements of gas and aerosol composition in the ground layer to analyze the impact of road works on ambient air quality in the London area, UK. Paired measurements characterized the content of pollutants in the windward and leeward parts of the road. Thus, under certain meteorological conditions, the difference between them can be interpreted as a contribution to the content of pollutants from processes occurring on the road itself (i.e., mainly emissions from cars and repair work). In [132], a box model, together with measurements at the Earth's surface, was used to estimate mercury emissions in Zurich, Switzerland. Unlike the previous study, instead of paired measurements, data from observations of mercury gases at a station in the city itself were used, as well as measurements in the background air of the peripheral part of the city, carried out in a separate non-overlapping period of time. This approach undoubtedly increases the error in emission estimates. Note that due to the locality of the measurements used to estimate emissions in both works, the assumption of weak vertical air mixing is used. For this purpose, for example, in the study [132] only days with temperature inversion in the surface layer were considered, i.e. with weak vertical air transfer. In the study [133], mobile spectroscopic measurements of NO_2 content in the troposphere are used in conjunction with a box model to estimate the total annual gas emissions from the territory of St Petersburg. According to the study results,

emission estimates vary significantly depending on the day of observation (almost 4 times relative to the minimum value).

Thanks to simultaneous remote spectroscopic measurements of CO_2 in the background and polluted air of St Petersburg, carried out as part of the EMME campaign, the value of the city's anthropogenic contribution to the gas content or Δc is estimated on a specific day. Considering that the main contribution to urban anthropogenic CO_2 emissions comes from stationary sources (for example, the network of thermal power plants in St Petersburg), we can assume that c depends on CO_2 emissions from the areas of distribution of air masses (hereinafter we will call such areas "paths"). Thus, Δc characterizes CO_2 emissions from certain parts of St Petersburg.

According to the box model equation (1), the measured value of Δc depends on the magnitude of local anthropogenic CO_2 emissions, wind speed and the length of the air mass movement path. In our approach, $\Delta c_{mod,\,i}$ is calculated from the box model equation (1) for a specific path of air mass movement (Δx_i) based on information about wind speed (u_i) and a priori CO2 emissions (E_i) (2). $\Delta c_{mod,\,i}$ characterizes the anthropogenic contribution of St Petersburg to the CO_2 content on the day i of EMME measurements based on modeling. Then, for each day i, the coefficient R_i is determined as the quotient between the measured and model Δc on these days (3). R is subsequently used to correct a priori anthropogenic CO_2 emissions on the territory of St Petersburg. Thus, R and subsequently adjusted a priori CO_2 emissions from the city will be a solution to the inverse problem of atmospheric transfer.

In contrast to (1), the variable H (height of the mixing layer) in equation (2) is not used explicitly here, since Δc characterizes the CO_2 content in the entire atmosphere and, thus, implicitly contains this parameter.

$$\Delta c_{mod,\,i} = \frac{E_i \Delta x_i}{u_i} \qquad (2)$$

$$R_i = \frac{\Delta c_{obs,i}}{\Delta c_{mod,i}} \quad (3)$$

To estimate $\Delta c_{mod,i}$, for each day of EMME measurements, different equations (2) with different input parameters are compiled. Figure 3 shows the positions of paired EMME measurements (connected by segments) together with a priori anthropogenic CO_2 emissions based on the ODIAC database for 2019. Note that with this consideration, one of the traces was repeated three times, since for the same pair of positions (A2-B2) CO_2 TC measurements were carried out on three different days. Thus, as a first approximation, no more than 5 noticeably different observation geometries are used.

Large anthropogenic sources of CO_2 are clearly visible in Figure 3 (11 dark green cells). Their position is in good agreement with the coordinates of the St Petersburg CHPs. According to ODIAC data for 2019, CO_2 emissions, which correlate with emissions from thermal power plants, are more than two orders of magnitude higher than all other anthropogenic gas emissions in the city and account for about 30% of total emissions.

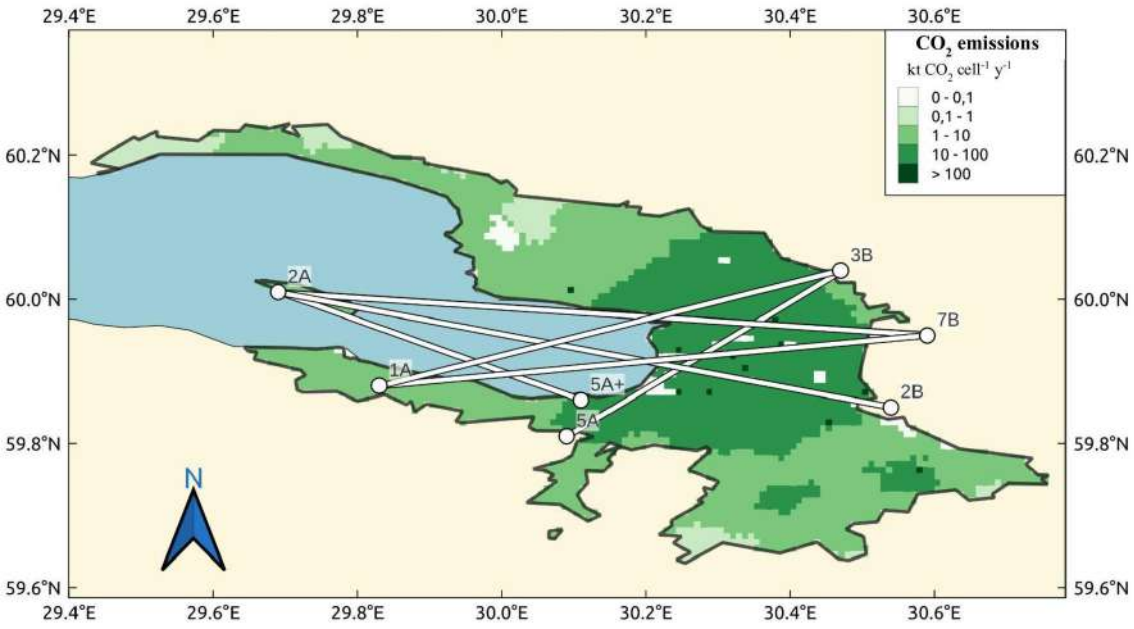

Figure 3: Anthropogenic CO_2 emissions in St Petersburg according to ODIAC data for 2019 and positions of paired CO_2 TC measurements within the framework of the EMME 2019 campaign.

The ODIAC inventory database for 2019 (E_i) is used as a priori information on the spatiotemporal distribution of anthropogenic CO_2 emissions in equation (2). The spatial resolution of ODIAC is ~1 km^2 on average for the entire earth's surface and ~0.43 km^2 for the territory of St Petersburg and its suburb [134].

The calculation results of the numerical weather forecast model WRF version 4.1.2 are used as wind speed data in (2). A numerical experiment using the WRF model was carried out in March-April 2019 with a spatial resolution of 8 km. Simulation data was output within an hour. Global forecast system (GFS) analysis data were used as initial and boundary conditions for WRF modeling (https://www.ncdc.noaa.gov/data-access/model-data/model-datasets/global-forcast-system-gfs). Wind speed values at the Earth's surface and the average in the 0-1350 m layer (a value close to the height of the Earth's boundary layer during the day) based on WRF modeling are used in the study.

In [26], straight lines connecting paired EMME measurements were taken as trajectories of air mass movements Δx from equation (2) (Figure 3). However, as, for example, noted in [22], the direction of the surface wind within the city may change to the opposite during the period of parallel measurements, i.e. within 3-4 hours.

To reduce the errors from a simple approximation of atmospheric air mass transport over a city and to define Δx In Equation (2), the STILT particle dispersion model [135] coupled with the WRF weather forecast model [105] (WRF-STILT) were used in the study. The details of using the WRF-STILT model will be discussed in the following chapters.

2.4 Uncertainty analysis of CO_2 emissions estimation using the DS method

Let us recall that when solving the inverse problem to estimate the total CO_2 emissions from the entire territory of St Petersburg, in studies [24, 26], a priori anthropogenic CO_2 emissions from the city territory were multiplied by correction factors calculated on the basis of the relationship between measured and model Δc (3). These multipliers, determined on specific days of EMME measurements (Figure 3),

were used to correct a priori anthropogenic CO_2 emissions from the entire territory of St Petersburg, and not from the city districts that make the greatest contribution to the measured CO_2 contents. However, these studies did not take into account the fact that the EMME campaign measurements mainly covered the central part of the city, where, according to ODIAC 2018 and 2019, the largest sources of anthropogenic CO_2 emissions are located. Accordingly, the use of correction factors obtained from EMME measurements and the box model (see Equations 2 and 3) to estimate total emissions from the city may lead to additional errors.

To quantify this factor, we present histograms that describe the distribution of anthropogenic CO_2 emissions from the ODIAC base throughout the entire territory of St Petersburg (Figure 4 a). In addition, three histograms of the distribution of emissions in the territories of St Petersburg covered by observations based on simplified straight-line traces during the measurement days of the EMME program in 2019 are presented (Figure 4 b). The histograms show the distribution of CO_2 emissions in relation to the total number of ODIAC data cells for the area of the entire city (Figure 4 a) and on selected simplified routes (Figure 3) - for 4, 7 and 9 days (Figure 4 b). Here we use ODIAC data for 2018, since this is the version used in [26]. 4, 7 and 9 days correspond to the measurement days of the EMME campaign, the data of which were used in [22, 24, 26].

From the presented histograms we can conclude that, according to ODIAC data, most of the territory of St Petersburg (Figure 4a) is occupied by CO_2 emissions with values less than ~20 kt km^{-2} $year^{-1}$. In turn, the smallest part of the city is occupied by emissions with values of more than ~40 kt km^{-2} $year^{-1}$. The areas covered by simplified air transport paths on EMME measurement days (Figure 4 b) mainly cover high emission values - from 15 to 55 kt km^{-2} $year^{-1}$.

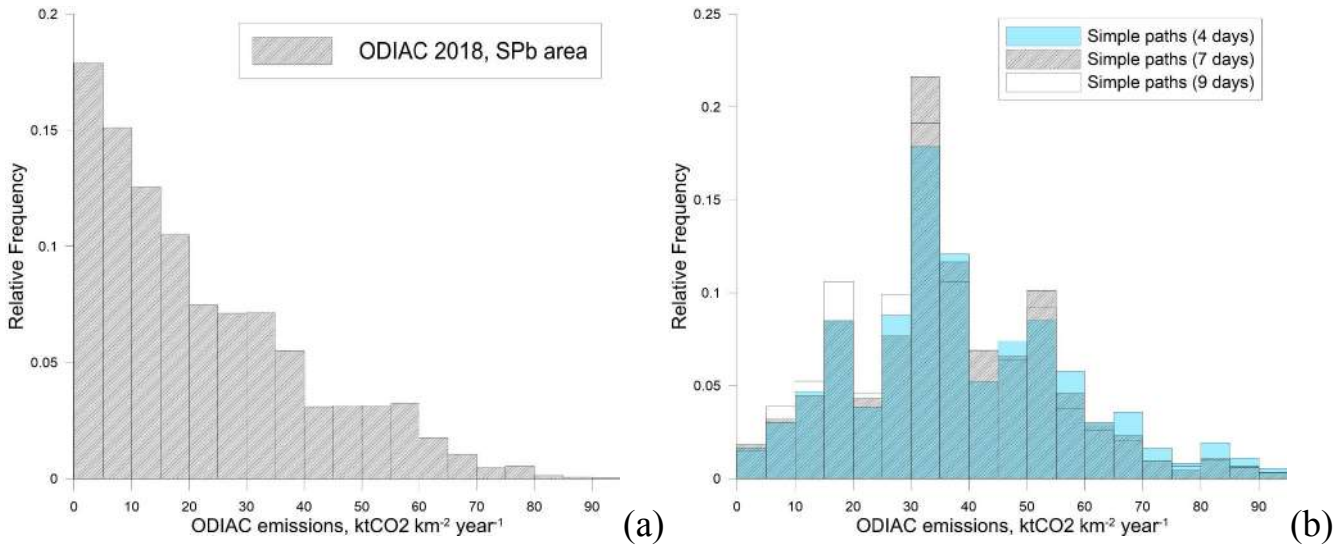

Figure 4: Histogram of the distribution of CO_2 emissions according to ODIAC data for 2018 on the entire territory of St Petersburg (a) and in the territories of straight air mass routes (b) with a width of 1 km on the days of EMME measurements.

Thus, systematic errors in determining the total anthropogenic CO_2 emissions of St Petersburg based on EMME measurements in 2019 [24, 26] and expressions (2) and (3) may be due to the fact that the measurements covered mainly parts of the city with very high specific CO_2 emissions.

Let's consider a simple example illustrating the influence of this factor. Let us assume that ODIAC data correctly describe the spatial distribution of anthropogenic CO_2 emissions in St Petersburg. In this case, the average specific CO_2 emissions according to ODIAC data for 2018 for the entire territory of St Petersburg, whose area is ~1400 km^2, are ~21.6 kt km^{-2} $year^{-1}$. Hence, by multiplying this specific emission value by the city area, we obtain the "true" value of the total CO_2 emission of St Petersburg. For the central part of the city with the highest CO_2 emissions according to ODIAC data (Figure 4, area ~1000 km^2), the average specific emission is approximately 28.8 kt km^{-2} $year^{-1}$. This is approximately 30% more than the average specific CO_2 emissions of the entire city. Accordingly, multiplying this value by the area of the entire city, we obtain an overestimate of the total anthropogenic CO_2 emissions of St Petersburg by 30% (relative to the "true" total emission).

Accordingly, the question arises: how is it possible to take this factor into account when estimating anthropogenic CO_2 emissions from the territory of St Petersburg, using paired DS IR measurements and a simple box model?

We propose an approach that consists in assessing anthropogenic CO_2 emissions only for the territories of St Petersburg covered by EMME measurements. It is proposed to cover the remaining areas of the city with a priori information - the ODIAC database for 2019. Equation (4) describes a new approach for estimating the total anthropogenic CO_2 emissions from the entire city. In (4), $\overline{R}$ is the average correction factor based on all EMME measurement days used; E_c - a priori anthropogenic CO_2 emissions from the territory of St Petersburg, covered by EMME measurements; E_{nc} - a priori anthropogenic CO_2 emissions from the territory of St Petersburg, not covered by EMME measurements.

$$\overline{E_s} = \overline{R} * E_c + E_{nc} \quad (4)$$

2.5 Assessment of the territory of St Petersburg covered by EMME measurements

In addition to modeling the trajectory of air mass movement, using the WRF-STILT model it is possible to estimate the spatiotemporal distribution of the contribution of St Petersburg to the CO_2 content based on EMME measurements. Let's imagine that in the St Petersburg area, on one of the observation days of the EMME campaign, a measurement of CO_2 was carried out in the leeward (polluted) part of the city x_{ri}, y_{rj} (point A). Having parallel measurements in the windward (background) part of the city (point B) and the direction of atmospheric transfer from A to B, we can describe the anthropogenic contribution of St Petersburg to the CO_2 TC as a function of time $\Delta c(t_m)$. The value of Δc at the measuring station x_{ri}, y_{rj} at point A at a certain time t_m depends on the transfer of CO_2 molecules from the territory remote from the station, which includes St Petersburg. If we trace where each of the particles, component Δc, moved to the measuring station x_{ri}, y_{rj} by the time t_m and at the same time mentally draw the trajectories of their movement on the geographical projection of the Earth, then on this projection the trajectories will form an area passing over the city and expanding deeper into the city, away from the measuring station. If we divide each trajectory into

segments that the particles covered per unit of time (for example, an hour), then it turns out that the lengths of the segments change. These two phenomena are associated with the fact that the speed and direction of the wind in space (including within the city) is constantly changing. If we assume that the measured Δc at time t_m depends only on the anthropogenic emissions of CO_2 sources in St Petersburg and the rate of particle transfer above them, then the residence time of particles in certain areas of the city will be a characteristic that describes the influence of specific parts of the city on the measured anthropogenic contribution Δc to point x_{ri}, y_{rj}.

The WRF-STILT model allows us to determine this characteristic based on the calculation of the time-reverse transport of particles in the atmosphere. In this study, using this model, numerical experiments were carried out on the transfer of particles back in time during the measurement days of EMME 2019. Thus, information was obtained on the spatiotemporal distribution of particles arriving at the leeward measurement point.

To model the transport of particles in space, meteorological data are used based on the high spatial resolution numerical weather prediction model WRF. WRF-STILT simulated the transport of 2000 particles from downwind EMME measurement sites separately for each of the nine campaign days. As part of the numerical experiments, particles moved back in time for 6 hours from 10 UTC, distributing throughout the territory of St Petersburg to an altitude of about 1500 m. Numerical experiments were carried out for each day of EMME measurements.

Then, based on the obtained model information, the parameter $f\left(x_i, y_{j,} t_m\right)$ was calculated by the model using equation (5). The variable f was determined for the windward space, relative to the measuring station $x_i, y_{j,}$, based on the total time (Δt) during which the model particles (p) arriving at the measuring station were in one or another part of space. Units of f are ppm μmol^{-1} m^2 s. Thus, the set of f values reflects the potential contribution of the windward part of the city to the measured Δc at a particular time t_m.

$$f\left(x_i, y_j, t_m\right) = \frac{m_{air}}{h\bar{\rho}(x_i, y_j, t_m)} \frac{1}{N_{tot}} \sum_{p=1}^{N_{tot}} \Delta t_{p,i,j,k} \quad (5)$$

In the equation (5) $\bar{\rho}$ – mean air density in the windward area of the city, relative to measurements; h – the height up to which the effect of the windward area of the city on particles released from the measurement point is taken into account; m_{air} – molar mass of air; N_{tot} – number of model particles released from the position of a measurement site (2000 in this study); x_r, t_r – position and time of measurements (or, in other words, the period from which the simulation of particle transport back in time was carried out); x_i, y_j, - the location to which the particles were transported back in time to the time t_m (for example, the position of the measurements).

However, f does not take into account the influence of anthropogenic CO_2 emissions on Δc. To correct this, we use expression (6). In it, the parameter $\Delta C_{m,i,j}$ [ppm] is calculated as the product of a set of values f [ppm μmol^{-1} m^2 s] and the corresponding territorial a priori emissions of CO_2 E [μmol m^{-2} s^{-1}]. The parameter $\Delta C_{m,i,j}$ characterizes the contribution of the windward part of the city to the anthropogenic contribution Δc at the measurement location x_i, y_j. It depends on the residence time of particles over specific areas of the city and on the spatial distribution and magnitude of a priori CO_2 emissions. For example, at high values of f, but at small or absent emissions E, $\Delta C_{m,i,j}$ will also be small or equal to zero, respectively, and vice versa. Thus, we can consider that the spatial distribution of the values of $\Delta C_{m,i,j}$ on a certain day of EMME measurements is a characteristic of the contribution of a particular part of the city to the measured Δc. Hence, by using the described method, it is possible to estimate the spatial coverage of EMME measurements on a specific day.

$$\Delta C(x_r, t_r) = f\left(x_i, y_i, t_m\right) E(x_i, y_i, t_m) \quad (6)$$

Figure 5 shows the values of $\Delta C_{m,i,j}(x_r, t_r)$ for the period of nine days of EMME 2019 measurements in percentage. The data are normalized relative to the total value of

$\Delta C_{m,i,j}(x_r, t_r)$ on the territory of St Petersburg for each day separately. The spatial distribution $\Delta C(x_r, t_r)$ (colored area) characterizes, according to the WRF-STILT model, the metropolitan areas that have the main influence on the formation of the measured anthropogenic contribution of the city to the CO_2 environment on each specific day. Also there are straight lines on the images which are connecting the positions of parallel measurements and characterizing the simplified movement of the air mass that day. In Figure 5, only the values of $\Delta C_{m,i,j}(x_r, t_r)$ are shown, which influence the total anthropogenic contribution by more than 0.01%.

Analysis of the city areas responsible for the formation of the anthropogenic contribution of St Petersburg based on modeling data indicates that the measurement of background and polluted CO_2 content on some days was carried out relative to different air masses (April 3, 4, 16 and 25). Accordingly, the use of EMME measurements that were obtained on these days and the box model (2) to estimate anthropogenic emissions in St Petersburg assumes a horizontal homogeneous distribution of CO_2 content in the air mass approaching the city from different directions.

In some cases, a straight line approximates air movement quite well (for example, March 21 and 27, April 1, 6 and 24), but in others it greatly simplifies the actual nature of the movement (for example, April 16 and 25). Apparently, on April 16 and 25, a difficult meteorological situation was observed, due to which $\Delta C_{m,i,j}(x_r, t_r)$, according to modeling data, is concentrated in one small area, and does not “stretch” across the city, as in other days. An analysis of the wind direction based on measurements from a weather station on the roof of the Physics Faculty of St Petersburg State University in Peterhof showed that on both days the wind direction at the Earth’s surface changed almost to the opposite. At the same time, the WRF model has large errors in modeling the direction of the surface wind on these two days (in some hours up to almost 180°). These facts may indicate that, firstly, measurements these days should not be used to assess the anthropogenic contribution in our study. Secondly, this may mean that difficulties in modeling the observed meteorological situation also lead to difficulties in interpreting measurements using numerical simulation.

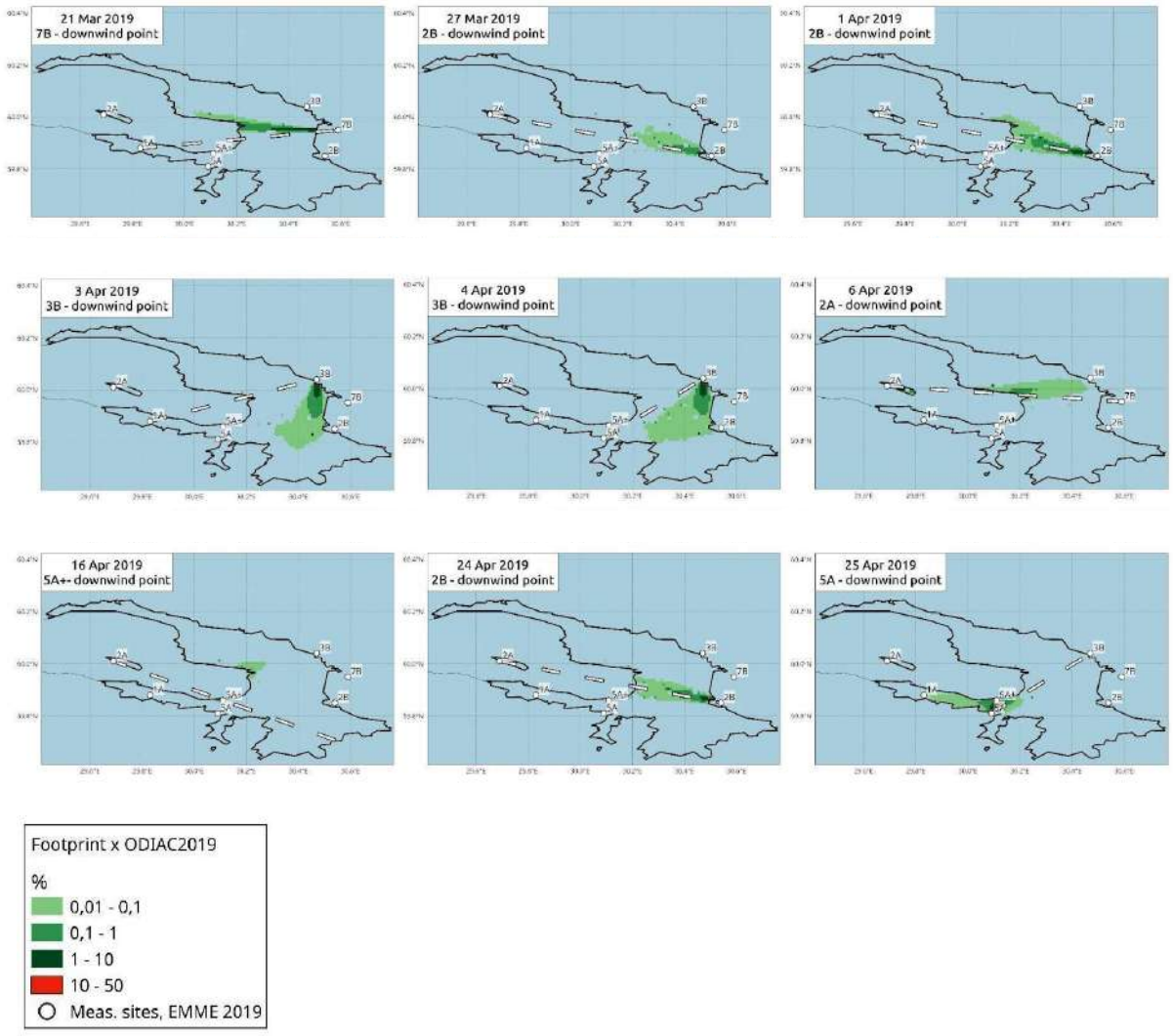

Figure 5: Spatial distribution of areas of formation of the St Petersburg anthropogenic contribution on different measurement days of the EMME 2019 program according to the WRF-STILT model ($\Delta C_{m,i,j}$)

Next, $\Delta C_{m,i,j}(x_r, t_r)$ were combined on certain days to estimate which part of the city is predominantly covered by EMME measurements. Figure 6 shows the total contribution of windward regions to the Δc EMME 2019 measurements for 7 (excluding April 16 and 25) and 5 (excluding April 3, 4, 16, 25) observation days based on the WRF-STILT simulation. The contribution in each individual cell is presented as a percentage relative to the total total contribution in the entire city for 7 days.

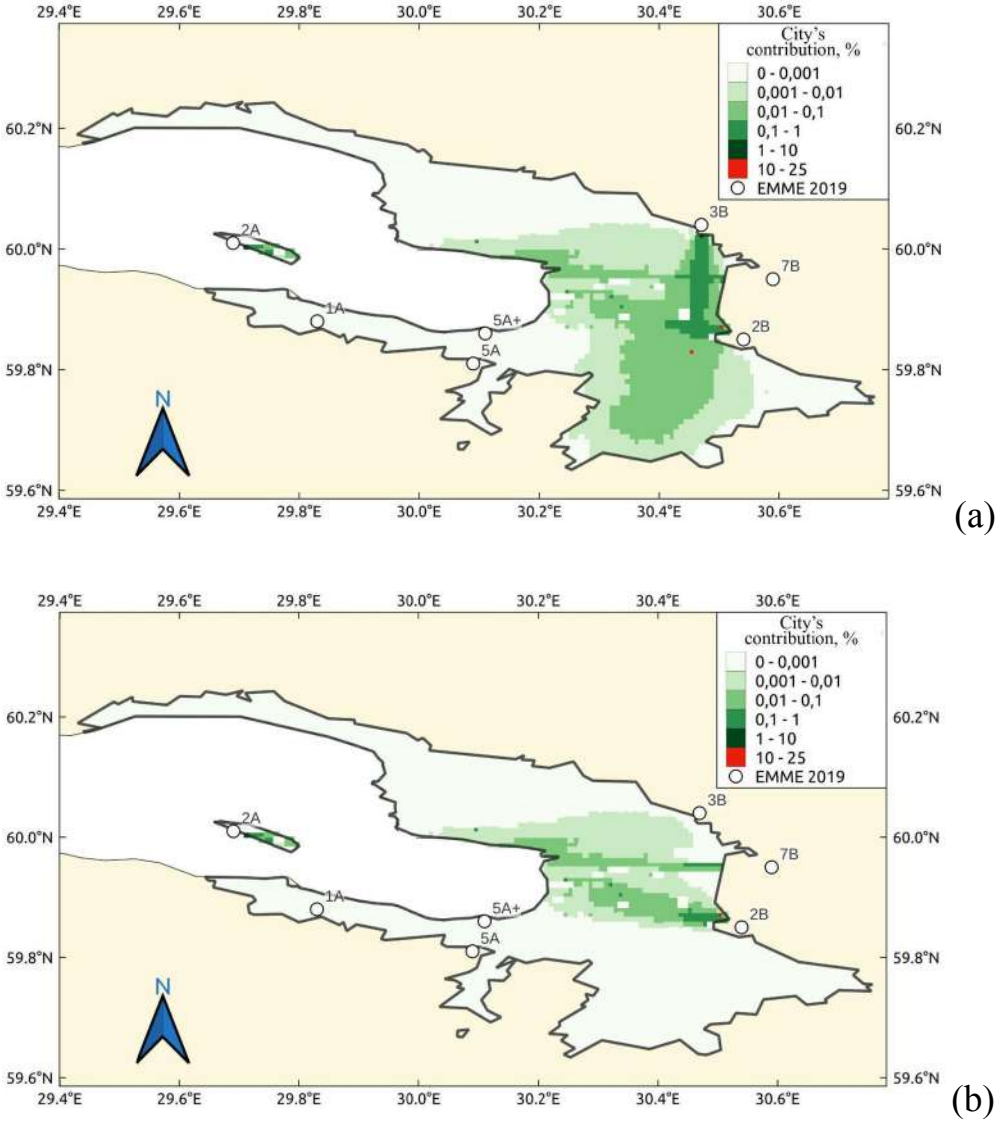

Figure 6: The region of St Petersburg, forming the anthropogenic contribution for 7 (a) and 5 (b) days of measurements of the EMME program in 2019

According to Figure 6 "a", over 7 days of EMME measurements, the largest area of the city is occupied by areas with anthropogenic influence in the range of 0-0.01%. However, their total impact is only ~3.3% of the total anthropogenic contribution for all 7 days. Next in terms of the size of the occupied area follow the values in the range of 0.01-0.1%, which amount to ~20.4% of the total anthropogenic contribution of St Petersburg (the center and south of the city). The area with the greatest impact (~76.3%) on the anthropogenic contribution of St Petersburg has a range of values 1-21% (25% in the legend) and occupies a very small area to the east of the city center. From Figure 6 "b" for 5 days of EMME measurements, we only note that the territorial coverage of the city's anthropogenic contribution is approximately two times smaller than for 7 days.

Since the regions of St Petersburg highlighted in Figure 6, according to the modeling data, characterize the part of the city with the greatest contribution to the measured values of Δc, we can say that these regions characterize the coverage of the city by EMME measurements for 7 and 5 days. From Figure 6 “a" it is clear that 7 days of measurements cover about half of the territory of St Petersburg and most combined heat and power plants. This is likely due to careful planning of measurements as well as meteorological conditions during the day. Thus, depending on meteorological conditions, the measured value of Δc is due to transfer from different parts of St Petersburg. According to Figures 3 and 6, measurements for 7 days do not cover that part of the city where, according to ODIAC 2019 data, specific CO_2 emissions are at least an order of magnitude lower than in the area covered by measurements. However, the total CO_2 emissions from the area not covered by measurements is approximately 50% of the total emissions of St Petersburg. In turn, 5 days of measurements cover approximately half the area of the city and mainly in the north. In this case, according to ODIAC, CO_2 emissions of St Petersburg, which are not covered by measurements, amount to more than 60% of the total emissions of the city.

2.6 Estimation of anthropogenic CO_2 emissions by differential spectroscopic method

Let's estimate the total anthropogenic CO_2 emissions of St Petersburg in 2019 based on DS IR measurements of the city's anthropogenic contribution, a priori anthropogenic CO_2 emissions from ODIAC data and the box model (2). Note that in this and other studies cited, the estimation of anthropogenic CO_2 emissions is given for the entire year 2019, despite the fact that the EMME campaign measurements were carried out over several days in March and April 2019. This approximation is put forward due to the small change in anthropogenic CO_2 emissions from month to month based on the 2019 ODIAC inventory database. Thus, the largest total difference between CO_2 emissions from the territory of St Petersburg per month is no more than 2% of the total

annual emissions of the city. As will be shown below, these 2% lie within the error of the estimation of CO_2 anthropogenic emissions.

2.6.1 Modeling the anthropogenic contribution of St Petersburg to CO_2 using a box model

To further correct a priori CO_2 emissions and new estimates of total anthropogenic CO_2 emissions in St Petersburg, we will use the box model of atmospheric transfer (equation 2). We use five days of measurements in which, according to WRF-STILT modeling, the approximate air mass transfer can be approximated by a straight line - March 21 and 27, April 1, 6 and 24. As mentioned earlier, measurements of background and polluted CO2 TCs on the four remaining days (April 3, 4, 16 and 25) may refer to different air masses, so the Δc values found on their basis probably have more uncertainty and are not used here to assess anthropogenic CO_2 emissions.

Using a priori anthropogenic CO_2 emissions along the approximate path of air mass movement according to WRF-STILT data, information on wind speed from the results of WRF numerical modeling and the box model (2), the difference in CO_2 TC measurements in the windward and leeward parts of St Petersburg was simulated. Table 1 shows the dates of the five days (first column); estimates of total anthropogenic CO_2 emissions from the path of air masses according to ODIAC data for 2018 and 2019 (second column); wind speeds at the Earth's surface and average in the 0-1350 m layer (third and fifth columns); model estimates of the anthropogenic contribution of St Petersburg in the form of $dTCCO_2$ [mol. cm^{-2}], obtained using the box model, at different wind speeds (fourth and sixth columns); $dTCCO_2$ according to EMME measurements in 2019 (seventh column).

According to the analysis, total anthropogenic emissions based on ODIAC 2018 data are significantly less than ODIAC 2019 (almost 3 times as of April 1). The exception is April 6, which is a reflection of the spatial heterogeneity of the refinements made in the ODIAC 2019 database. Note that $dTCCO_2$ from the city territory based on modeling, ODIAC 2019 data and using surface wind speed, has a better agreement with

measurements (not taking into account 6 - April), however, on 3 out of 5 days the measured values are overestimated. When using average wind speeds in the layer up to 1350 m, the average difference between model data and measurements increases, and on all days the model underestimates $dTCCO_2$ based on measurements. It is worth highlighting the case of April 6, when the model value was more than 4 times less than the measured value. In turn, the average deviation of the model $dTCCO_2$ according to ODIAC 2018 data in relation to measurements turned out to be less by about 34% when using surface wind speed and by more than 100% when using average speeds in a layer up to 1350 m.

Table 1: Differences between CO_2 TC ($dTCCO_2$) in the windward and leeward parts of St Petersburg for 5 days in March and April 2019 based on the box model (for ODIAC 2018 and 2019) and EMME measurements in 2019; $dTCCO_2$ in [mol. cm^{-2} 10^{19}]; WS (wind speed) in [m s^{-1}] near the surface (a) and averaged in a layer 0-1350 m (b).

Date	**ODIAC, $MtCO_2$ y^{-1} (2018/2019)**	**Mean WS (~30 m)**	**WRF-STILT $dTCCO_2$ a**	**Mean WS (0-1350 m)**	**WRF-STILT $dTCCO_2$ b**	**$dTCCO_2$ (EMME)**
21.03	3.7/7.09	7.2	0.56/1.07	11.2	0.36/0.69	1.13
27.03	8.0/14.3	3.2	1.09/1.95	7	0.5/0.89	1.67
01.04	6.2/15.2	6.4	0.6/1.48	10.5	0.37/0.9	0.98
06.04	2.9/3.1	3.6	0.87/0.93	5.4	0.58/0.62	4.24
24.04	5.2/12.8	2.6	1.3/3.3	5.9	0.59/1.45	2.2

2.6.2 Estimates of total CO_2 anthropogenic emissions of St Petersburg

Using calculations of $dTCCO_2$ by the box model and subsequently equations (3) and (4), we estimated the correction factor R and the total CO_2 anthropogenic emissions of St Petersburg for 2019. Let us recall that the correction of anthropogenic CO_2

emissions is performed only for the part of the city that, according to the WRF-STILT model, is covered by EMME measurements (more than 0.001%, see Figure 6 “b”). New estimates of CO_2 anthropogenic emissions from St Petersburg in 2019, obtained using method (4), based on various a priori information and approximations, are given in Table 2.

According to the analysis, a change in the methodology for solving the inverse problem, without changing other features of the interpretation of measurements, led to a noticeable decrease in estimates of anthropogenic emissions - from 65 Mt y^{-1} [26] to 46 Mt y^{-1}. Hence, the decrease was ~30%, which is close to the estimate of errors in CO_2 emissions due to the coverage of predominantly the central part of St Petersburg by EMME measurements [26]. Variations in a priori anthropogenic emissions, wind speed and the type of considering of the measurements on certain days (three similar measurement geometries - March 27, April 1 and 24) lead to significant changes in anthropogenic emissions estimates from 46 to 105 Mt y^{-1} with a standard deviation or random error of 19 Mt y^{-1}. The resulting total CO_2 emissions of St Petersburg are on average 2.3 and 1.4 times higher than emissions based on the ODIAC inventory database for 2018 and 2019. A change in a priori information from 2018 to 2019 leads to an increase in estimates of anthropogenic CO_2 emissions using the proposed methodology by approximately 50%. This is due to the difference between the total CO_2 emissions of St Petersburg according to ODIAC data for 2018 and 2019.

Correction of anthropogenic CO_2 emissions in St Petersburg, by multiplying a priori ODIAC data for 2019 from the entire city, as in an early study [26], leads to an increase in estimates from Table 2 by ~22-55% (not shown in the table).

At the same time, the final value of the total anthropogenic CO_2 emissions of St Petersburg in 2019 based on the current method can be given as 91±19 Mt y^{-1}. It was obtained as the average between estimates based on the box model, ODIAC database for 2019 and the average wind speed in the 0-1350 m layer. The results and methods of this study are presented in [25].

Table 2: Estimates of CO_2 anthropogenic emissions of St Petersburg for 2019 (except ODIAC 2018) based on a priori (ODIAC) and adjusted data; WS_{surf} and WS_{avg} – wind speed at the Earth's surface and average in the 0-1350 m layer according to ERA5 reanalysis data.

Special conditions of estimation		**Total CO_2 anthropogenic emissions of St Petersburg, Mt y^{-1}**	
A priori emissions of CO_2		ODIAC 2018	ODIAC 2019
		31	49
Three separate sets of measurements for A2-B2 path	WS_{surf}	46	63
	WS_{avg}	66	88
Mean by three sets of measurements fo A2-B2 path	WS_{surf}	52	76
	WS_{avg}	72	105

2.7 Main results and conclusion

In the current chapter it was shown that:

1. The accuracy of estimating anthropogenic CO_2 emissions from the territories of large cities based on solving the inverse problem of atmospheric transfer depends on many factors. These include the number and errors of measurements of CO_2 content in the atmosphere, spatial coverage of measurements, the complexity of the atmospheric transport model, the quality of a priori information, etc.

2. When assessing the total anthropogenic CO_2 emissions of St Petersburg using the DS IR method and a one-dimensional box model of atmospheric transport, the geometry and number of measurements are important. Large systematic errors in estimates of total emissions can be caused by such factors as strong spatial heterogeneity of anthropogenic specific CO_2 emissions in the city; using measurements in limited areas of the city; differences in a priori anthropogenic CO_2 emissions.

3. The proposed method for solving the inverse problem of atmospheric transfer for estimating the total anthropogenic CO_2 emissions of St Petersburg, taking into

account the spatial coverage of the city territory by measurements, presents the values of anthropogenic CO_2 emissions for 2019 in the range of 52–105 Mt y^{-1}. This wide range is due to the use of different wind speeds as well as prior CO_2 emissions in the box model. Correction of anthropogenic CO_2 emissions using the old method, i.e. throughout St Petersburg, leads to an increase in estimates by ~22-55%.

The assessment of the total anthropogenic CO_2 emission of St Petersburg for 2019 based on the current method is 91±19 Mt y^{-1} and was obtained as the average between estimates based on the ODIAC database for 2019 and the average wind speed in the 0-1350 m layer.

Chapter 3. Validation of WRF-Chem modelling of CO_2 transport in St Petersburg using in situ and remote measurements

3.1 Three-dimensional modelling of CO_2 transport in the atmosphere

In the previous chapter, the inverse problem of estimating anthropogenic CO_2 emissions from St Petersburg is solved using a very simple one-dimensional box model of atmospheric transport. We point out that the use of this model is justified in the case of relatively small spatial scales (kilometers and tens of kilometers) and little changes of meteorological conditions during the period of paired DS measurements. In addition, a condition for using the box model is the direction of air mass transfer from the windward measurement position to the leeward one. In this case, the difference between measurements with greater confidence should minimize the influence of other factors on the measured signal and highlight the contribution of CO_2 emissions from the city. However, if it is impossible to carry out measurements under such conditions, for the subsequent interpretation of the anthropogenic contribution of the city to CO_2 content, another class of numerical models of atmospheric transport should be considered. One of these is a three-dimensional numerical model of weather prediction and composition of the troposphere and lower stratosphere with high spatial resolution WRF-Chem (Weather Research and Forecast - Chemistry) [106]. It has been used for many years for research in a wide range of atmospheric sciences.

The uncertainties in modeling tropospheric CO_2 transport using WRF-Chem are being studied by many scientists. For example, in [136], the average CO_2 content in the troposphere (XCO_2) based on WRF-Chem modeling and measurements with a Bruker 125HR IR Fourier spectrometer in the area of Saint-Denis (France, Reunion Island, Indian Ocean) for a period of more than a year have an mean difference (MD) and standard deviation of the difference (SDD) of about -0.09 and 0.2%, respectively, with a high correlation coefficient of 0.9. In [23], similar studies were carried out in Berlin (Germany) using a series of mobile Bruker EM27/SUN Fourier transform spectrometers

over a period of about a month. In this case, the MD between the measured and model values of XCO_2 is 0.2-0.5%.

In work [137], to analyze the quality of the WRF-Chem numerical model to simulate the transport of CO_2 on the territory of St Petersburg, local measurements of the surface mixture ratio of this gas, obtained using the equipment of the resource center of St Petersburg State University “Geomodel” are used. However, the main disadvantage of this approach for model validation is that the CO_2 content near the Earth's surface characterizes a small volume of air. Therefore, from such data it is possible to obtain information about anthropogenic CO_2 emissions only under certain meteorological conditions, i.e. this validation is not enough. In turn, the average gas mixing ratio in the layer from the Earth’s surface to a given height in the atmosphere or XCO_2 characterizes all factors influencing the CO_2 content in the layer under consideration (for example, anthropogenic sources, horizontal and vertical transport, biogenic contribution, etc.). Thus, the study [138] showed that the MD and SDD between WRF-Chem modeling data and XCO_2 measurements in the St Petersburg region are -1 and 0.5% before correction of chemical boundary conditions and -0.6 and 0.5% after the correction.

Adapting the model to the conditions of St Petersburg and the surrounding area is an important task also because of the possible influence of vegetation on the CO_2 content during the growing season. Thus, St Petersburg borders on large forested areas located both on the territory of the Leningrad region and in the neighboring country - Finland [139].

The aim of this chapter of the dissertation is a comprehensive assessment of the ability of the three-dimensional numerical model WRF-Chem to describe spatiotemporal changes in CO_2 content in St Petersburg over a period of about a year. The assessment is carried out based on a comparison of the WRF-Chem modeling results with measurements of the state of the atmosphere and CO_2 content on the territory of St Petersburg and border areas, including the southern part of Finland. The agreement of the WRF-Chem model results with independent simulation data is also analyzed.

Let us recall that adapting the model and validating its ability to simulate the transport of CO_2 in the atmosphere is an important step in solving the inverse problem of atmospheric transport, since the solution of the inverse problem (i.e. assessments of anthropogenic CO_2 emissions) strongly depends on the quality of the direct operator (numerical model of atmospheric transport).

3.2 Measurements of CO_2 content and atmospheric state

On the territory of St Petersburg in Peterhof in 2019-2020, measurements of the total CO_2 content in the atmosphere were carried out. The measuring station is based at the Faculty of Physics of St Petersburg State University (SPbU, 59.88°N, 29.83°E). Peterhof is located approximately 25 km from the center of St Petersburg, being part of it. It is located in a slightly urbanized part of the city and is surrounded mainly by mixed forest and fields. On the territory of Peterhof and the adjacent territory there are no large stationary sources of CO_2, in contrast to the central part of St Petersburg.

Scientists at the Finnish Meteorological Institute (FMI, Helsinki, Finland) and the University of Helsinki (UHEL) (60.20°N, 24.96°E) are making observations of near-surface CO_2 content and many other atmospheric parameters from the roof of the institute [140]. The measurement site is located in a partially urbanized area of the city of Helsinki, which is surrounded by roads, parks, gardens, forest areas, and mainly administrative buildings. The predominant type of vegetation in the area is mixed forest. Due to the relative proximity of Helsinki and St Petersburg (about 330 km) and similar climatic features of these regions, measurements from the Helsinki station are used in the study to further validate the modeling data for surface CO_2 transport.

Also, to adapt the model of biogenic CO_2 fluxes, data on CO2 emissions and absorption by vegetation obtained during measurements at a Finnish background station are used. The station is located away from the anthropogenic influence of Helsinki in southern Finland and is surrounded predominantly by coniferous forests.

In addition to information on the gas content in the atmosphere, to validate the WRF-Chem CO_2 transport modeling, measurement data of the most important for

atmospheric transport meteorological parameters - wind speed and direction - are used. Meteorological measurements are carried out both in Peterhof on the basis of St Petersburg State University, and in Helsinki on the basis of FMI and UHEL. Below there are the characteristics of the instruments and descriptions of the measurements used in the study to validate the WRF-Chem simulation data.

3.2.1 Meteorological parameters

Regular measurements of meteorological parameters, including wind speed and direction, near the Earth's surface are carried out in Peterhof, at the Faculty of Physics of SPbU. Measurements are performed using the Weather station WXT536 on the roof of the Physics Department (height ~18-20 m) and are available at the output approximately every 10 seconds (https://www.campbellsci.com.au/wxt536). The measuring device was provided by the resource center (RC) of SPbU "Geomodel".

Measurements of wind speed and direction near the Earth's surface in Helsinki are carried out at the SMEAR III Kumpula station, which is located on the premises of the UHEL Faculty of Physics. The meteorological measurements themselves are carried out on the roof of the faculty at a height of approximately 30 m above ground level (https://www.atm.helsinki.fi/smear/index.php/smear-iii/measurements). Wind speed and direction are measured using a Vaisala WAA141 weather station, while air temperature measurements are taken using a Pt100 thermometer. The data is obtained from https://smear.avaa.csc.fi and is available every 1 minute.

In Voeikovo (Leningrad region), aerological measurements of vertical profiles of such meteorological parameters as wind speed and direction, air temperature, etc. are carried out at 0 and 12 UTC. Measurements are performed from the ground to altitudes of ~30 km. Upper air data are freely available at http://weather.uwyo.edu/upperair/sounding.html.

To compare the measured profiles of meteorological parameters with the WRF-Chem numerical simulation data, the model profiles are linearly interpolated to the measured pressure profiles to altitudes of about 50 hPa or ~20 km (the upper limit of

the WRF-Chem simulation data). Figure 7 shows the examples of vertical profiles of air temperature, wind speed and direction according to measurements and modeling by WRF-Chem (before and after interpolation to the measured profile) in Voeykovo for 19 Dec 2019 12 UTC. From the examples it is clear that the interpolated model profile differs little from the original model profile.

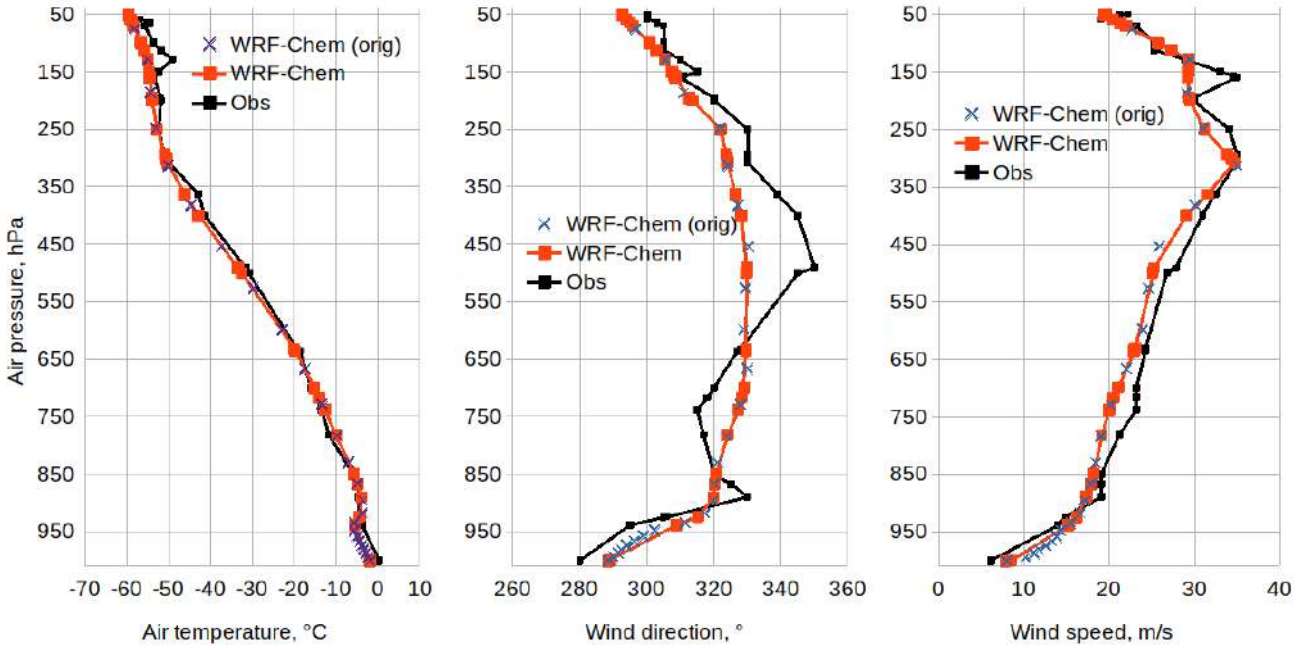

Figure 7: Vertical profiles of air temperature, direction and wind speed (from left to right) in Voeykovo for 19 Dec 2019 12 UTC according to measurements and modeling by WRF-Chem; designation "WRF-Chem orig" - WRF-Chem modeling data before interpolation; "WRF-Chem" - WRF-Chem simulation data after interpolation to measured profile heights.

3.2.2 Near-surface CO_2 mixing ratio

In situ measurements of near-surface CO_2 mixing ratio in Helsinki have been carried out since 2010 on the roof of the FMI building at a height of about 36 m above ground level [140]. The measurements are performed with a Picaro gas analyzer model G1301 and are based on the cavity ring-down spectroscopy (CRDS) method. The device is calibrated 2-3 times a year according to WMO/GAW standards (https://community.wmo.int/activity-areas/gaw). The average difference between the measurements of this device and the standard (systematic error) is 0.01-0.04 ppm, and

the standard deviation of the difference (random error) is 0.02–0.07 ppm. Data is available every 1 hour.

3.2.3 Column averaged CO_2 mixing ratio (XCO_2)

The retrievals of column averaged CO_2 mixing ratio in a dry atmosphere (XCO_2) are used in this study. XCO_2 values were obtained based on measurements of incoming solar IR radiation using a calibrated Bruker EM27/SUN Fourier-transform IR spectrometer. The spectra are measured in the range of 4000–12000 cm^{-1} with a resolution of 0.5 cm^{-1}. To interpret the spectra and retrieve the vertical profile of CO_2 mixing ratio, the algorithm described in [70] was used. XCO_2 values were calculated as the average mixing ratio of the entire dry atmosphere based on the retrieved profile. Independent studies have shown that systematic and random errors in retrieved XCO_2 values based on measurements with the Bruker EM27/SUN instrument can reach ~0.5 and 0.025–0.075%, respectively [70, 71, 130]. Retrieved XCO2 values are available with ~1 min frequency for 3-4 hours per day from Jan 2019 to Mar 2020. However, the time series has many gaps, both during the day and for the entire study period, which is mainly due to meteorological conditions. In total 83 days of measurements are available. Let us recall that measurements using one spectrometer were carried out in Peterhof as part of an international campaign to measure the content, assess anthropogenic emissions of greenhouse gases (including CO_2) from the territory of St Petersburg (EMME) and validate satellite measurements [141].

3.3 WRF-Chem model

The WRF-Chem (Weather Research and Forecasting - Chemistry) numerical model was created to predict the weather and composition of the lower atmosphere (troposphere and lower stratosphere). In this study the WRF-Chem model is used to simulate the transport of CO_2 in the troposphere in St Petersburg (Russia), Helsinki (Finland) and adjacent areas for the period from Jan 2019 to Mar 2020. In this time

interval, complex measurements of CO_2 content are available in the study areas both at the Earth's surface and in the entire atmosphere.

3.3.1 Description of a WRF-Chem numerical experiment

Modeling of CO_2 transport was carried out on four areas, of which three were nested in a parent one for more correct setting of boundary conditions on modeling areas with the highest spatial resolution (Figure 8). The outer parent region (d01) covers an area of 800x800 km^2 with a spatial resolution (Δx) of 8 km. The region includes part of North-West Russia, southern Finland, Estonia and Latvia. The second area (d02) is a subsidiary of d01 with an area of about 320x320 km^2 and Δx=4 km. The two smallest areas - d03 and d04 - have the same areas (about 110x110 km^2) and Δx (2 km). At the same time, d03 is nested in d02 and covers the territory of St Petersburg, while d04 is nested in d01 and covers the city of Helsinki. Vertically, the calculation was performed at 25 hybrid model levels with an upper limit at the atmospheric pressure level of 50 hPa, which approximately corresponds to an altitude of 18-20 km. Above 20 km, the CO_2 content is taken into account from the modeling data of the CAMS service; this is described in detail in Chapter 3.3.2. The simulation time step (Δt) is 40 s for area d01, 20 s for d02 and 10 s for areas d03 and d04. In this numerical experiment, CO_2 is considered as a completely inert gas, i.e. without taking into account chemical transformations. The modeling takes into account four main factors influencing the dynamics of CO_2 in the atmosphere - (1) atmospheric transport, (2) chemical boundary conditions, (3) anthropogenic sources and (4) biogenic absorption and release of CO_2. The last three factors within the WRF-Chem model are described below. To make the most efficient use of available CO_2 and atmospheric measurements, WRF-Chem simulation data is output at a frequency of 10 minutes.

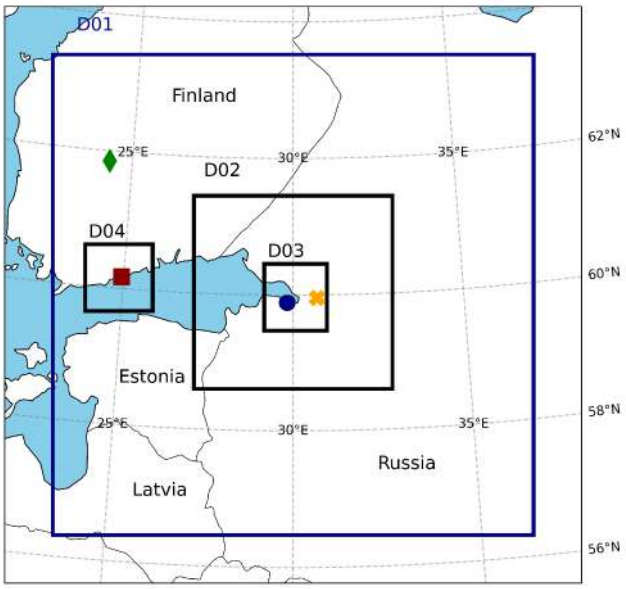

Figure 8: WRF-Chem modeling domains; symbols indicate measuring stations; Peterhof, St Petersburg (blue circle); Voeykovo (orange cross); Helsinki, Kumpula (red square); SMEAR II Hyytiälä forest (green diamond).

Table 3 lists the atmospheric processes whose subgrid-scale parameterization was used in the WRF-Chem simulation. The large number of physical processes described indicates the complexity of the WRF-Chem model and the high requirements for validation with additional measurement-based information.

Note that all processes from the table, except for vertical transport and convective cloudiness, were modeled using parameterization in all four modeling domains. In the case of vertical transfer, parameterization schemes were used only for regions d01 and d02 (Δx 8 and 4 km, respectively). For regions d03 and d04 (Δx=2 km), vertical transport was modeled by solving the differential equation of vertical transport in an approximate form. This approach is considered more correct when modeling with Δx<5 km [105].

Table 3: Atmospheric processes taken into account in WRF-Chem on a subgrid-scale and names of schemes

Process	Name of scheme	Source
Transfer of long-wave EM radiation in the atmosphere	RRTM Longwave Scheme	[142]

Process	Name of scheme	Source
Transfer of short-wave EM radiation in the atmosphere	Dudhia Shortwave Scheme	[143]
Earth's boundary layer model	Mellor–Yamada–Janjic	[144]
Earth's surface layer model	Eta Similarity Scheme	[145, 146]
Model of land-surface layer interaction	Unified Noah land-surface scheme for non-urban landcover surface energy fluxes	[147]
Vertical transport and convective clouds	The Grell 3D ensemble cumulus convection scheme	[148]
Microphysics of clouds	WRF Single–moment 6–class Schemes	[149]
Urban effect	Building Effect Parameterization (BEP)	[150]

To set the initial (IC) and boundary (BC) meteorological conditions, data from the ERA5 meteorological reanalysis are used, obtained by combining modeling and measurement data using the 4DVar assimilation algorithm. ERA5 data have a horizontal spatial resolution of 0.25° (~25 km) and are distributed vertically at 137 hybrid levels, covering the atmospheric layer from the Earth's surface to about 80 km [151, 152]. Meteorological IC and BC include such parameters as atmospheric pressure, wind speed and direction, air temperature, specific humidity and geopotential. Meteorological BC are set every 6 hours throughout the entire modeling period.

To specify chemical BC, CarbonTracker Near-Real Time v.2022-1 (CT-NRT.v2022-1) data are used. The data are CO_2 mixing ratio values on a global scale with a spatial resolution of 2x3° (~200x300 km^2) at 35 vertical hybrid levels from the Earth's surface to an altitude of about 200 km [153]. CarbonTracker data are maintained by scientists from NOAA ESRL, Boulder, Colorado, USA (http://carbontracker.noaa.gov). CT-NRT.v2022-1 data are generated using the global

numerical atmospheric transport model TM5 and assimilation of local ground, ship, mast and aircraft gas measurements (https://gml.noaa.gov/ccgg/carbontracker/CT2019B/). In the current work chemical BC are set every 6 hours.

CO_2 anthropogenic emissions

For anthropogenic CO_2 emissions, the ODIAC (Open-source Data Inventory for Anthropogenic CO_2) inventory database with a global spatial distribution and high resolution (0.43 km^2 for the modeling area) are used [134]. Data for 2019 are available as sums for each month of the year.

Figure 9 shows anthropogenic CO_2 emissions according to ODIAC data for March 2019 for the territories of St Petersburg and Helsinki in tCO_2 per month. The white circle in Figure 9 marks the positions of the measuring stations (Peterhof, St Petersburg and Kumpula, Helsinki). According to ODIAC data, the spatial distribution of anthropogenic CO_2 emissions across the territory of St Petersburg is heterogeneous and tends to peak in the central part of the city with a decrease towards the periphery. CO_2 emissions from the territory of Helsinki are significantly lower than in St Petersburg, and also have a more uniform spatial distribution. Using the example of March 2019, the average specific anthropogenic CO_2 emissions from the territory of Helsinki are approximately 2.3 times lower than in St Petersburg.

The values of CO_2 emissions according to ODIAC data, which corresponded to the position of CHPs in St Petersburg and Helsinki according to https://openinframap.org, are placed on the first four vertical model levels (heights of 50-200 m above the Earth's surface). The total anthropogenic CO_2 emission of St Petersburg according to ODIAC data for 2019 is ~49.1 Mt y^{-1}.

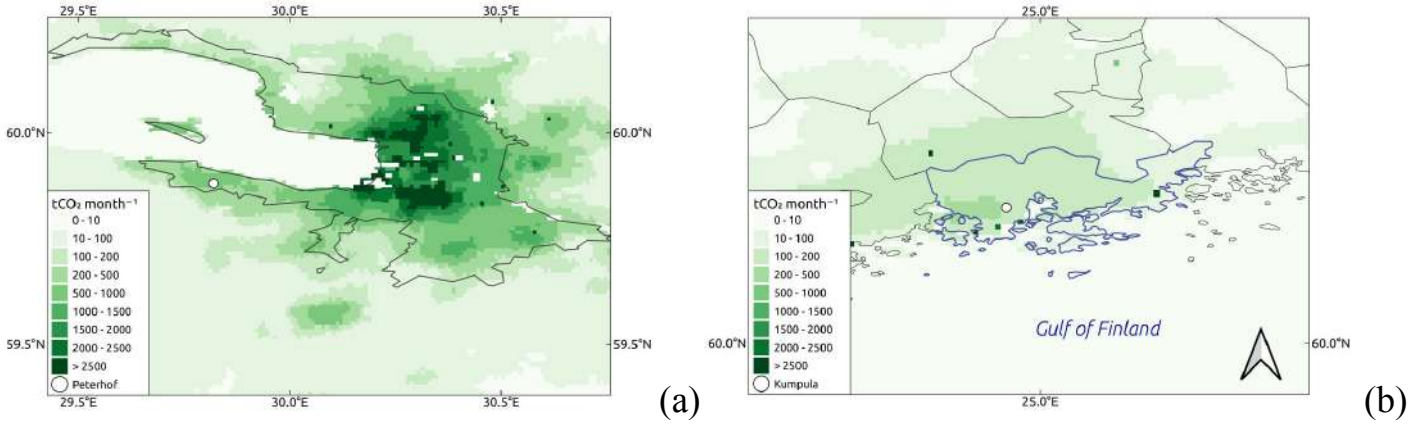

Figure 9: Spatial distribution of anthropogenic CO_2 emissions according to ODIAC data for March 2019 for the territory of St Petersburg (a) and Helsinki (b); the positions of the measuring stations Peterhof and Kumpula are highlighted with white circles; The territory of Helsinki is highlighted with an additional outline.

CO_2 biogenic fluxes

The territories of the cities of St Petersburg and Helsinki are surrounded by various types of vegetation - from evergreen spruce trees to meadows. Therefore, the biogenic factor (absorption and release of CO_2 by vegetation during the growing season) can have a noticeable effect on the gas content in the atmosphere during the late spring, summer and early autumn. The study [44] showed that the CO_2 content in the troposphere is subject to seasonal changes, which is most likely influenced by plant activity during the growing season. A study [154] shows that the start of the growing season in southern Finland occurs around the end of March to the beginning of April. WRF-Chem modeling uses the VPRM (Vegetation Photosynthesis and Respiration Model) model [155], which is part of the version of WRF-Chem used, to account for the uptake and release of CO_2 by vegetation as a result of photosynthesis. Calculation of CO_2 emission and absorption by vegetation is performed in parallel with the WRF-Chem model.

The VPRM provides an explicit estimate of CO_2 uptake from photosynthesis (Gross Ecosystem Exchange or GEE) during solar daytime and CO_2 release (respiration) during nighttime (Respiration or Resp) for seven vegetation types. The sum of these

components determines the CO_2 flux caused by plant activity during the growing season (Net Ecosystem Exchange or NEE). A detailed description of the model is presented in [155]. GEE and Resp in the VPRM model are functions of surface air temperature, reflected short-wave solar radiation in certain wavelength ranges, and the amount of photosynthetic active radiation absorbed by plants.

In this study, the VPRM model is optimized by adjusting the Resp parameter based on measurements at the Finnish station "SMEAR II Hyytiälä Forest" for one vegetation type (out of seven taken into account), which is predominant in the station area - needleleaf forest. Measurements of characteristics of biogenic activity at SMEAR stations are described in Appendix A.

In the VPRM model, the parameter Resp is calculated using linear regression on surface air temperature (T_{air}). Based on the measurements of T and Resp, linear regression parameters a and b are selected for a specific vegetation type. Table A1 shows the original parameters a and b and those adapted by measurements to the conditions in the Hyytiälä station area. These parameters have been added to one of the WRF-Chem model code scripts and are available for selection before running the model.

This optimization allowed us to reduce the average difference between the simulation data and the Resp measurements by more than 10% relative to the original parameters a and b. Figure B1 (Appendix B) shows the time series of GEE and Resp from the WRF-Chem VPRM simulation with adjusted parameters a and b and measurements at Hyytiälä. The model reproduces the temporal variability of the parameters with a high correlation coefficient of about 0.9. Moreover, on average, the model underestimates the GEE measured at the Finnish station and overestimates Resp by approximately 11.7 and 6.9%, respectively. The greatest differences are observed in summer, i.e. during the peak of vegetation season.

Note that according to calculations of the VPRM using the example of June 2019, biogenic CO_2 emissions in St Petersburg on average amount to ~3% of the city's anthropogenic emissions according to the ODIAC data for 2019. This allows us to say that the main contribution to the CO_2 content in the atmosphere on the territory of St

Petersburg is provided by emissions from anthropogenic sources (energy, road transport, industries, etc.).

Other sources and sinks of CO_2

In addition to the above factors, the CO_2 content in the Earth's atmosphere depends on processes that are less significant at the city scale. One of them is the absorption and release of CO_2 by water surfaces [156].

St Petersburg is located on the shore of a large water body - the Gulf of Finland of the Baltic Sea. To assess the possible impact of the surface of the Gulf of Finland on CO_2 content in St Petersburg, a separate study was carried out, based on a number of independent studies and experimental data. To estimate CO_2 emissions from the water surface (F), parameterization (7) from studies [157 - 159] is used.

$$F = 0.251 \times U^2 \times \left(\frac{Sc}{660}\right)^{-0.5} \times K_0 \times \left(e_{sea} - e_{air}\right) \qquad (7)$$

where U - wind speed near the water surface; Sc - a function of water surface temperature (Schmidt number); K_0 - function of water surface temperature and salinity (solubility coefficient); e_{sea} and e_{air} - partial pressures of CO_2 in water and air above water surface.

To calculate F, data on the partial content of CO_2 in the water of the Gulf of Finland, temperature and salinity of water based on ship measurements SOCOM (Surface Ocean pCO2 Mapping intercomparison, http://www.bgc-jena.mpg.de/SOCOM/), data on partial CO_2 pressure based on ground-based spectroscopic measurements in Peterhof with a Bruker 125HR IR Fourier spectrometer and wind speed data in the surface layer based on measurements at the Finnish island station are used. The instrument Bruker 125HR was provided by SPbU RC "Geomodel".

The results indicate that CO_2 emissions from the water surface, according to parameterization (7), significantly depend on variations in wind speed and the ratio between the partial pressure of CO_2 in water and air. The possible contribution of the

water surface of the Gulf of Finland to the CO_2 content is very small in relation to the anthropogenic contribution (1.7-3%). Therefore, in the current study, the contribution of the surface of the Gulf of Finland to CO_2 content is not taken into account in the modeling. A more detailed description of the methods and results obtained is given in the study [160].

The contribution to CO_2 content from forest fires was taken into account only through chemical boundary conditions.

3.3.2 Adaptation of the WRF-Chem model to St Petersburg

Correction of the chemical boundary conditions

The analysis indicates that the CarbonTracker data used to specify chemical IC and BC in WRF-Chem modeling overestimates ground-based XCO_2 measurements based on Bruker EM27/SUN measurements in Peterhof for the period Jan 2019-Mar 2020 by an average of 3.3 ppm with an SDD of 1.3 ppm (Figure 10). This may indicate that CarbonTracker data is subject to a local source of errors, which may be errors in a priori anthropogenic CO_2 emissions and the inability to take into account local features of their distribution in the St Petersburg region due to the coarse spatial resolution of CarbonTracker data. Thus, CarbonTracker data needs to be adjusted before being used as chemical IC and BC.

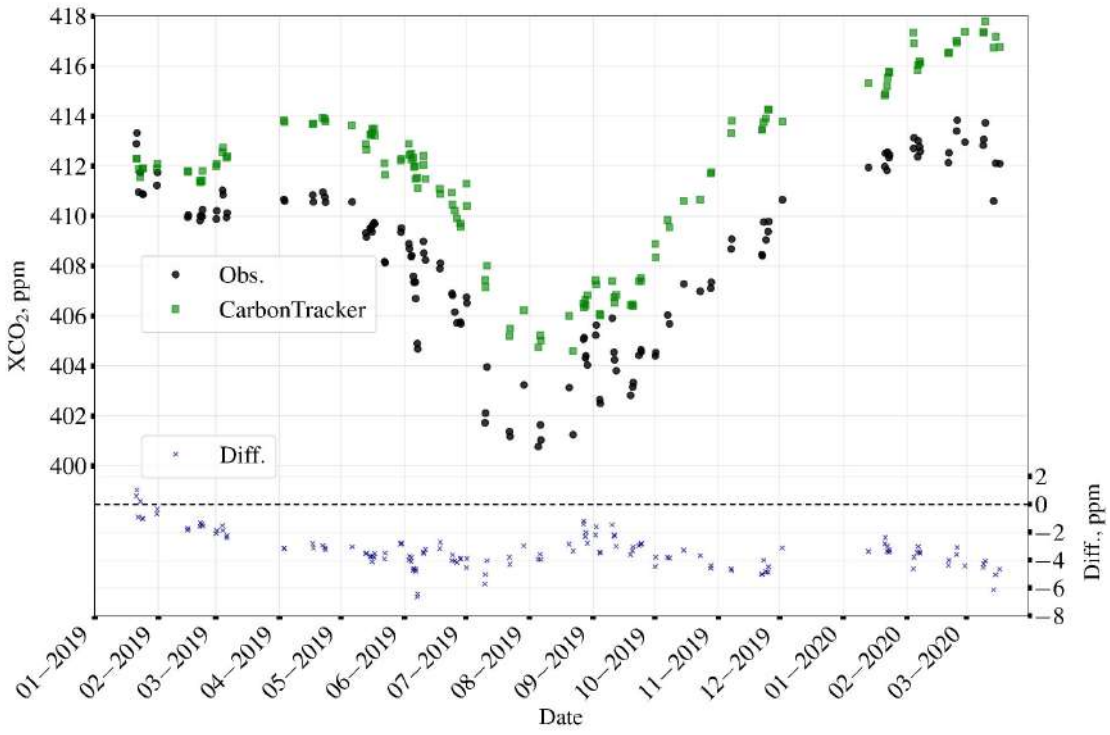

Figure 10: XCO_2 time series according to Bruker EM27/SUN measurements and CarbonTracker v2022-1 modeling for Jan 2019 – Mar 2020, as well as the difference between them (Obs-CarbonTracker, scale on the right).

In WRF-Chem simulations, CarbonTracker data is defined at the domain boundaries. However, there are no XCO_2 measurements in this area and direct correction by comparison with measurements is not possible. In order to correct chemical BC using measurements in Peterhof, it can be assumed that, under certain conditions, the CO_2 content in the air mass arriving at Peterhof is due only to transfer from a remote area (for example, from the boundaries of the modeling domain). Such conditions can be achieved in the absence of the influence of large local anthropogenic sources of CO_2 and biogenic gas emissions on the CO_2 content in Peterhof. Accordingly, we will filter pairs of CarbonTracker data and Bruker EM27/SUN measurements in Peterhof according to these criteria.

In [161], a study was conducted to identify wind directions at which the Bruker 125HR instrument in Peterhof can record the anthropogenic contribution of St Petersburg to the CO_2 content. Therefore, to take into account the first criterion, an analysis of XCO_2 measurements using the Bruker EM27/SUN device and surface wind direction in Peterhof was carried out. Based on the results of the analysis, measurements

during wind directions corresponding to transfer from the territory of St Petersburg (20-150°) were excluded. To account for the second criterion, CarbonTracker measurement and modeling data are filtered by the period in which the biogenic contribution is greatest. According to VPRM modeling data, it corresponds to the period from early spring to mid-autumn.

After filtering, out of 128, 14 pairs of XCO_2 values remained based on Bruker EM27/SUN and CarbonTracker measurements in St Petersburg. It can be assumed that the filtered XCO_2 values characterize the total CO_2 content in St Petersburg, which is primarily associated with the transfer of air masses from the boundaries of the WRF-Chem modeling area. Thus, due to selection, the CO_2 content in these air masses changed slightly when transferred from the border of the region to Peterhof. The MD between filtered pairs of model and measured XCO2 values is about -1.8 ppm (~-0.4%), i.e. CarbonTracker data predominantly overestimates XCO_2 measurements in St Petersburg. This is the rationale for adjusting (reducing) CarbonTracker data by approximately 0.4% for use as chemical BC. Therefore, to set BC the CO_2 mixing ratios by CarbonTracker were reduced by 0.4% at all vertical levels.

Accounting for CO_2 content in the entire atmosphere

As already mentioned in the chapter describing the model, WRF-Chem takes into account processes in the troposphere and lower stratosphere (up to about 18-20 km). In turn, the reconstructed XCO_2 values based on ground-based spectroscopic measurements in Peterhof characterize the entire atmosphere. Not-considering the CO_2 content above 18-20 km according to WRF-Chem data can lead to an artificial overestimation of XCO_2 relative to the measured values. In our study [138], to take into account CO_2 above approximately 20 km, we use reanalysis data from the Copernicus Atmosphere Monitoring Service (CAMS) version v21r2 [162].

Note that XCO_2 values in the St Petersburg region for the period from January 2019 to March 2020 in a layer up to about 70 km by CAMS overestimate measurements with the Bruker EM27/SUN instrument by an average of 2.2 ppm or ~0.5%. For further

use of the CAMS reanalysis data above approximately 20 km, the data were reduced by ~0.5%.

As a result, XCO_2 according to WRF-Chem modeling data (XCO_{2wrf}) is calculated as follows:

$$XCO_{2\,wrf} = \frac{(TCCO_{2\,wrf,<20\,km} + TCCO_{2\,CAMS,>20\,km})}{(TC_{air,wrf} - TC_{water,wrf}) * 10^6} \quad (8)$$

$$TCCO_{2\,wrf,<20\,km} = \sum_{i=1}^{N} \Delta P_i * CO_{2\,i} \quad (9)$$

where $TCCO_{2\,wrf,<20\,km}$- the number of CO_2 molecules in the layer from the Earth's surface to approximately 20 km according to WRF-Chem modeling data; $TCCO_{2\,CAMS,>20\,km}$ - the number of CO_2 molecules in the layer above approximately 20 km according to CAMS reanalysis data; $TC_{air,wrf}$ and $TC_{water,wrf}$ - the number of air and water molecules in the entire atmospheric column; N is the number of WRF-Chem vertical levels; ΔP_i is the pressure of the selected vertical layer i according to WRF-Chem data; $CO_{2\,i}$ is the CO_2 mixing ratio at vertical level i according to WRF-Chem data.

3.4 Validation of WRF-Chem modelled data

3.4.1 Comparison of the modelled and observation data

Near-surface wind speed and direction

According to the analysis results, the WRF-Chem model represents changes in wind speed and direction at the Earth's surface in St Petersburg and Helsinki with noticeably different errors. MD reaches -1.7 m/s and 38.2° for St Petersburg and -0.8 m/s and 21.6° for Helsinki. On average, the model has a better fit for the Helsinki area. The SDD for wind speed is close in both cities and is 1.5-1.6 m/s. However, the wind

direction SDD is greater in Helsinki (48.2°) than in St Petersburg (29.3°). The overestimation of surface wind speed by the WRF-Chem model may be due to difficulties in representing calm weather conditions, such as at night or during the cold season (see [163, 164]). Also, the excess of the surface wind speed by the model relative to the measurements can be caused by the close location of St Petersburg and Helsinki to the territory of the Gulf of Finland (Baltic Sea). This can lead to the formation of local circulations in the Earth's boundary layer with a horizontal scale less than the spatial resolution of the WRF-Chem simulation [165]. In addition, the characteristics of local air circulation may be influenced by another relatively large body of water located near St Petersburg - Lake Ladoga. The correlation coefficients (CCs) between WRF-Chem data and surface wind speed and direction measurements are 0.76 and 0.80 for Peterhof and 0.67 and 0.78 for Helsinki. Similar estimates were obtained in studies [166, 136].

Figure 11 shows histograms of the distribution of wind direction and speed at the Earth’s surface in Peterhof (Jan 2019-Mar 2020) and Helsinki (2019) according to measurement and modeling data. First, let us note how clearly different the wind direction distributions at the Earth's surface are in the two cities over a period of about a year. In Peterhof, the prevailing directions are in the ranges of 140-180° (SSE-S) and 220-260° (WSW), and speeds are 1-4 m/s. In Helsinki, the distribution of wind direction is more complex and does not have clear predominant ranges. However, 100-120°, 200-240° and 280-320° can be distinguished, which correspond to ESE, SSW-WSW and WNW-NNW. Only one of these wind direction ranges intersects with the prevailing values in Peterhof - 200-240°. Perhaps such differences, given the relatively close location of the two cities, are due to local features that affect small-scale dynamic processes. Analysis of changes in wind direction by season indicates that the left hump in the distribution in Helsinki is associated mainly with directions in spring and summer. In turn, the left hump in the distribution of wind directions in Peterhof according to measurement data is caused by wind directions in the winter and autumn periods.

The WRF-Chem model largely follows the prevailing wind directions in both cities. However, in Peterhof the model does not reproduce one of the two predominant wind direction intervals - 140-180°. In turn, in Helsinki, according to modeling data, two main ranges of wind directions are distinguished - 80-120° and 220-260°. These overlap with the two observed predominant ranges. However, the model does not repeat the third range of directions - 280-320°. The analysis indicates that the WRF-Chem model represents the surface wind direction less well in Helsinki than in Peterhof. This is also indicated by the SDD assessment given above.

The distribution of surface wind speed in Peterhof and Helsinki is similar. The ranges of the most frequent surface wind speeds in the two cities are close and are 1-3 m/s in Peterhof and 2-4 m/s in Helsinki. The model partially repeats the shape of the distribution of measured wind speeds both in Peterhof and Helsinki. The range of the most frequent wind speed values according to the model in the two cities is 2-4 m/s. As shown by analyzing MD, and as seen in Figure 11, WRF-Chem overestimates the surface wind speed in both cities. However, the model better replicates the wind speed distribution in Helsinki. Analysis of the distribution of wind parameters in Peterhof for the period of 2019 only (as in Helsinki) indicates that it remains almost unchanged in relation to the entire period (Jan 2019-Mar 2020).

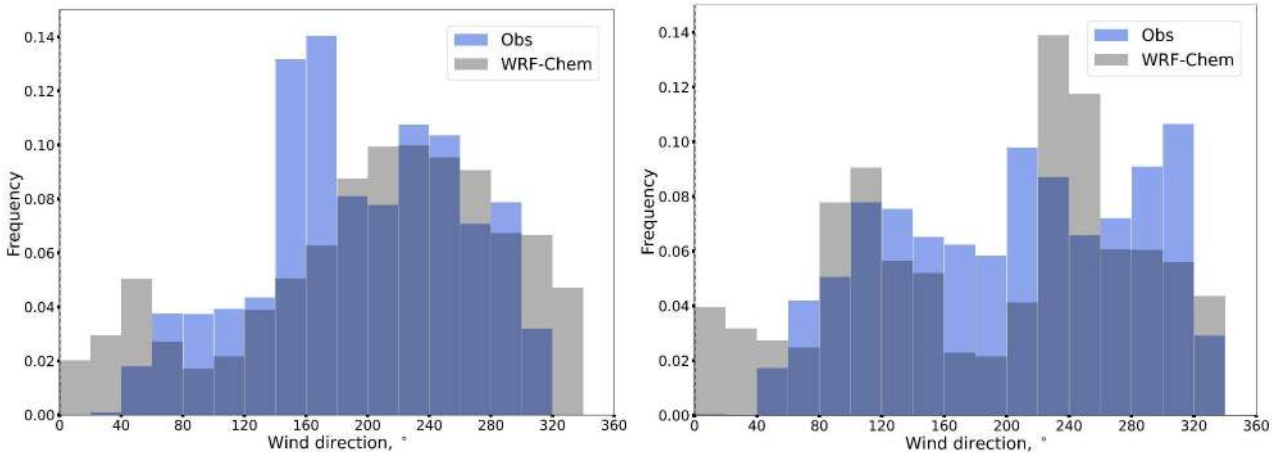

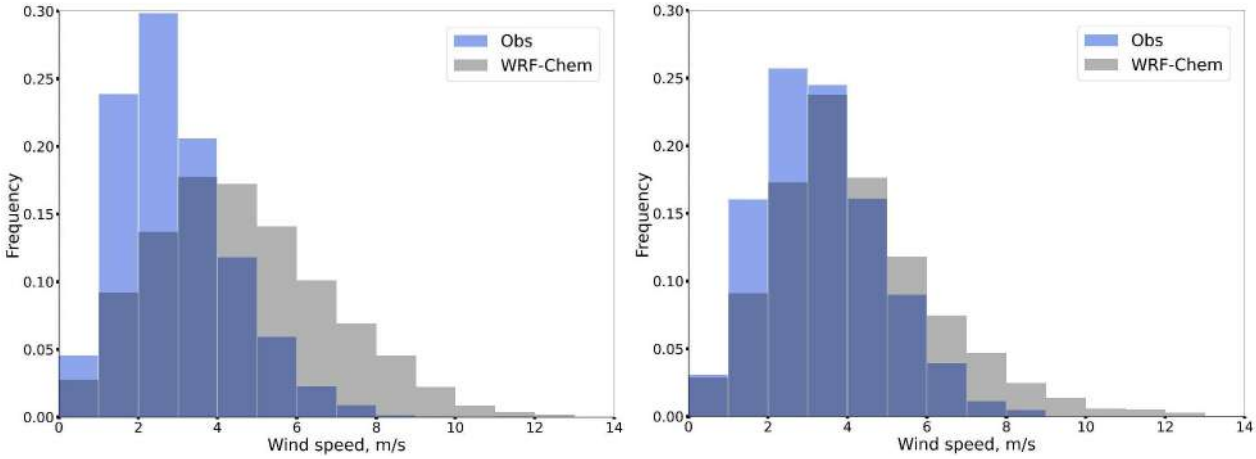

Figure 11: Histograms of the distribution of surface wind parameters (direction - top, speed - bottom) in Peterhof (left) for Jan 2019-Mar 2020 and Helsinki (right) for 2019 according to WRF-Chem modeling and measurements

Vertical distribution of meteorological parameters near St Petersburg

Based on the analysis of aerological measurements and modeling data of vertical profiles of meteorological parameters in Voeikovo for Jan 2019-Mar 2020 we can say that the WRF-Chem model is capable of simulating the vertical profile of changes in wind speed and direction and air temperature in the troposphere in the St Petersburg region.

The air temperature from the modeling data is in best agreement with measurements, having a MD of 0.4°C, SDD of 2.5°C, and a CC of 0.99. MD and SDD for wind speed reach 0.5 and 4.1 m/s, and for direction - 12.1 and 28.3°. In the upper troposphere, wind speed, according to measurement and modeling data, can take values of more than 40-50 m/s, which explains the relatively large value of SDD. CC for wind speed and direction are 0.93 and 0.86, respectively.

According to the results of comparison of vertical profiles of wind speed and direction from modeling and measurement data, using the WRF-Chem model it is possible to describe the variation of CO_2 content in the troposphere. In addition, the

vertical profile of air temperature according to the simulation data corresponds well to the measured one. This probably means that the model can also be used to qualitatively describe the vertical atmospheric transport of CO_2 in the St Petersburg region.

Near-surface CO_2 mixing ratio in Helsinki

Figure 12 shows the temporal change in the near-surface CO_2 mixing ratio according to WRF-Chem modeling and measurements in Helsinki for the period 2019. Table 4 shows the main statistical characteristics of the mismatch of these data. For average values, confidence intervals are given at a confidence level of 95%, calculated based on [167]:

$$\overline{VMR_{CO_2}} \pm z\frac{SD}{\sqrt{N}} \text{ [ppm]} \quad (10)$$

where $\overline{VMR_{CO_2}}$ - mean near-surface CO_2 mixing ratio; z - quantile of normal distribution or Student's T test for 95% confidence level; SD - standard deviation of CO_2 near-surface mixing ratio from the mean; N - size of the dataset.

The WRF-Chem modeling data have a fairly similar pattern of change to ground-based observations - the CC for the entire period was about 0.73. The MD and SDD between measurements and simulation data are 0.15 and 1.68%. On average, near-surface CO_2 content in Helsinki in 2019 is lower according to modeling than measured data. In addition, we note the very close natural variability (standard deviation from the mean) of observational and modeling data - about 9.5-9.7 ppm.

According to Figure 12, one can observe the emerging growing season, the most active influence of which begins around April and ends in October. At the same time, the decrease in near-surface CO_2 content in the period from April to August (peak of the biogenic influence) relative to the period from January to April is underestimated according to the model by approximately 3 ppm.

The exclusion of biogenic influence leads to an increase in MD from 0.15 to 0.45%, but to a decrease in SDD from 1.68 to 1.56%. Probably the small variability of

MD between the modeling data and measurements when taking into account and not taking into account the biogenic contribution to the modeling area is associated with the influence of air transport from the boundaries of the modeling area and the strong daily variation of this factor, which can partially smooth out the discrepancy.

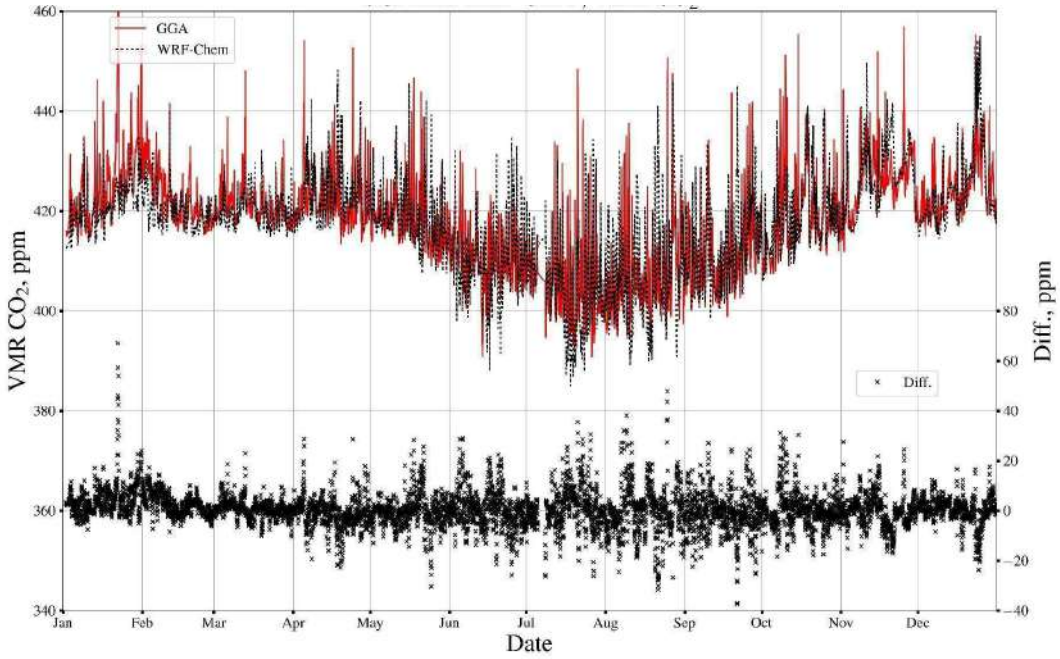

Figure 12: Time series of near-surface CO2 mixing ratio in Helsinki (in ppm) according to WRF-Chem modelling and measurements for 2019 and the difference between them (Obs-WRF-Chem, scale on the right); GGA - measurement data.

Table 4: Statistical characteristics of the difference between the hourly average near-surface CO_2 mixing ratio according to WRF-Chem data and measurements in Helsinki for the period 2019; % values are given relative to the mean value based on measurements; SD – standard deviation, MD – average difference, SDD – standard deviation of the difference, CC – correlation coefficient; For average values, a confidence interval is given at a confidence level of 95%.

Data	**Size of the dataset**	**Mean and SD, ppm**	**MD and SDD, ppm (%)**	**CC**
Observations - WRF-Chem	8565	**418.0**±0.2 and **9.7**/ 417.4±0.2 and 9.5	0.6±0.15 and 7.0 (0.15±0.04 and 1.7)	0.73

Of the 8565 pairs of measured and model values with a step of 10 minutes, about 59.6% of all values have a difference of less than 1% (4.2 ppm), about 32.6% of pairs with a difference from 1 to 3% (4.2-12.5 ppm) and only ~8% of pairs with a difference of more than 3%. Among the largest differences, values reaching 10-15% (40-60 ppm)

are observed, but there are very few of them (about 9 pairs or 0.1% of the entire sample) and can probably be attributed to anomalous values.

Let's try to find out what mainly causes the errors in modeling the surface CO_2 mixing ratio in Helsinki in 2019. Let's consider the change in the differences between the measured and model values when the modeling error in wind speed and direction changes. No obvious connection was found between the errors in modeling the surface CO_2 content and the errors in modeling the wind at the Earth's surface in Helsinki; the CC is ~0.1. However, considering modeling errors of more than 3% (i.e., more than ~12 ppm), taking into account the sign of the error, a not very obvious opposite relationship was revealed between the modeling errors of surface CO_2 content and wind speed. When considering errors from 12 ppm, the CC is about 0.4 with a sample size of more than 699 pairs (out of 8565). When the error threshold is increased to 17 ppm, the CC increases to 0.48, however, with a sample size of only 282 pairs. It was found that when the sign of the largest errors in modeling the surface CO_2 content changes (more than 3%), the sign of the error in modeling the surface wind speed changes to the opposite. This is logical, since when the surface wind speed is overestimated according to the model data, the model surface CO_2 content should decrease. Thus, we can say that the largest errors in modeling the surface CO_2 content in Helsinki (more than 3%) are caused by errors in modeling the surface wind speed.

Figure 13a shows the diurnal variation of surface CO_2 content at the Helsinki station based on WRF-Chem modeling and measurements. Time is given in UTC. Confidence intervals are highlighted in color. As can be seen from the graph, the model in general simulates the change in the surface CO_2 mixing ratio during the day. Thus, WRF-Chem repeats the increase in CO_2 content at 4-5 UTC with a subsequent decrease to 15 UTC and further growth. As noted above, the model predominantly underestimates the surface CO_2 content relative to measurements - to approximately 1.5 ppm at night and to less than 1 ppm during the day. Analysis of the daily variation of surface CO_2 content and wind speed for individual seasons (graphs not shown) for 2019 in Helsinki indicate that the shape of the overall average daily variation (Figure 13 a) is likely caused by the influence of vegetation during the growing season (from about

mid-spring to the beginning of autumn) and a pronounced diurnal variation in wind speed in spring and summer (maximum at 12-14 UTC). In winter, the surface CO_2 content has a relatively smooth diurnal variation with an increase of approximately 5 ppm by 12 UTC (according to measurements), while in summer the CO_2 content varies during the day up to 10 ppm or more. The winter increase is likely caused by more frequent calm conditions and more temperature inversions. The WRF-Chem model represents the average daily cycle worst of all in winter, and better in spring. This is possibly due to the average overestimation of surface wind speed in Helsinki according to the modeling data. Confidence intervals based on measurement and modeling data are close and constitute ~1 ppm, increasing slightly towards 11-12 UTC.

Analysis of changes in the near-surface CO_2 mixing ratio depending on the day of the week indicates that the modeling data repeats the decrease in gas content on weekends - Saturday and Sunday - according to measurement data (on average by 1-1.5 ppm). The decrease in near-surface CO_2 content is likely due to a decrease in the use of transport on these days, as well as the temporary cessation of the work of some enterprises. Such information is not explicitly specified through the anthropogenic CO_2 emissions of the ODIAC database and is apparently contained in the chemical boundary conditions of the CarbonTracker database, which are specified within a 6-hour interval.

Analysis of the seasonal change in the surface CO_2 mixing ratio in Helsinki for 2019 (Figure 13 b) based on measurement and modeling data indicates, firstly, that it is possible to describe it using the WRF-Chem model. Secondly, there is a pronounced decrease in the surface CO_2 content by July with a subsequent increase, as indicated above. The amplitude of the changes is about 24 ppm (~5-6% of the measured average). The worst agreement between measurement and modeling data is observed in January-February (3-4 ppm) and July (1-2 ppm). However, in July (as in most months), the confidence intervals for the measured and simulated data overlap, suggesting that the differences between the monthly averages of the two data sets during this period are not significant. On average, the confidence intervals for measurement and modeling data are close and amount to ~0.5 ppm.

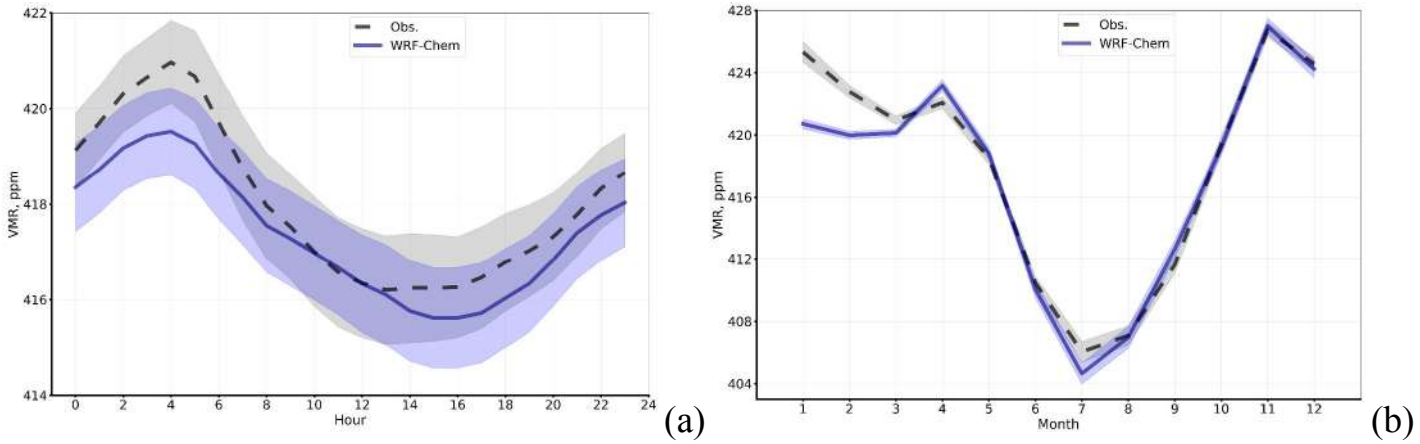

Figure 13: Daily (a) and seasonal (b) variation of the near-surface CO_2 mixing ratio in Helsinki according to WRF-Chem data and measurements in 2019; time is given in UTC (a) and in months (b); The confidence intervals of the means for the 95% confidence level are highlighted in color.

XCO_2 in St Petersburg

The time series of XCO_2 (the average mixing ratio in the entire atmosphere) from WRF-Chem simulations and Bruker EM27/SUN measurements are very close, having a CC of ~0.95 (Figure 14, Table 5). The model simulates the measured decrease and subsequent increase in XCO_2 caused by plant activity during the growing season (approximately May to October 2019). Analysis of individual components of XCO_2 according to WRF-Chem modeling data shows that in general seasonal variation of XCO_2 is due to chemical BC. Within the modeling domain, the VPRM model simulates local features of the biogenic fluxes that adjust its impact on CO_2 content. MD and SDD between the simulation and measurement data are -1.3 and 1.2 ppm, respectively (~-0.3%). The analysis indicates that systematic bias in XCO_2 modeling may be due to errors in chemical boundary conditions as well as errors in atmospheric transport modeling.

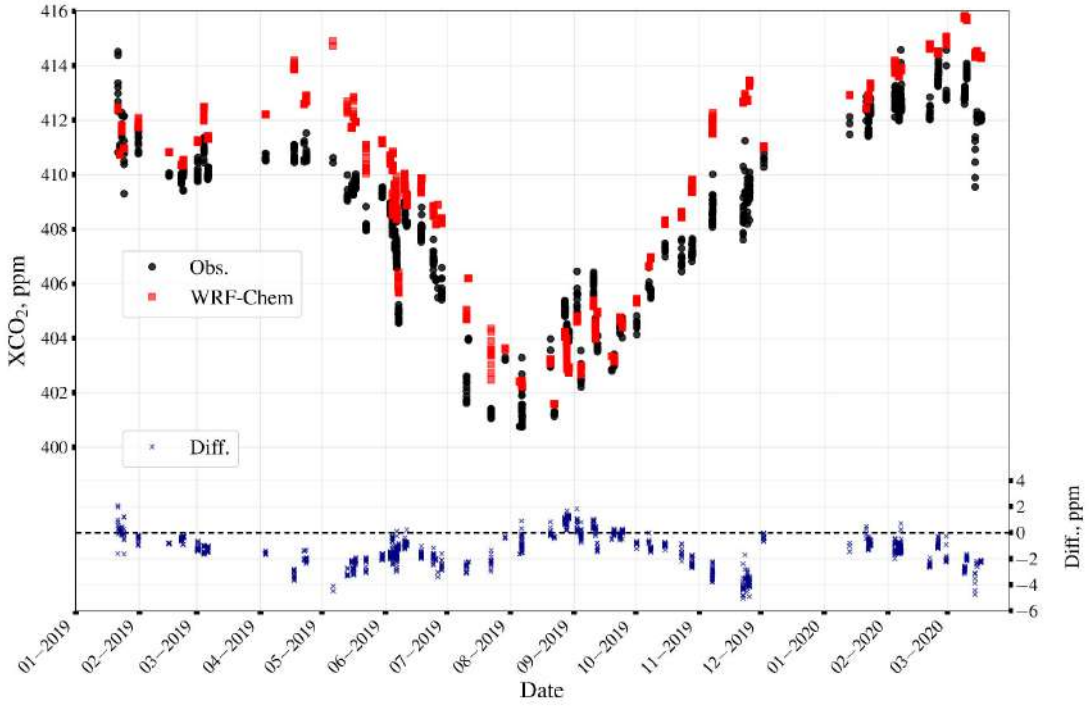

Figure 14: Time series of XCO_2 in St Petersburg according to Bruker EM27/SUN measurements and WRF-Chem modeling for Jan 2019 – Mar 2020, as well as the difference between them (Obs-WRF-Chem, scale on the right).

Table 5: Statistical characteristics of the XCO_2 difference according to Bruker EM27/SUN measurements and WRF-Chem modeling in St Petersburg for Jan 2019 – Mar 2020; % values are relative to average XCO_2 based on measurements; SD – standard deviation, MD – mean difference, SDD – standard deviation of the difference, CC – correlation coefficient; For average values, a confidence interval is given at a confidence level of 95%.

Data	Mean and SD, ppm	MD and SDD, ppm (%)	CC
Observations - WRF-Chem	**408.4±0.2** and **3.4**/ 409.7±0.2 and 3.9	-1.3±0.07 and 1.2 (-0.3±0.02 and 0.3)	0.95

A series of numerical experiments by WRF-Chem with a simplified specification of chemical BC along the vertical, as well as using information on the water vapor content based on spectroscopic measurements with a Bruker 125HR instrument, led to a MD between the modeling data and measurements of approximately 0.6%, i.e. twice as high as the results from Table 5 [138]. At first, this is due to errors in specifying chemical BC in the upper troposphere layer. Secondly, the higher MD value is caused by the use of a limited set of measured atmospheric water vapor data to calculate XCO_2. Thus, measurement data of the total water vapor content using the Bruker instrument are

available for only 77 days of the period Jan 2019-Mar 2020 in the form of daily averages. The results of the current study show that correct specification of chemical BC and the use of information on atmospheric water vapor content from WRF-Chem modeling data lead to improved agreement between model and measured XCO_2 values in St Petersburg. More detailed information about the methods and results is given in [138].

Let us evaluate the contribution of three main factors influencing the dynamics of XCO_2 in the St Petersburg region - (1) transport from the boundaries of the modeling domain (chemical boundary conditions), (2) anthropogenic CO_2 emissions and (3) absorption and release of CO_2 by vegetation during the growing season. Using the WRF-Chem model, CO_2 transport from the three listed sources is modeled as three separate variables - $XCO_{2\ BC}$, $XCO_{2\ Ant}$ and $XCO_{2\ Bio}$. The sum of these variables (11), after vertical integration, gives the CO_2 total column or XCO_2, which is analyzed above:

$$XCO_2 = XCO_{2\,BC} + XCO_{2\,Ant} + XCO_{2\,Bio} \qquad (11)$$

This approach allows us to analyze several scenarios in which we will vary the three components of XCO_2. Firstly, we will be able to understand the significance of each of the three factors, and secondly, evaluate which of the scenarios will lead to less systematic and random error in XCO_2 modeling. Note that $XCO_{2\,Ant}$ and $XCO_{2\,Bio}$ depend only on anthropogenic and biogenic activity within the modeling domain. The influence of anthropogenic CO_2 emissions and vegetation activity outside the modeling domain is specified through BC. Thus, taking $XCO_{2\,Ant}$ and $XCO_{2\,Bio}$ in (11) as 0 ppm excludes the influence of anthropogenic and biogenic activity only inside the modeling domains.

Table 6 lists 9 scenarios, including the control one (Control), and gives a brief description of what they involve. Figure 15 shows the values of MD (a) and SDD (b) between the Bruker EM27/SUN measurement data and WRF-Chem modeling in St Petersburg for Jan 2019-Mar 2020. Confidence intervals for the 95% probability are plotted on the MD graph.

First, note that for all scenarios, the SDD varies from approximately 0.30 to 0.33%, which is ~0.1 ppm. We can assume that the SDD remains almost unchanged. Excluding the biogenic contribution (scenario 2) leads to an increase in MD by approximately 0.1%, while excluding only the anthropogenic contribution (scenario 3) leads to a slight decrease in MD by 0.05% relative to control scenario 1. It should be noted that the MDs for the first five scenarios overlap in confidence interval and the differences between them can be considered statistically insignificant. The smallest MD is observed for scenario 6 (reduction of chemical boundary conditions by 0.3%), while the confidence interval does not overlap with the MD of the other scenarios. With a subsequent decrease in the contribution of CO_2 transfer from the boundaries of the modeling area (scenarios 7-9), the MD increases relatively strongly (up to ~0.7%).

Table 6: Scenarios of variation of XCO_2 components in St Petersburg for Jan 2019-Mar 2020 according to WRF-Chem modeling data; $XCO_{2\,BC}$, $XCO_{2\,Ant}$ and $XCO_{2\,Bio}$ - XCO_2 values based on modeling data in the area of near-surface measurements in Peterhof from the boundaries of the modeling domain, biogenic activity and anthropogenic emissions, respectively.

N	Name	Description
1	Control	Control numerical experiment WRF-Chem $XCO_2 = XCO_{2\,BC} + XCO_{2\,Ant} + XCO_{2\,Bio}$
2	Without $XCO_{2\,Bio}$	$XCO_2 = XCO_{2\,BC} + XCO_{2\,Ant}$
3	Without $XCO_{2\,Ant}$	$XCO_2 = XCO_{2\,BC} + XCO_{2\,Bio}$
4	Without $XCO_{2\,Bio}$ and $XCO_{2\,Ant}$	$XCO_2 = XCO_{2\,BC}$
5	$XCO_{2\,BC}$ reduced by 0.1%	$XCO_2 = XCO_{2\,BC}*0.999 + XCO_{2\,Ant} + XCO_{2\,Bio}$
6	$XCO_{2\,BC}$ reduced by 0.3%	$XCO_2 = XCO_{2\,BC}*0.997 + XCO_{2\,Ant} + XCO_{2\,Bio}$
7	$XCO_{2\,BC}$ reduced by 0.5%	$XCO_2 = XCO_{2\,BC}*0.995 + XCO_{2\,Ant} + XCO_{2\,Bio}$
8	$XCO_{2\,BC}$ reduced by 0.7%	$XCO_2 = XCO_{2\,BC}*0.993 + XCO_{2\,Ant} + XCO_{2\,Bio}$
9	$XCO_{2\,BC}$ reduced by 1%	$XCO_2 = XCO_{2\,BC}*0.990 + XCO_{2\,Ant} + XCO_{2\,Bio}$

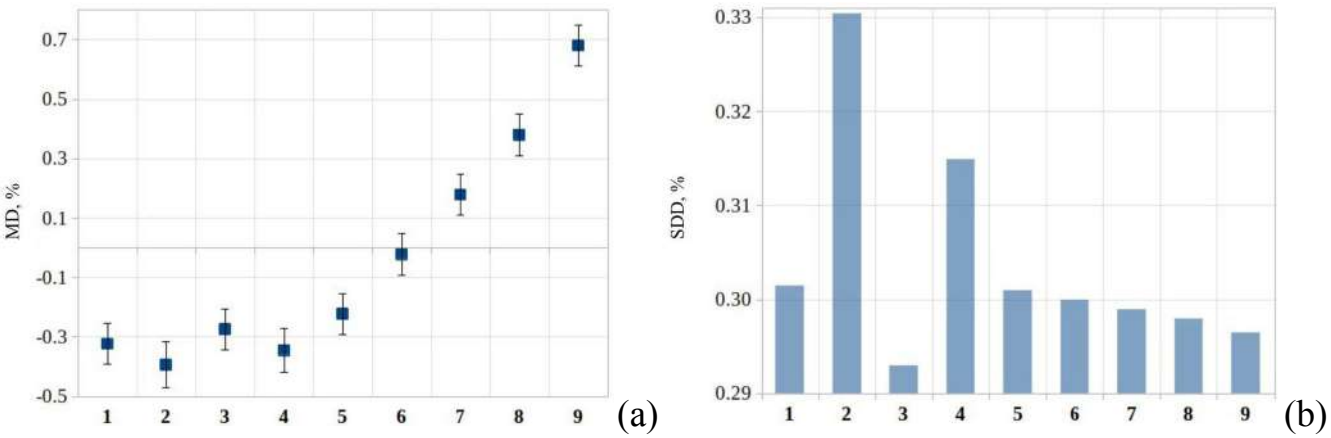

Figure 15: MD (a) and SDD (b) between XCO_2 according to Bruker EM27/SUN measurements and WRF-Chem modeling for nine scenarios in St Petersburg for Jan 2019-Mar 2020; for a description of the scenarios, see Table 6; Values are given in % relative to average XCO_2 based on measurements.

Thus, a reduction in the contribution from chemical boundary conditions to XCO_2 on the territory of St Petersburg can be achieved with their additional reduction by another 0.3%. However, the SDD will remain virtually unchanged and will also be ~0.3%. It can be assumed that the SDD value is determined by errors in a priori anthropogenic CO_2 emissions and errors in modeling the biogenic contribution. The fact that the exclusion of both factors does not lead to noticeable changes in the CO_2 may indicate, for example, errors in the spatial distribution of CO_2 emissions or their daily, weekly or monthly variations.

3.4.2 Comparisons of WRF-Chem simulation results with independent model data

Due to the coarser spatial resolution of the CAMS v21r2 reanalysis relative to the WRF-Chem simulation data, the comparison is made only with respect to XCO_2. Thus, the study [168] compared the values of the surface mixture ratio of CO_2 and XCO_2 based on the CAMS reanalysis of an earlier version (v18r3) and measurements (local and remote) in the area of St Petersburg (Russia) for 2018. It is shown that the differences in the surface CO_2 mixing ratios based on CAMS reanalysis data and local measurements depend significantly on the season and vary by up to 3%. The same applies to correlation, which varies from 0.26 to 0.81 depending on the month. However, this was to be expected due to the dependence of the surface CO_2 mixing ratio

on the local features of the territory of St Petersburg, which cannot be taken into account at a spatial resolution of more than 100 km.

Analysis of XCO_2 comparison according to WRF-Chem and CAMS data for the period from January 2019 to March 2020 indicates their closeness. Thus, MD and SDD are 0.15 and 0.3% with a very high correlation (CC = ~0.96). The WRF-Chem data generally slightly underestimate XCO_2 relative to the CAMS data. Moreover, the greatest differences are observed during the vegetation season - approximately from May to October 2019 (on some days up to more than 5 ppm). This may indicate differences between the two models in representing the biogenic contribution to CO_2 content. Note that the variation of XCO_2 based on the CAMS reanalysis is smoother compared to WRF-Chem. Their standard deviations from the mean are about 3.4 and 4.2 ppm, respectively. This may be due to the coarser spatial resolution of the CAMS data, which smoothes out the local features of the anthropogenic influence of St Petersburg on XCO_2.

Figure 16 shows the differences between XCO_2 data in St Petersburg based on measurements (Bruker EM27/SUN) and modeling (WRF-Chem, CAMS v21r2 and CarbonTracker v2022-1). Note that CAMS and CarbonTracker data are available at 3 and 6 h rates, respectively, making the minimum time step for matching to be 6 h. It can be concluded that the WRF-Chem simulation data best matches the measurements. The MDs for WRF-Chem, CAMS and CarbonTracker are 1.3, 2.3 and 3.3 ppm (0.3, 0.5 and 0.8%), respectively. The better agreement between the measured data and the WRF-Chem simulations is likely due to the higher spatial resolution relative to the CAMS and CarbonTracker data.

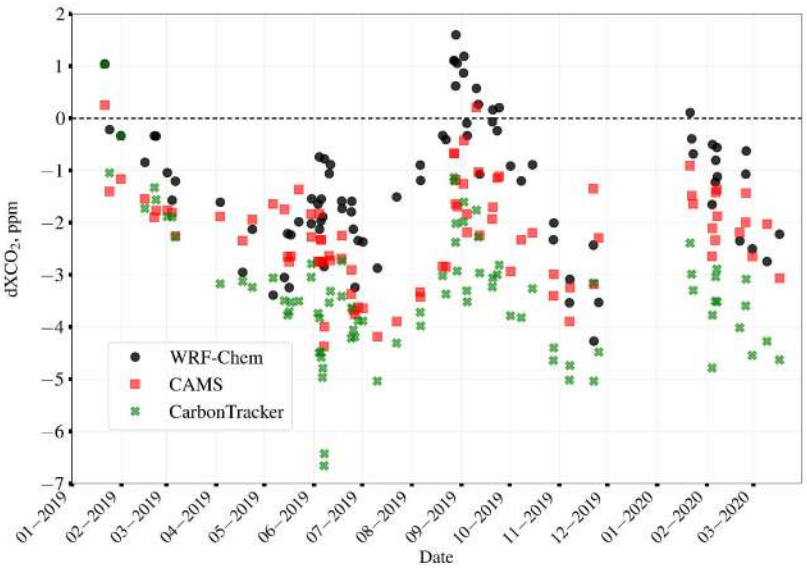

Figure 16: Differences between XCO2 in the St Petersburg area according to measurement data (Bruker EM27/SUN) and modeling (WRF-Chem, CAMS v21r2, CarbonTracker v2022-1) for Jan 2019 – Mar 2020.

3.5 Compliance of XCO_2 modeling errors with modern requirements

To date, many studies have assessed the ability of the WRF-Chem model to represent the surface abundance, vertical profile, and whole-atmosphere CO_2 content over time scales ranging from daily to multi-year [23, 136, 138]. Errors in XCO_2 modeling in studies are usually less than 0.1% or about 0.5 ppm.

In studies [22, 24, 95] it is shown that the city's anthropogenic contribution to CO_2 content, measured using paired high-precision spectrometers, ranges from less than ~0.5 to 5 ppm. This characteristic has a direct connection with anthropogenic CO_2 emissions from the city and was obtained using parallel spectroscopic measurements of XCO_2. The essence of such measurements is to reduce the influence of the main factors on the CO_2 content and highlight the influence of anthropogenic gas emissions from the territory of the city under study. With this approach, taking into account that the model qualitatively represents atmospheric transport, by varying the a priori anthropogenic emissions of the city, the best agreement between the modeling results and XCO_2 measurements can be achieved.

The a priori emissions adjusted in this way will be a solution to the inverse problem of atmospheric transport. However, if XCO_2 measurements are available with only one instrument, then during modeling it is important to correctly take into account other influencing factors (i.e., CO_2 transport from the boundaries of the modeling domain, biogenic contribution, etc.). Therefore, with this approach, the acceptable error in modeling CO_2 transport depends on the magnitude of the anthropogenic contribution. For example, if the anthropogenic contribution of a city to the total CO_2 content according to measurement data is 5 ppm, then with a modeling error of 1 ppm the systematic error of adjusted anthropogenic CO_2 emissions will be 20%. If the contribution from measurement data is 1 ppm, then with the same modeling error the systematic error of posterior emissions will be 100%.

Based on the range of the anthropogenic contribution of St Petersburg from [22, 24], we can say that to assess the city's anthropogenic emissions using only one measuring instrument, the modeling error should be ~1 ppm (0.2%) or lower.

Figure 17 shows histograms of the distribution of errors in XCO_2 modeling using WRF-Chem (a - original modeling data, b - XCO_2 from chemical boundary conditions reduced by 0.3%) in St Petersburg for Jan 2019-Mar 2020. The histograms highlight in green the error intervals that can be considered acceptable (from -1 to 1 ppm), according to the above research analysis. The selected error interval for the data of the original numerical experiment (Figure 17 a) accounts for approximately 35% (425) of all error values. The shift of the distribution to the left and the analysis given above indicate that the most likely reason for the overestimation of XCO_2 according to the modeling data is errors of a systematic nature, for example, errors in chemical boundary conditions. A decrease in XCO_2 from chemical boundary conditions by 0.3% (Figure 17 b) shifts the error distribution to the right and the acceptable range for XCO_2 modeling from -1 to 1 ppm accounts for ~60% of all errors.

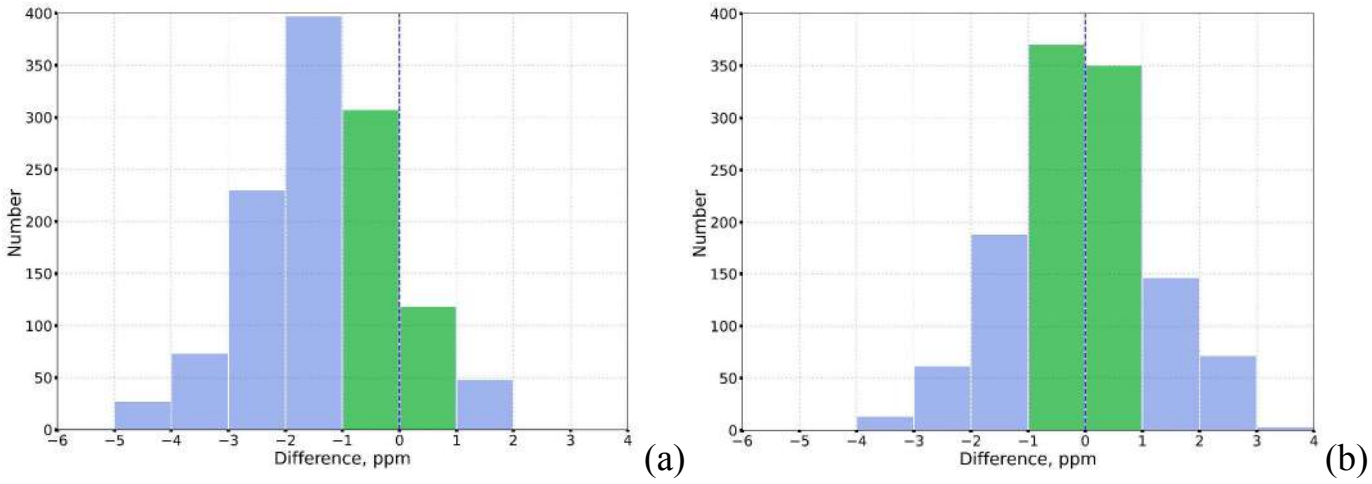

Figure 17: Histogram of error distribution for XCO_2 modeling using WRF-Chem (a - $XCO_2 = XCO_{2\,BC} + XCO_{2\,Ant} + XCO_{2\,Bio}$; b - $XCO_2 = XCO_{2\,BC}*0.997 + XCO_{2\,Ant} + XCO_{2\,Bio}$, see Table 6) in St Petersburg for Jan 2019-Mar 2020.

3.6 Main results and conclusion

The chapter provides the analysis results of a comprehensive validation of the ability of the WRF-Chem numerical model to describe changes in CO_2 in the troposphere in the St Petersburg region. The results indicate that using the WRF-Chem model it is possible to simulate the annual change in CO_2 at the Earth's surface and in the entire atmosphere. The results of this study were published in [169].

1. Using the model, it is possible to represent the seasonal and daily variations in gas content associated with the influence of vegetation. The correlation with the near-surface CO_2 mixing ratio at a station in Helsinki (distance from St Petersburg is ~300 km) is high (CC = ~0.73) with the modeling error and its standard deviation being 0.15±0.04 and 1.7%.
2. The WRF-Chem model simulates the temporal change in the average dry atmosphere CO_2 mixing ratio (XCO_2) in the St Petersburg region with a very high correlation coefficient of ~0.95. The modeling errors for XCO_2 are ~-0.3±0.02% with a standard deviation of 0.3%, which is consistent with estimates from independent studies for other cities. Systematic error is most likely due to errors in the chemical boundary conditions.

3. The time series of XCO_2 in St Petersburg obtained using the WRF-Chem model is consistent with independent data sets based on numerical simulations and CAMS and CarbonTracker measurements. However, the WRF-Chem data agrees slightly better with the measurements. This is probably due to the ability of the WRF-Chem model to take into account the influence of local dynamic features of the study area, as well as the specific spatial distribution of a priori CO_2 sources and sinks. This emphasizes the importance of high spatial resolution weather prediction models and atmospheric gas composition to estimate anthropogenic CO_2 emissions.
4. Analysis of measurements and modeling of CO_2 total content in St Petersburg over a period of more than a year indicated that data on the spatiotemporal distribution of CO_2 in the atmosphere CarbonTracker Near-Real Time v.2022-1 (CT-NRT.v2022-1) are overestimated at the boundaries of the modeling area. Reducing the CarbonTracker data by 0.4% resulted in a modeling error of ~0.3%, which is almost 2 times less than in an earlier study using the original CarbonTracker data. The analysis showed that an additional decrease in the chemical boundary conditions by another ~0.3% will lead to an almost complete decrease in the systematic difference, but will not change its standard deviation.
5. The study showed that using the WRF-Chem model it is possible to simulate the annual variation of CO_2 in the atmosphere in the St Petersburg region with high spatial resolution (2 km). If the recommendations given in this study are followed, the errors in modeling CO_2 emissions in most cases will meet the requirements, which, as we indicated, are 1 ppm or less, which need to be put forward by numerical models when solving inverse problems for estimating anthropogenic CO_2 emissions (0.2%). Thus, we can say that the WRF-Chem model can be used to solve inverse problems for estimating anthropogenic CO_2 emissions from the territory of St Petersburg, provided that the model is adapted to the study area and careful validation of modeling data was carried out.

Chapter 4. Estimation of anthropogenic CO_2 emissions in St Petersburg using the WRF-Chem model

4.1 WRF-Chem modelling of St Petersburg anthropogenic contribution to CO_2 TC

As already indicated in Chapter 2, in 2019, as part of the EMME measurement campaign, paired spectroscopic measurements of CO_2 were carried out in the windward and leeward parts of St Petersburg, the difference between which, under certain meteorological conditions, can be interpreted as the contribution of St Petersburg to the CO_2 content. Based on the WRF-Chem numerical experiment on CO_2 transport in the St Petersburg region in Jan 2019-Mar 2020, described in Chapter 3, it is possible to obtain an estimate of the model anthropogenic contribution of St Petersburg and compare it with EMME measurements. To do this, from each model cell corresponding to paired measurements with two Bruker EM27/SUN IR Fourier spectrometers for the 8 best days of measurements in March-April 2019, CO_2 TC values were obtained in units [mol. cm^{-2}]. These are 21 and 27 March, 1, 3, 4, 6, 16 and 24 April 2019. The data were selected according to the criteria described in [22], which are related to meteorological conditions and the position of certain measurements near large local sources of CO_2. Then, the difference is determined between the model data in the corresponding cells ($dTCCO_2$).

As discussed in Chapter 3, the uncertainty in modeling CO_2 in the troposphere depends on factors such as errors in the modeling of physical atmospheric processes, errors in chemical boundary conditions, and CO_2 emissions and sinks. Comparison of CO_2 TC from modeling data with measurements provides an estimate of the overall modeling error of this parameter, which includes all of the listed factors.

Let us calculate the influence of the error in modeling CO_2 transport using the WRF-Chem model on the estimate of $dTCCO_2$. To do this, we calculate $dTCCO_2$ as the difference between model cells on the measurement days of EMME 2019, which are separated from each other by an azimuthal angle corresponding to the atmospheric transport modeling error. We will take the average difference between the model and

measured vertical profile of the wind direction (12.7° or 5%, see Chapter 3) (Figure 18) as the error in modeling atmospheric transport. If the distance between two model cells that correspond to the paired measurement positions on a particular day is ~30 km, using a simple trigonometric transformation, it can be determined that the angle α=12.7° relative to the position of the windward cell corresponds to a distance of ~4 km around the leeward cell. Accordingly, to estimate $dTCCO_2$, we calculate the difference between each pair of windward and leeward cells in 8 days of EMME measurements. The total number of such pairs for each day is 8-15. An example of such cells is highlighted in red in Figure 18.

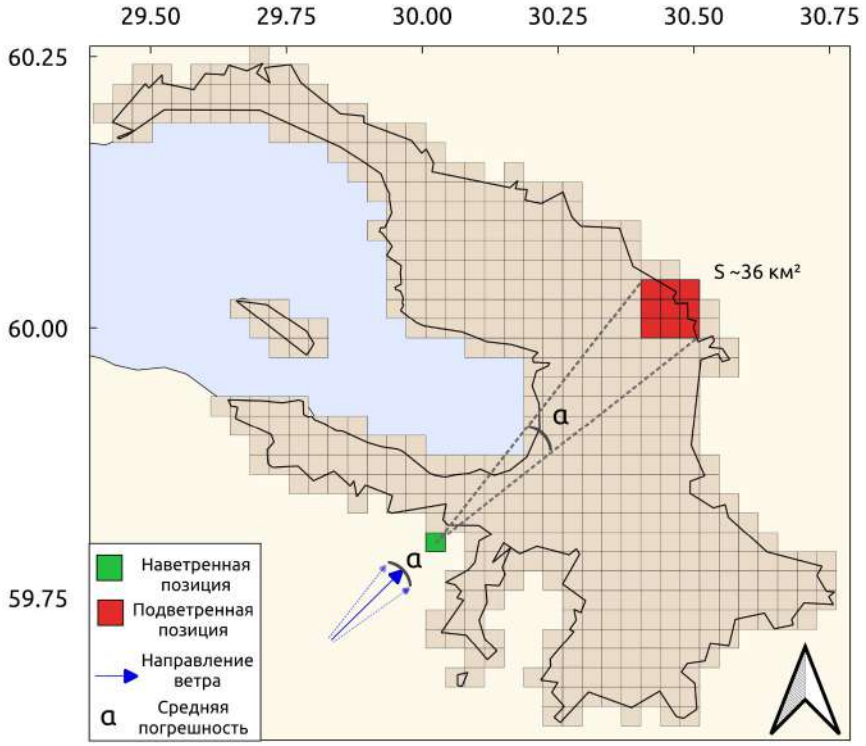

Figure 18: Schematic representation of the effect of wind direction modeling error on $dTCCO_2$ between windward and leeward positions around St Petersburg; grid - spatial coverage of St Petersburg with WRF-Chem modeling data with a step of 2 km; S - the area of the selected region.

Figure 19 shows $dTCCO_2$ time series at 10 minutes (left) and daily average (right) for each of the 8 days of March-April 2019 from paired EMME measurements and WRF-Chem simulations. The graphs show simulation data from paired cells with the best fit to measurements (blue curve), the worst fit (green curve), and the spatial average of all simulated $dTCCO_2$ values for a given day (red curve). Note that the simulation data with the best fit are on average 2.4 km away from the "true" EMME measurement

positions. In turn, the $dTCCO_2$ simulation data with the worst agreement with the measurements are on average 3.7 km away from the true observation positions.

As can be seen in Figure 19, the best-fit simulation data agrees well with measurements on all days except April 24, when the model significantly underestimates $dTCCO_2$. For the best fit between the simulation data and the measurements, the mean difference (MD) and standard deviation of the difference (SDD) are 6.7 and 36.9%, respectively. The correlation coefficient (CC) between the simulation data and measurements is 0.78. If we exclude 24 April, then MD and SDD decrease to -0.3 and 33.2%, CC increases to 0.84.

On 24 April 2019, the simulation data greatly underestimate $dTCCO_2$ based on measurements (by about 70%). This may be due to errors in transport modeling or errors in specifying chemical boundary conditions. Analysis of $dTCCO_2$ separately from three factors ($OC\ CO_{2\ Ant}$, $OC\ CO_{2\ Bio}$, $OC\ CO_{2\ BC}$) shows that to achieve agreement between measurement and modeling data on 24 April, anthropogenic emissions need to be increased by approximately 2.5 times (i.e. by 250%) or completely eliminate the contribution to $dTCCO_2$ from chemical boundary conditions. The first scenario is most likely not plausible, since such a strong CO_2 source would have been noticeable on other days of EMME measurements. In turn, the influence of CO_2 transfer from chemical boundary conditions could be the cause of such an error.

The WRF-Chem simulation data from the cells with the worst agreement with the measurements have MD and SDD of 52.5 and 102.5%, respectively. CC is 0.67. The exclusion of 24 April leads to a change in MD and SDD to 36 and 99% with a CC of 0.73.

In turn, the spatially averaged model $dTCCO_2$ repeats the measured values with a relatively high CC of 0.69. At the same time, MD and SDD are 17.2 and 55.1%, respectively. On two of the eight days (1 April and 24 April), the spatially averaged model $dTCCO_2$ values are negative, in contrast to the measurements. This is due to the fact that the CO_2 content transported from the boundaries of the modeling domain to the windward areas of the city was generally greater than in the leeward areas of the city.

The exclusion of 24 April leads to a decrease in MD and SDD to 3.1 and 41.9%, CC increases to 0.82.

When averaging the daily cycle of $dTCCO_2$ (Figure 19 on the right), SDD decreases by ~7-10%, and MD increases slightly (by 1-6%). For example, averaging the daily cycle for spatially averaged model $dTCCO_2$ leads to a change in MD and SDD to 4.7 and 34.6%.

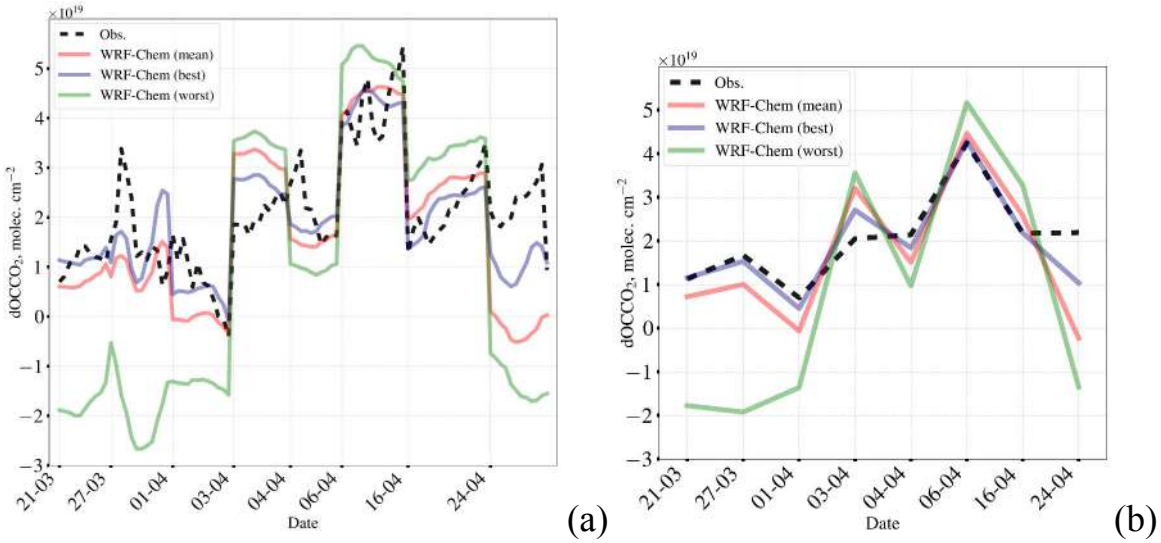

Figure 19: Time series of $dTCCO_2$ averaged over 10 minutes (a) and daily average (b) for 8 days of March-April 2019 according to paired measurements (EMME) and WRF-Chem modeling; simulation data from cells with the best fit to measurements (blue curve); with the worst fit (green curve); averaged over space on a specific day (red curve).

The analysis shows that the average error in modeling the direction of atmospheric transport of 12.7° (about 5% relative to measurements) can lead to errors in modeling the anthropogenic contribution of up to more than 50%. However, the average transport modeling error used as an example is assumed to be the same throughout the entire territory of St Petersburg, although the closest aerological measurements are carried out in Voeikovo and only twice a day (at a distance of about 20 km from the center of St Petersburg). In addition, this error characterizes, on average, a vertical layer covering approximately the entire troposphere and part of the lower stratosphere. The error in modeling the wind profile on a specific day, time period and at a certain altitude can be less than 5% (even close to 0%).

A likely optimal solution would be to consider a spatial averaged $dTCCO_2$ of about 36 km2 around the “true” downwind position of the EMME measurements

according to modelled data (red area in Figure 18 and red curve in Figure 19). From this we conclude that the WRF-Chem model describes the change in the anthropogenic contribution of St Petersburg to the CO_2 content with an average error of ~35% (excluding 24 April and using averaged daily values).

Let us note once again that the resulting error in $dTCCO_2$ modeling includes the error in modeling atmospheric transport and the error in a priori CO_2 emissions (anthropogenic and biogenic). However, it does not include the influence of the number of measurements used, the amount of a priori information, diurnal variability of the measured $dTCCO_2$ and other possible factors. Thus, the influence of the first factor was observed when excluding measurements taken on 24 April 2019, and when averaging modeling and measurement data per day. This was shown to reduce the $dTCCO_2$ simulation error from 55 to 35% (i.e. ~20%). The influence of the second factor was not studied for the WRF-Chem model, but was partially analyzed for the one-dimensional box model of atmospheric transport. Thus, a change in a priori anthropogenic CO_2 emissions according to the ODIAC 2018 database to ODIAC 2019 leads to an increase in emission estimates for St Petersburg by ~30%. A third factor (diurnal variability of measured $dTCCO_2$) was assessed in a study [22]. Its contribution to the error was 33% for 9 days of measurements. For the case from the current study (7 days of measurements, excluding 24 April), this factor contributes to an error of ~27%. If we take into account these errors in this form, then the total error in $dTCCO_2$ modeling and subsequently the error in estimating anthropogenic CO_2 emissions of St Petersburg for 2019 will be ~57%. However, since the error in modeling CO_2 transport is known with greater certainty (approximately 35%), then in this study, to estimate the error in anthropogenic CO_2 emissions in St Petersburg, we will leave only this uncertainty, keeping in mind that the real error may be greater.

Previously, it was shown that the random error in modeling the CO_2 TC in St Petersburg for 83 days from January 2019 to March 2020 using the WRF-Chem model is 0.3%. Such significant differences between the early and current values of the random error (34-37%) can be explained by the fact that in this case the error estimate is based on only 7 days of measurements in March and April. Obviously, with an increase in the

sample of measurements, the random error should decrease. In addition, Chapter 3 provides an estimate of the uncertainty in modeling CO_2 TC (as XCO_2), while here we estimate the uncertainty in modeling $dTCCO_2$. The difference between the model values of CO_2 TC can also increase the random and, as a consequence, the total error in the $dTCCO_2$ modeling.

4.2 Estimation of St Petersburg CO_2 anthropogenic emissions by solving the inverse problem using the WRF-Chem model

Using the WRF-Chem model, we will conduct a series of numerical experiments to simulate the anthropogenic contribution of St Petersburg ($dTCCO_2$) for 7 days of EMME measurements in 2019, excluding 24 April.

In each of the numerical experiments we will change the anthropogenic CO_2 emissions of St Petersburg. That set of modified a priori anthropogenic CO_2 emissions, at which the $dTCCO_2$ modeling data will have the smallest difference with $dTCCO_2$ data based on paired spectroscopic measurements, will serve as a solution to the inverse problem of estimating anthropogenic CO_2 emissions in St Petersburg for 2019. Let us recall that the assessment of emissions is for the entire year based on single measurements in March and April 2019. It is justified in this work by the probable low seasonal variability of anthropogenic CO_2 emissions of St Petersburg (according to the ODIAC data for 2019).

Descriptions of eight numerical experiments are given in Table 7. The first is a control experiment with “reference” emissions and chemical boundary conditions. Based on the results of the control numerical experiment, a conclusion is drawn on how to adjust the a priori information in order to achieve a better agreement between the model and measured $dTCCO_2$ values. In 2-6 numerical experiments, anthropogenic CO_2 emissions in St Petersburg increased by 5, 10, 15, 20 and 25%. For the 7th numerical experiment, anthropogenic CO_2 emissions of St Petersburg were increased only in that part of the city that, according to the STILT modeling results (Figure 6 a), is covered by measurements. And finally, in the 8th numerical experiment, anthropogenic CO_2

emissions were increased by 20% in cells corresponding to the positions of the St Petersburg CHPs.

Table 7: Description of WRF-Chem numerical experiments; SPb - entire territory of St Petersburg.

Experiment	Description
1 (control)	CO_2 anthropogenic emissions - ODIAC 2019
2	ODIAC 2019 (SPb) + 5%
3	ODIAC 2019 (SPb) + 10%
4	ODIAC 2019 (SPb) + 15%
5	ODIAC 2019 (SPb) + 20%
6	ODIAC 2019 (SPb) + 25%
7	ODIAC 2019 (SPb) + 25% + STILT
8	ODIAC 2019 (CHP) + 20%

Figure 20 shows the total $dTCCO_2$ modeling errors based on a comparison of modeling and measurement data for 7 days of March and April 2019 in St Petersburg in % relative to measurements. The total errors are calculated as the square root of the sum of the squares of the average difference between the modeling and measurement data (systematic modeling error) and its standard deviation (random modeling error).

The graph shows that the best agreement is observed with an increase in anthropogenic emissions by 20% only from the territories of CHPs (~34%). At the same time, the agreement deteriorates to more than ~39% when emissions increase to 25% from the entire city territory. The change in MD with an increase in anthropogenic emissions from the entire territory of St Petersburg is almost linear.

Considering that the integrated anthropogenic CO_2 emissions of St Petersburg based on ODIAC 2019 data are 49.1 Mt y^{-1}, their increase from the territories of thermal power plants by 20% leads to emissions of the city of ~62.3 ± 21 Mt y^{-1}. It is possible that an increase in a priori CO_2 emissions from the positions corresponding to the city's

thermal power plants by more than 20% will further reduce the total error $dTCCO_2$ and better correct a priori emissions.

As can be seen from Figure 20, an increase in anthropogenic emissions by 20% from the entire territory of St Petersburg and only from the approximate positions of the CHPs leads to a difference of ~4% between the modeling errors. At the same time, the modeling error with an increase in emissions by 20% only from the positions of CHPs is close to the error of the experiment, where CO_2 emissions from the entire territory of St Petersburg increased by 5 and 10%, as well as to the control experiment (difference ~2%).

This indicates the ambiguity of estimates of anthropogenic CO_2 emissions in St Petersburg based on the method for solving the inverse problem of atmospheric transport. For example, an increase in the a priori total anthropogenic CO_2 emissions for the entire St Petersburg for 2019 according to ODIAC data by 5% will lead to a value of ~51 Mt y^{-1}. In turn, as already mentioned above, an increase of 20% in a priori emissions only from the territories of CHPs will lead to an estimate of 62.3 Mt y^{-1}, i.e. about 22% more.

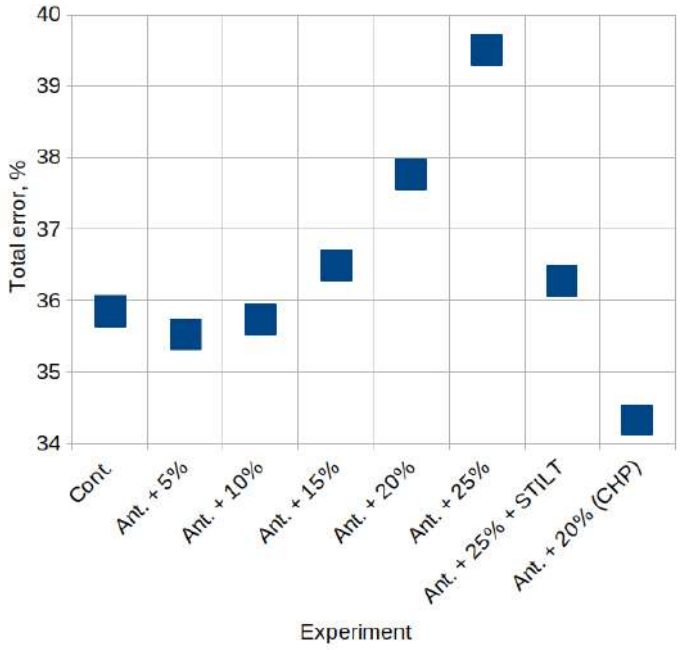

Figure 20: Total modeling error of $dTCCO_2$ for 7 days of March-April 2019 in St Petersburg; differences are given in % relative to measurements.

4.3 Comparison of independent estimates of anthropogenic CO_2 emissions of St Petersburg

Table 8 provides estimates of total anthropogenic CO_2 emissions from St Petersburg based on the current study and other sources of information. The overall range of estimates for 2019 is 49-91 Mt y^{-1}. In this case, the range of estimates based on the method for solving the inverse problem of atmospheric transport is 62-91 Mt y^{-1}. The value of the total anthropogenic CO_2 emission from St Petersburg for 2019 (62 Mt y^{-1}) obtained in this chapter is consistent with the value obtained using the box model (65 Mt y^{-1}) within the error limits. In this case, the average estimate for all given values based on solving the inverse problem is 73 with a standard deviation of 13 Mt y^{-1}.

The difference with the estimate of CO_2 emissions for St Petersburg for 2019, obtained using the HYSPLIT dispersion model [24], is at least ~16 Mt y^{-1}. This is likely due to differences in the description of atmospheric transport in the models used and in the a priori information and number of EMME measurements used.

The estimate of total CO_2 emissions of St Petersburg for 2015 using the inventory method according to data from [170] is at least 27% less than estimates based on solving the inverse problem of atmospheric transfer (taking into account the error). However, the fact that the inventory-based estimate is given for 2015 does not allow us to say with confidence about the errors of the inventory method.

The estimate based on the 2019 ODIAC inventory database is 49 Mt y^{-1} with an error of ~15 Mt y^{-1}. If we consider the edges of the ranges of estimates taking into account errors, then anthropogenic CO_2 emissions of St Petersburg based on the ODIAC data are lower than the city emissions obtained using the WRF-Chem model (62±21 Mt y^{-1}) by ~11%. The both estimates are consistent within the error range of 41-64 Mt y^{-1}.

Table 8: Total anthropogenic emissions of CO_2 from St Petersburg for 2019 from on a priori (ODIAC 2019) and aposteriori data

Method	**Source**	**CO_2 anthropogenic emissions, Mt y^{-1}**	**Errors**
Inventory	[170]	29.6 (2015)	-
	ODIAC 2018	31 (2018)	from ~30-40% [20]
	ODIAC 2019	49 (2019)	
Inverse problem of atmospheric transport	[24] Dispersion model HYSPLIT + ODIAC 2018	75.8 (2019)	-
	[26] Box model + ODIAC 2018	65 (2019)	from ~19 Mt y^{-1}
	Current study - Box model + ODIAC 2019	91 (2019)	
	Current study - WRF-Chem + ODIAC 2019 + (Ant 20% from positions of CHPs)	62 (2019)	~21 Mt y^{-1}

4.4 Main results and conclusion

In this part of the study, the total CO_2 anthropogenic emissions from the entire territory of St Petersburg for 2019 were assessed by solving the inverse problem of atmospheric transport. The assessment was carried out using paired spectroscopic measurements of CO_2 and the WRF-Chem numerical model of weather prediction and tropospheric composition of high spatial resolution.

The total anthropogenic CO_2 emission of St Petersburg for 2019 based on solving the inverse problem of atmospheric transport using the WRF-Chem model is ~62±21 Mt

y^{-1}. This estimate is at least 27% higher than the inventory data for 2015. This also was found in other studies for St Petersburg [24, 26].

At the same time, the entire range of emission estimates for St Petersburg, obtained using differential spectroscopic measurements of the CO_2 TC during the EMME campaign and various atmospheric transfer models, is 62-91 Mt y^{-1}. All estimates are consistent with each other within the error range (19-21 Mt y^{-1}).

The mean estimate of CO_2 anthropogenic emissions of St Petersburg in 2019 based on solving the inverse problem is 73 Mt y^{-1} with a standard deviation of 13 Mt y^{-1}.

Summary

This dissertation is devoted to the study of methods for assessing anthropogenic emissions of the greenhouse gas CO_2 from the territory of large cities using the example of the Russian megapolis of St Petersburg. Methods for estimating CO_2 emissions based on solving the inverse problem of atmospheric transport were considered. The work examines the influence of the choice of atmospheric transport model, a priori information (a priori distribution and values of anthropogenic CO_2 emissions) and measurement data of the total CO_2 content in the atmosphere on estimates of anthropogenic CO_2 emissions in St Petersburg.

According to the study, the errors in assessing anthropogenic CO_2 emissions in St Petersburg using spectroscopic measurements of gas content in the atmosphere and a one-dimensional box model of atmospheric transport depend on the spatial distribution of CO_2 emissions within the city; spatial coverage of measurements; quality of a priori information; complexity of the atmospheric transport model. Taking into account the limited spatial coverage of paired spectroscopic measurements of CO_2 content in the atmosphere leads to a decrease in estimates of anthropogenic emissions of St Petersburg by ~22-55%.

The study indicates a small contribution of the water surface of the Gulf of Finland to estimates of CO_2 anthropogenic emissions of St Petersburg, even under extreme meteorological conditions. Accordingly, when assessing anthropogenic CO_2 emissions of St Petersburg, the contribution of the water surface of the Gulf of Finland can be neglected.

Using the example of 2019, the work shows that in ~60% of cases, the WRF-Chem three-dimensional numerical weather prediction and tropospheric composition model can be used to solve the inverse problem of estimating CO_2 anthropogenic emissions from St Petersburg (modeling error ~0.2%). Based on the sensitivity analysis of the model, it was concluded that the random error in modeling the CO_2 content in the atmosphere may be associated with errors in the spatial distribution of a priori CO_2 emissions and their temporal variation.

It is shown that the complexity of the atmospheric transport model, the quality of a priori information and the spatial coverage of measurements of CO_2 content in the atmosphere leads to a wide range of estimates of anthropogenic CO_2 emissions in St Petersburg from ~62 to more than 90 Mt y^{-1}. In this case, the average estimate for all given values based on solving the inverse problem is 73 Mt y^{-1} with a standard deviation of 13 Mt y^{-1}. Estimates based on solving the inverse problem of atmospheric transport exceed the values based on the inventory by 11-27%. This indicates the importance of independent methods for assessing CO_2 emissions, which will allow validating and, if necessary, adjusting existing inventories of carbon dioxide emissions into the atmosphere.

The development of this independent method for assessing anthropogenic CO_2 emissions is especially relevant now in connection with (1) the operation and preparation for launches of satellite systems that measure CO_2 TC with high spatial resolution; (2) the availability of high-precision spectrometers that allow ground-based remote measurements of CO_2 TC; and (3) the development of three-dimensional numerical models of atmospheric transport with high spatial resolution, which can resolve gas transport at the scale of a large city, taking into account the physical properties of urban buildings.

This study and a number of cited works indicate the promise of a method for estimating anthropogenic CO_2 emissions based on high-precision spectroscopic measurements of the gas content in the atmosphere and modeling of atmospheric transport. To implement it, it is necessary to establish appropriate regular measurements in large cities both in Russia and other countries. Similar measurements have been implemented for several years in large European cities (Munich, Paris).

Acknowledgements

The author thanks his scientific supervisor - Doctor of Physical and Mathematical Sciences Timofeev Yuri Mikhailovich (St Petersburg State University) - and Doctor of Physical and Mathematical Sciences - Smyshlyaev Sergei Pavlovich (RSHU) for invaluable support in the academic and life spheres, transferred knowledge and experience in the scientific fields of remote measurements, solving inverse problems of atmospheric optics and numerical modeling of the chemical composition of the Earth's atmosphere, for an endless number of discussions and disputes, critical, strict, but a fair view of the research being carried out, for support during the writing of the dissertation and simply for a friendly attitude.

The author is grateful to the team of scientists from the National Oceanic and Atmospheric Administration (NCAR), the University Corporation for Atmospheric Research (UCAR), the National Oceanic and Atmospheric Administration (NOAA) and the Air Force (AFWA), USA, who developed, are developing and are distributing the numerical data free of charge model WRF-Chem. The author also expresses gratitude to the team of scientists from the Department of Atmospheric Physics of St Petersburg State University and the Voeikov Main Geophysical Observatory and specifically Maria Vladimirovna Makarova for organizing and leading the EMME measurement campaign, the data of which are used in my dissertation. The author thanks the resource center of St Petersburg State University "Geomodel" for providing measuring equipment. The author is also grateful to scientists Juha Hatakka and Ivan Mammarella from the Finnish Meteorological Institute and the University of Helsinki for providing measurements of near-surface CO_2 content and biogenic gas fluxes in Finland (data obtained in 2020). The author would like to thank the NOAA ESRL science team for free access to CarbonTracker data (data acquired 2021). Finally, the author thanks colleagues from the Max Planck Institute for Biogeochemistry (Jena, Germany) for their assistance with the VPRM model (communication during the period 2020-2021).

The author also thanks the rest of the team of the Department of Atmospheric Physics of St Petersburg State University and Ozone Layer and Upper Atmosphere

Research Laboratory (O3Lab), in particular Yana Akselevna Virolainen, Alexander Viktorovich Polyakov, Anatoly Vasilievich Poberovsky and Evgeniy Vladimirovich Rozanov for the shared experience in conducting research, writing articles, analyzing various measurement data and in life issues.

The author expresses special gratitude to his colleagues - Alexander Mahura (University of Helsinki, Finland), Roman Nuterman (Niels Bohr Institute, Denmark) and Suleiman Mostamandi (King Abdullah University of Science and Technology, Saudi Arabia), who made a great contribution to the development of the author as young scientist through many informal discussions, seminars, practical classes, scientific internships and generally long-term scientific cooperation.

The author also thanks the team of the Scientific Research Center for Ecological Safety of the Russian Academy of Sciences (SRCES RAS), and in particular Viktor Ivanovich Gorny, and the team of the Laboratory for Modeling the Middle and Upper Atmosphere of the Russian State University of Humanities for valuable comments on individual parts of the dissertation, received during informal conversations and scientific seminars. The author also specially thanks the team of the Russian State University of Humanities and O3Lab for providing access to computing resources.

List of abbreviations and conventions

EM - electromagnetic

IR - infrared

IPCC - Intergovernmental Panel on Climate Change

WMO - World Meteorological Organization

ppm - parts per million

USD - The United States dollar

GDP - gross domestic product

CHP - Combined Heat and Power plant

GAW - The Global Atmosphere Watch

NOAA ESRL - National Oceanic and Atmospheric Administration, Earth System Research Laboratories

SMEAR - Station for Measuring Ecosystem-Atmosphere Relations

ICOS - Integrated Carbon Observation System

JR-STATION - Japan–Russia Siberian Tall Tower Inland Observation Network

RAS - Russian Academy of Sciences

SPbU - St Petersburg State University

GGA - Greenhouse Gas Analyzer

TCCON - Total Carbon Column Observing Network

COCCON - COllaborative Carbon Column Observing Network

NDACC - Network for the Detection of Atmospheric Composition Change

TOVS - Television Infrared Observation Satellite Operational Vertical Sounder

IMG - Interferometric Monitor for Greenhouse gases

GOSAT - Greenhouse gases Observing SATellite

SCIAMACHY - The SCanning Imaging Absorption spectroMeter for Atmospheric CartograpHY

IASI - Infrared Atmospheric Sounding Interferometer

OCO - Orbiting Carbon Observatory

AIRS - Atmospheric Infra-Red Sounder

TES - Tropospheric Emission Spectrometer

IKFS-2 - InfraKrasnii Furie Spectrometer-2

TanSat - Exploratory Satellite for Atmospheric CO2

SOCOL - SOlar Climate Ozone Links

MPI-ESM - Max Planck Institute Earth System Model

MEZON - Model for Evaluation of oZONe trends

WRF-Chem - Weather Research and Forecasting model coupled with Chemistry

ODIAC - Open-source Data Inventory for Anthropogenic CO_2

TC - total column

DS - differential spectroscopic

EMME - Emission Monitoring Mobile Experiment

HYSPLIT - The Hybrid Single-Particle Lagrangian Integrated Trajectory model

UTC - Coordinated Universal Time

GFS - Global forecast system

STILT - the Stochastic Time-Inverted Lagrangian Transport model

IC - initial conditions

BC - boundary conditions

Literature

[1] Wallace, J.; Hobbs, P. Atmospheric Science—An Introductory Survey, 2nd ed. *Elsevier Academic Press: Amsterdam*, *The Netherlands*, P. 484, 2006.

[2] Seinfeld, J.H.; Pandis, S.N. Atmospheric Chemistry and Physics: From Air Pollution to Climate Change, 2nd ed. *John Wiley & Sons, Inc.: Hoboken, NJ, USA*, P. 1225, 2006.

[3] Timofeyev Yu.M., A.V. Polyakov, V. Deler, D. Shpenkuh, D. Ortel. Analysis of spectra measured by SI-1 device. *Sovremennye problemy distantsionnogo zondirovaniya Zemli iz kosmosa*, 15(3): 236–242, 2018, (in Russian).

[4] Keeling, C.D. The Concentration and Isotopic Abundances of Carbon Dioxide in the Atmosphere. *Tellus*, 12: 200-203, 1960.

[5] Keeling, C. D, Piper, S. C, Bacastow, R. B, Wahlen, M., Whorf, T. P, Heimann, M., Meijer, H. A. Exchanges of Atmospheric CO2 and ^{13}CO2 with the Terrestrial Biosphere and Oceans from 1978 to 2000. *I. Global Aspects. UC San Diego: Scripps Institution of Oceanography,* 117: 83-113, 2001.

[6] F. Dentener, R. Derwent, E. Dlugokencky, E. Holland, I. Isaksen, J. Katima, V. Kirchhoff, P. Matson,P. Midgley, M. Wang. The Carbon Cycle and Atmospheric Carbon Dioxide In: “Climate Change 2001: The Scientific Basis. Contribution of Working Group I to the Third Assessment Report of the Intergovernmental Panel on Climate Change”. *Cambridge University Press, Cambridge, United Kingdom and New York, NY, USA*, 2001.

[7] Eyring, V., N.P. Gillett, K.M. Achuta Rao, R. Barimalala, M. Barreiro Parrillo, N. Bellouin, C. Cassou, P.J. Durack, Y. Kosaka, S. McGregor, S. Min, O. Morgenstern, Y. Sun. Human Influence on the Climate System. In “Climate Change 2021: The Physical Science Basis. Contribution of Working Group I to the Sixth Assessment Report of the Intergovernmental Panel on Climate Change”. *Cambridge University Press, Cambridge, United Kingdom and New York, NY, USA*, 2021.

[8] Bindoff, N.L., P.A. Stott, K.M. AchutaRao, M.R. Allen, N. Gillett, D. Gutzler, K. Hansingo, G. Hegerl, Y. Hu, S. Jain, I.I. Mokhov, J. Overland, J. Perlwitz, R. Sebbari, X. Zhang. Detection and Attribution of Climate Change: from Global to Regional. In “Climate Change 2013: The Physical Science Basis. Contribution of Working Group I to the Fifth Assessment Report of the Intergovernmental Panel on Climate Change”. *Cambridge University Press, Cambridge, United Kingdom and New York, NY, USA*, 2013.

[9] Stips, A., Macias, D., Coughlan, C., Garcia-Gorriz E., X. San Liang. On the causal structure between CO_2 and global temperature. *Sci Rep*, 6: 21691, 2016.

[10] Chan, D., & Wu, Q. Attributing Observed SST Trends and Subcontinental Land Warming to Anthropogenic Forcing during 1979–2005. *Journal of Climate*, 28(8): 3152-3170, 2015.

[11] Seneviratne, S.I., X. Zhang, M. Adnan, W. Badi, C. Dereczynski, A. Di Luca, S. Ghosh, I. Iskandar, J. Kossin, S. Lewis, F. Otto, I. Pinto, M. Satoh, S.M. Vicente-Serrano, M. Wehner, B. Zhou. Weather and Climate Extreme Events in a Changing Climate. In “Climate Change 2021: The Physical Science Basis. Contribution of Working Group I to the Sixth Assessment Report of the Intergovernmental Panel on Climate Change”. *Cambridge University Press, Cambridge, United Kingdom and New York, NY, USA*, 2021.

[12] Forster, P., T. Storelvmo, K. Armour, W. Collins, J.-L. Dufresne, D. Frame, D.J. Lunt, T. Mauritsen, M.D. Palmer, M. Watanabe, M. Wild, H. Zhang. The Earth’s Energy Budget, Climate Feedbacks, and Climate Sensitivity. In “Climate Change 2021: The Physical Science Basis. Contribution of Working Group I to the Sixth Assessment Report of the Intergovernmental Panel on Climate Change”. *Cambridge University Press, Cambridge, United Kingdom and New York, NY, USA*, 2021.

[13] United Nations Framework Convention on Climate Change (UNFCCC). Kyoto Protocol to the United Nations Framework Convention on Climate Change. 2303: 162, 1998.

[14] United Nations Framework Convention on Climate Change (UNFCCC). The Paris Agreement - Publication. *Paris Climate Change Conference - November 2015*. 2018.

[15] Lwasa, S., K.C. Seto, X. Bai, H. Blanco, K.R. Gurney, Ş. Kılkış, O. Lucon, J. Murakami, J. Pan, A. Sharifi, Y. Yamagata. Urban systems and other settlements. In "IPCC, 2022: Climate Change 2022: Mitigation of Climate Change. Contribution of Working Group III to the Sixth Assessment Report of the Intergovernmental Panel on Climate Change". *Cambridge University Press, Cambridge, UK and New York, NY, USA*, 2022.

[16] D. McMorrow. Methods for Remote Determination of CO2 Emissions. *JASON The MITRE Corporation*. P. 198, 2011

[17] A. Agustí-Panareda, D. Brunner. D5.4 Final report on service elements for CO2 emission and transport model integration. *CHE Consortium*, P. 49, 2020.

[18] K. Rypdal, W. Winiwarter. Uncertainties in greenhouse gas emission inventories — evaluation, comparability and implications. *Environmental Science & Policy*, 4(2–3): 107-116, 2001.

[19] EPA (2022) Inventory of U.S. Greenhouse Gas Emissions and Sinks: 1990-2020. *U.S. Environmental Protection Agency*, *EPA 430-R-22-003*, P. 841, 2022.

[20] T. Oda, R. Bun, V. Kinakh, P. Topylko, M. Halushchak, G. Marland, T. Lauvaux, M. Jonas, S. Maksyutov, Z. Nahorski, M. Lesiv, O. Danylo, J. Horabik-Pyzel. Errors and uncertainties in a gridded carbon dioxide emissions inventory. *Mitig Adapt Strateg Glob Change*, 24: 1007–1050, 2019.

[21] COllaborative Carbon Column Observing Network. [https://www.imk-asf.kit.edu/english/COCCON.php]

[22] Makarova, M. V., Alberti, C., Ionov, D. V., Hase, F., Foka, S. C., Blumenstock, T., Warneke, T., Virolainen, Y. A., Kostsov, V. S., Frey, M., Poberovskii, A. V., Timofeyev, Y. M., Paramonova, N. N., Volkova, K. A., Zaitsev, N. A., Biryukov, E. Y., Osipov, S. I., Makarov, B. K., Polyakov, A. V., Ivakhov, V. M., Imhasin, H. Kh., Mikhailov, E. F. Emission Monitoring Mobile Experiment (EMME): an overview

and first results of the St. Petersburg megacity campaign 2019. *Atmos. Meas. Tech.*, 14: 1047–1073, 2021.

[23] Zhao, X., Marshall, J., Hachinger, S., Gerbig, C., Frey, M., Hase, F., and Chen, J. Analysis of total column CO2 and CH4 measurements in Berlin with WRF-GHG. *Atmos. Chem. Phys.*, 19: 11279–11302, 2019.

[24] Ionov, D. V., Makarova, M. V., Hase, F., Foka, S. C., Kostsov, V. S., Alberti, C., Blumenstock, T., Warneke, T., Virolainen, Y. A. The CO2 integral emission by the megacity of St Petersburg as quantified from ground-based FTIR measurements combined with dispersion modelling. *Atmos. Chem. Phys.*, 21: 10939–10963, 2021.

[25] Timofeyev, Y.M., Nerobelov, G.M., Poberovskii, A.V. Experimental Estimates of Integral Anthropogenic CO2 Emissions in the City of St. Petersburg. *Izv. Atmos. Ocean. Phys*. 58: 237–245, 2022.

[26] Y. M. Timofeyev, G. M. Nerobelov, Ya. A. Virolainen, A. V. Poberovskii, S. C. Foka. Estimates of CO2 anthropogenic emission from the megacity St. Petersburg. *Dokl. Earth Sci*. 494(1): 753–756, 2020.

[27] Kovats, R.S., R. Valentini, L.M. Bouwer, E. Georgopoulou, D. Jacob, E. Martin, M. Rounsevell, J.-F. Soussana. Europe. In “Climate Change 2014: Impacts, Adaptation, and Vulnerability. Part B: Regional Aspects.Contribution of Working Group II to the Fifth Assessment Report of the Intergovernmental Panel on ClimateChange”. *Cambridge University Press, Cambridge, United Kingdom and New York, NY, USA*, 2014.

[28] Flato, G., Gillett, N., Arora, V., Cannon, A. Anstey, J. Modelling Future Climate Change; Chapter 3 in “Canada’s Changing Climate Report”. *Government of Canada, Ottawa, Ontario*, 2019.

[29] V.M. Kattsov and S.M. Semenov. Assessment report on climate change and its consequences in Russian Federation. General Summary. *Roshydromet*, P. 56, 2014.

[30] I.A. Serebritskii. Experience of St Petersburg in managing adaptation to climate change and mitigating anthropogenic impact on the climate system. Information and

analytical note. Web resource - [https://www.infoeco.ru/index.php?id=8780], (in Russian).

[31] Trading Economics. Web resource - [https://tradingeconomics.com]

[32] The World Bank (population change data). Web resource - [https://data.worldbank.org/indicator/SP.POP.TOTL]

[33] P. A. Arias, N. Bellouin, E. Coppola, R. G. Jones, G. Krinner, J. Marotzke, V. Naik, M.D. Palmer, G.K. Plattner, J. Rogelj, M. Rojas, J. Sillmann, T. Storelvmo, P.W. Thorne, B. Trewin. Technical Summary. In "Climate Change 2021: ThePhysical Science Basis. Contribution of Working Group I to the Sixth Assessment Report of the Intergovernmental Panel on Climate Change". *Cambridge University Press, Cambridge, United Kingdom and New York, NY, USA*, 2021.

[34] United Nations Environment Programme (UNEP) Ozone Secretariat. The Montreal Protocol on Substances that Deplete the Ozone Layer, which entered into force January 1, 1989, 26 I.L.M.: 1541, 1550, 1987.

[35] Amendment to the Montreal Protocol on Substances that Deplete the Ozone Layer (Kigali Amendment), 2016.

[36] Gulev, S.K., P.W. Thorne, J. Ahn, F.J. Dentener, C.M. Domingues, S. Gerland, D. Gong, D.S. Kaufman, H.C. Nnamchi, J. Quaas, J.A. Rivera, S. Sathyendranath, S.L. Smith, B. Trewin, K. von Schuckmann, R.S. Vose. Changing State of the Climate System. In "Climate Change 2021: The Physical Science Basis. Contribution of Working Group I to the Sixth Assessment Report of the Intergovernmental Panel on Climate Change". *Cambridge University Press, Cambridge, United Kingdom and New York, NY, USA*, 2021.

[37] WMO. WMO Greenhouse Gas Bulletin - The State of Greenhouse Gases in the Atmosphere Based on Global Observations through 2017. 14: P. 9, 2018.

[38] International Energy Agency (IEA). World Energy Outlook 2021. *IEA, Paris*, P. 386, 2021.

[39] The World Bank (data on gross domestic product for a period of more than 50 years to 2021 worldwide and in individual countries). Web resource - [https://data.worldbank.org/indicator/NY.GDP.MKTP.CD].

[40] Bach W., Crane A.J., Berger A.L., Longhetto A. Carbon dioxide: current views and developments in energy/climate research. *Conference on climate and energy: carbon dioxide, Erice, Italy, 16 Jul 1982*, P. 525, 1983.

[41] T. DeVries. The Ocean Carbon Cycle. *Annual Review of Environment and Resources*, 47(1): 317-34, 2022.

[42] Kirschbaum M.U.F., Mueller R. Net Ecosystem Exchange. *Cooperative Research Centre for Greenhouse Accounting,* P. 139, 2001.

[43] Archer, D., Brovkin, V. The millennial atmospheric lifetime of anthropogenic CO_2. *Climatic Change*. 90: 283–297, 2008.

[44] Timofeyev, Y.M., G.M., Poberovskii, A.V., Filippov N.N. Determining Both Tropospheric and Stratospheric CO2 Contents Using a Ground-Based IR Spectroscopic Method. *Izv. Atmos. Ocean. Phys*. 57: 286–296, 2021.

[45] Nikitenko, A.A., Timofeev, Y.M., Virolainen, Y.A., Nerobelov G.M., Poberovskii A.V. Comparison of Stratospheric CO2 Measurements by Ground- and Satellite-Based Methods. *Atmos Ocean Opt*. 35: 341–344, 2022.

[46] Friedlingstein, P., O'Sullivan, M., Jones, M. W., Andrew, R. M., Hauck, J., Olsen, A., Peters, G. P., Peters, W., Pongratz, J., Sitch, S., Le Quéré, C., Canadell, J. G., Ciais, P., Jackson, R. B., Alin, S., Aragão, L. E. O. C., Arneth, A., Arora, V., Bates, N. R., Becker, M., Benoit-Cattin, A., Bittig, H. C., Bopp, L., Bultan, S., Chandra, N., Chevallier, F., Chini, L. P., Evans, W., Florentie, L., Forster, P. M., Gasser, T., Gehlen, M., Gilfillan, D., Gkritzalis, T., Gregor, L., Gruber, N., Harris, I., Hartung, K., Haverd, V., Houghton, R. A., Ilyina, T., Jain, A. K., Joetzjer, E., Kadono, K., Kato, E., Kitidis, V., Korsbakken, J. I., Landschützer, P., Lefèvre, N., Lenton, A., Lienert, S., Liu, Z., Lombardozzi, D., Marland, G., Metzl, N., Munro, D. R., Nabel, J. E. M. S., Nakaoka, S.-I., Niwa, Y., O'Brien, K., Ono, T., Palmer, P. I., Pierrot, D., Poulter, B., Resplandy, L., Robertson, E., Rödenbeck, C., Schwinger, J., Séférian, R., Skjelvan, I., Smith, A. J. P., Sutton, A. J., Tanhua, T., Tans, P. P., Tian, H., Tilbrook, B., van der Werf, G., Vuichard, N., Walker, A. P., Wanninkhof, R., Watson, A. J., Willis, D., Wiltshire, A. J., Yuan, W., Yue, X., Zaehle, S. Global Carbon Budget 2020, *Earth Syst. Sci. Data*, 12: 3269–3340, 2020.

[47] Yue T.X., Zhang L.L., Zhao M.W., Wang Y.F., Wilson J. Space- and ground-based CO2 measurements: A review. *Science China Earth Sciences*, 59: 2089–2097, 2016.

[48] Różański K., Chmura Ł., Gałkowski M., N. Jarosław, Z. Mirosław, B. Jakub, O'D. Simon. Monitoring of Greenhouse Gases in the Atmosphere – A Polish Perspective. *Papers on Global Change*, 23: 111–126, 2016.

[49] V.I. Binenko, A.I. Reshetnikov, N.O. Shevchuk. The variability of anomalies of surface air temperature and the concentration of greenhouse gases on the basis of ground and satellite measurements at the regional level. Uchenie zapiski RGGMU, 38: 175-187, 2015, (in Russian).

[50] Timofeev Yu.M., I.A. Berezin, Ya.A. Virolainen, M.V. Makarova, A.V. Polyakov, A.V. Poberovsky, N.N. Filippov, S.Ch. Foka. Spatial-temporal CO2 variations near St. Petersburg based on satellite and ground-based measurements. *Izvestiya, atmospheric and oceanic physics*, 55(1): 65-72, 2019.

[51] Rokotyan N.V., Imasu R., Zakharov V.I., Gribanov K.G., Khamatnurova M.Yu. The amplitude of the CO2 seasonal cycle in the atmosphere of Ural by ground-based and satellite remote sensing techniques. *Optica atmosphere i okeana*, 27(9): 819–825, 2014, (in Russian).

[52] S.-J. Wang, L. Cao, N. Li. Responses of the ocean carbon cycle to climate change: Results from an earth system climate model simulation. *Advances in Climate Change Research*, 5(3): 123-130, 2014.

[53] WMO. The Global Atmosphere Watch Programme: 25 Years of Global Coordinated Atmospheric Composition Observations and Analyses. *WMO*, P. 48, 2014.

[54] WMO. Global Atmosphere Watch measurements guide. *WMO*, P. 87, 2001.

[55] What is the Global Greenhouse Gas Reference Network? Web resource - [https://gml.noaa.gov/ccgg/ggrn.php].

[56] Earth System Research Laboratories. Web resource - [https://www.esrl.noaa.gov/]

[57] Hari P., E. Nikinmaa, T. Pohja, E. Siivola, J. Bäck, T. Vesala, M. Kulmala. Station for Measuring Ecosystem-Atmosphere Relations: SMEAR. *Physical and Physiological Forest Ecology. Springer, Dordrecht*, 471–487, 2013.

[58] Hazan L., Tarniewicz J., Ramonet M., Laurent O., Abbaris A. Automatic processing of atmospheric CO_2 and CH_4 mole fractions at the ICOS Atmosphere Thematic Centre. *Atmos. Meas. Tech.*, 9: 4719–4736, 2016.

[59] Alferov A.M., Blinov V.G., Gitarsky M.L., Grabar V.A., Zamolodchikov D.G., Zinchenko A.V., Ivanova N.P., Ivakhov V.M., Karaban R. .T., Karelin D.V., Kalyuzhny I.L., Kashin F.V., Konyushkov D.E., Korotkov V.N., Krovotyntsev V.A., Lavrov S.A., Marunich A.S. ., Paramonova N.N., Romanovskaya A.A., Trunov A.A., Shilkin A.V., Yuzbekov A.K. Monitoring greenhouse gas fluxes in natural ecosystems. *Monograph. Saratov: Amrit,* P. 279, 2017 (in Russian).

[60] Belikov D., Arshinov M., Belan B., Davydov D., Fofonov A., Sasakawa M., Machida T. Analysis of the Diurnal, Weekly, and Seasonal Cycles and Annual Trends in Atmospheric CO_2 and CH_4 at Tower Network in Siberia from 2005 to 2016. *Atmosphere*, 10(11): 689, 2019.

[61] M.Yu. Arshinov, B.D. Belan, D.K. Davydov, G.M. Krekov, A.V. Fofonov, S.V. Babchenko, G. Inoue, T. Machida, Sh. Maksutov, M. Sasakawa, K. Shimoyama. The dynamics in vertical distribution of greenhouse gases in the atmosphere. *Optica atmospheri i okeana*, 25(12): 1051-1061, 2012 (in Russian).

[62] Foka S.Ch., M.V. Makarova, A.V. Poberovsky, Yu.M. Timofeev. Temporal variations in CO2, CH4 and CO concentrations in Saint-Petersburg suburb (Peterhof). *Optica atmospheri i okeana*, 32(10): 860–866, 2012 (in Russian).

[63] Makarova M.V., D.K. Arabadzhyan, S.Ch. Foka, N.N. Paramonova, A.V. Poberovskii, Yu.M. Timofeev, N.V. Pankratova, V.S. Rakitin. Estimation of Nocturnal Area Fluxes of Carbon Cycle Gases in Saint Petersburg Suburbs. *Russ. Meteorol. Hydrol*. 43: 449–455, 2018.

[64] Arabadzhyan D.K., Paramonova N.N., Makarova M.V., Poberovsky A.V. Analysis of temporal variability of methane concentration in the atmosphere based on ground-based observations. *Vestnik SPbGU*, 2(4): 204-215, 2015 (in Russian).

[65] Arefiev V.N., N.E. Kamenogradsky, F.V. Kashin, A.V. Shilkin. Background component of carbon dioxide concentration in the near-surface air. *Izv. RAN. Physica atmospheri i okeana*, 50(6): 655–662, 2014 (in Russian).

[66] Total Carbon Column Observing Network. Web resource - [http://www.tccon.caltech.edu/]

[67] Wunch D., Toon G.C., Blavier J.-F.L., Washenfelder R.A., Notholt J., Connor B.J., Griffith D.W.T., Sherlock V., Wennberg P.O. The Total Carbon Column Observing Network. *Phil. Trans. R. Soc. A*, 369(1943): 2087–2112, 2011.

[68] Hase F., Hannigan J., Coffey M.T., Goldman A., Hopfner M., Jones N. B., Rinsland C.P., Wood S.W. Intercomparison of retrieval codes used for the analysis of high-resolution, ground-based FTIR measurements. *Journal Of Quantitative Spectroscopy & Radiative Transfer*, 87: 25-52, 2004.

[69] Zeng Z.-C., Natraj V., Xu F., Chen S., Gong F.-Y., Pongetti T. J., Sung K., Toon G., Sander S.P., Yung Y.L. GFIT3: a full physics retrieval algorithm for remote sensing of greenhouse gases in the presence of aerosols. *Atmos. Meas. Tech.*, 14: 6483–6507, 2021.

[70] Frey M., Sha M.K., Hase F., Kiel M., Blumenstock T., Harig R., Surawicz G., Deutscher N. M., Shiomi K., Franklin J. E., Bösch H., Chen J., Grutter M., Ohyama H., Sun Y., Butz A., Mengistu Tsidu G., Ene D., Wunch D., Cao Z., Garcia O., Ramonet M., Vogel F., Orphal J. Building the COllaborative Carbon Column Observing Network (COCCON): long-term stability and ensemble performance of the EM27/SUN Fourier transform spectrometer. *Atmos. Meas. Tech.*, 12: 1513–1530, 2019.

[71] Frey M., Hase F., Blumenstock T., Groß J., Kiel M., Mengistu Tsidu G., Schäfer K., Sha M. K., Orphal J. Calibration and instrumental line shape characterization of a set of portable FTIR spectrometers for detecting greenhouse gas emissions. *Atmos. Meas. Tech.*, 8: 3047–3057, 2015.

[72] Hase F., Frey M., Blumenstock T., Groß J., Kiel M., Kohlhepp R., Mengistu Tsidu G., Schäfer K., Sha M. K., Orphal J. Application of portable FTIR

spectrometers for detecting greenhouse gas emissions of the major city Berlin. *Atmos. Meas. Tech.*, 8: 3059–3068, 2015.

[73] De Mazière M., Thompson A.M., Kurylo M.J., Wild J.D., Bernhard G., Blumenstock T., Braathen G.O., Hannigan J.W., Lambert J.-C., Leblanc T., McGee T.J., Nedoluha G., Petropavlovskikh I., Seckmeyer G., Simon P.C., Steinbrecht W., Strahan S.E. The Network for the Detection of Atmospheric Composition Change (NDACC): history, status and perspectives. *Atmos. Chem. Phys.*, 18: 4935–4964, 2018.

[74] Barthlott S., Schneider M., Hase F., Wiegele A., Christner E., González Y., Blumenstock T., Dohe S., García O.E., Sepúlveda E., Strong K., Mendonca J., Weaver D., Palm M., Deutscher N.M., Warneke T., Notholt J., Lejeune B., Mahieu E., Jones N., Griffith D. W.T., Velazco V. A., Smale D., Robinson J., Kivi R., Heikkinen P., Raffalski U. Using XCO2 retrievals for assessing the long-term consistency of NDACC/FTIR data sets. *Atmos. Meas. Tech.*, 8: 1555–1573, 2015.

[75] Timofeyev Yu., Ya. Virolainen, M. Makarova, A. Poberovsky, A. Polyakov, D. Ionov, S. Osipov, H. Imhasin. Ground-based spectroscopic measurements of atmospheric gas composition near Saint Petersburg (Russia). *J. Mol.Spectr.*, 323: 2–14, 2016.

[76] Virolainen Y.A. Methodical Aspects of the Determination of Carbon Dioxide in Atmosphere Using FTIR Spectroscopy. *J Appl Spectrosc*. 85: 462–469, 2018.

[77] Makarova M.V., O. Kirner, Yu.M. Timofeev, A.V. Poberovskii, Kh.Kh. Imkhasin, S.I. Osipov, B.K. Makarov. Analysis of methane total column variations in the atmosphere near St. Petersburg using ground-based measurements and simulations. *Izvestiya, Atmospheric and Oceanic Physics*, 51(2): 177–185, 2015.

[78] M. Zhou, Q. Ni, Z. Cai, B. Langerock, W. Nan, Ya. Yang, Ke. Che, Dongxu Yang, Ting Wang, Yi Liu, Pucai Wang. CO2 in Beijing and Xianghe Observed by Ground-Based FTIR Column Measurements and Validation to OCO-2/3 Satellite. *Observations.Remote Sens*, 14: 3769, 2022.

[79] Peylin P., F.M. Bre´on, S. Serrar, Y. Tiwari, A. Che´din, M. Gloor, T. Machida, C. Brenninkmeijer, A. Zahn, P. Ciais. Evaluation of Television Infrared Observation

Satellite (TIROS-N) Operational Vertical Sounder (TOVS) spaceborne CO2 estimates using model simulations and aircraft data. *J. Geophys. Res.*, 112: D09313, 2007.

[80] H. Kobayashi, A. Shimota, K. Kondo, E. Okumura, Y. Kameda, H. Shimoda, T. Ogawa. Development and evaluation of the interferometric monitor for greenhouse gases: a high-throughput Fourier-transform infrared radiometer for nadir Earth observation. *Appl. Opt.* 38: 6801-6807, 1999.

[81] Observing Systems Capability Analysis and Review Tool (OSCAR). Web resource - https://space-test.oscar.wmo.int/oscar-test/instruments/view/img

[82] Crevoisier C., Chédin A., Matsueda H., Machida T., Armante R., Scott N.A. First year of upper tropospheric integrated content of CO_2 from IASI hyperspectral infrared observations. *Atmos. Chem. Phys.*, 9: 4797–4810, 2009.

[83] Kulawik S.S., Jones D.B.A., Nassar R., Irion F.W., Worden J.R., Bowman K.W., Machida T., Matsueda H., Sawa Y., Biraud S. C., Fischer M.L., Jacobson, A.R. Characterization of Tropospheric Emission Spectrometer (TES) CO_2 for carbon cycle science. *Atmos. Chem. Phys.*, 10: 5601–5623, 2010.

[84] C. Moustafa T., T. S. Pagano, H. H. Aumann, R. Atlas, C. Barnet, J. Blaisdell, L. Chen, M. Divakarla, E. J. Fetzer, M. Goldberg, C. Gautier, S. Granger, S. Hannon, F. W. Irion, R. Kakar, E. Kalnay, B. H. Lambrigtsen, S.-Y. Lee, J.L. Marshall, W. Wallace Mcmillan, L. Mcmillin, E.T. Olsen, H. Revercomb, P. Rosenkranz, W.L. Smith, D. Staelin, L.L. Strow, J. Susskind, D. Tobin, W. Wolf, L. Zhou. AIRS. *Bulletin of the American Meteorological Society*, 87(7): 911-926, 2006.

[85] M. Reuter, H. Bovensmann, M. Buchwitz, J. P. Burrows, B. J. Connor, N. M. Deutscher, D. W. T. Griffith, J. Heymann, G. Keppel-Aleks, J. Messerschmidt, J. Notholt, C. Petri, J. Robinson, O. Schneising, V. Sherlock, V. Velazco, T. Warneke, P. O. Wennberg, D. Wunch. Retrieval of atmospheric CO2 with enhanced accuracy and precision from SCIAMACHY: Validation with FTS measurements and comparison with model results. *J. Geophys. Res.*, 116: D04301, 2021.

[86] Peiro, H., Crowell, S., Schuh, A., Baker, D. F., O'Dell, C., Jacobson, A. R., Chevallier, F., Liu, J., Eldering, A., Crisp, D., Deng, F., Weir, B., Basu, S., Johnson,

M. S., Philip, S., Baker, I. Four years of global carbon cycle observed from the Orbiting Carbon Observatory 2 (OCO-2) version 9 and in situ data and comparison to OCO-2 version 7. *Atmos. Chem. Phys.*, 22: 1097–1130, 2022.

[87] Yang, D., Liu, Y., Boesch, H. et al. A New TanSat XCO2 Global Product towards Climate Studies. *Adv. Atmos. Sci.*, 38: 8–11, 2021.

[88] O'Dell, C. W., Eldering, A., Wennberg, P. O., Crisp, D., Gunson, M. R., Fisher, B., Frankenberg, C., Kiel, M., Lindqvist, H., Mandrake, L., Merrelli, A., Natraj, V., Nelson, R. R., Osterman, G. B., Payne, V. H., Taylor, T. E., Wunch, D., Drouin, B. J., Oyafuso, F., Chang, A., McDuffie, J., Smyth, M., Baker, D. F., Basu, S., Chevallier, F., Crowell, S. M. R., Feng, L., Palmer, P. I., Dubey, M., García, O. E., Griffith, D. W. T., Hase, F., Iraci, L. T., Kivi, R., Morino, I., Notholt, J., Ohyama, H., Petri, C., Roehl, C. M., Sha, M. K., Strong, K., Sussmann, R., Te, Y., Uchino, O., Velazco, V. A. Improved retrievals of carbon dioxide from Orbiting Carbon Observatory-2 with the version 8 ACOS algorithm. *Atmos. Meas. Tech.*, 11: 6539–6576, 2018.

[89] Pearman, G. I., Hyson, P., Fraser, P. J. The global distribution of atmospheric carbon dioxide: 1. Aspects of observations and modeling. *J. Geophys. Res.*, 88(C6): 3581-3590, 1983.

[90] Jiang, X., Q. Li, M.-C. Liang, R.-L. Shia, M. T. Chahine, E. T. Olsen, L. L. Chen, Y. L. Yung. Simulation of upper tropospheric CO 2 from chemistry and transport models. *Global Biogeochem. Cycles*, 22: GB4025, 2008.

[91] Wang Q., Mustafa F., Bu L., Yang J., Fan C., Liu J., Chen W. Monitoring of Atmospheric Carbon Dioxide over a Desert Site Using Airborne and Ground Measurements. *Remote Sens.*, 14: 5224, 2022.

[92] Cheng Y. , An X., Yun F., Zhou L., Liu L., Fang S., Xu L. Simulation of CO2 variations at Chinese background atmospheric monitoring stations between 2000 and 2009: Applying a CarbonTracker model. *Chin. Sci. Bull.*, 58: 3986–3993, 2013.

[93] Park C., Park S.-Y., Gurney K.R., Gerbig C., DiGangi J.P., Choi Y., Hwa W.L.. Numerical simulation of atmospheric CO2 concentration and flux over the Korean

Peninsula using WRF-VPRM model during Korus-AQ 2016 campaign. *PLoS ONE*, 15(1): e0228106, 2020.

[94] Balsamo G., Engelen R., Thiemert D., Agusti-Panareda A., Bousserez N., Broquet G., Brunner D., Buchwitz M., Chevallier F., Choulga M., Denier Van Der Gon H., Florentie L., Haussaire J.-M., Janssens-Maenhout G.,Jones M.W., Kaminski T., Krol M., Le Quéré C., Marshall J., McNorton J., Prunet P., Reuter M., Peters W., Scholze M. The CO2 Human Emissions (CHE) Project: First Steps Towards a European Operational Capacity to Monitor Anthropogenic CO2 Emissions. *Front. Remote Sens.*, 2: 707247, 2021.

[95] Cory R. Martin, N. Zeng, A. Karion, K. Mueller, S. Ghosh, I. Lopez-Coto, K.R. Gurney, T. Oda, K. Prasad, Y. Liu, R.R. Dickerson, J. Whetstone. Investigating sources of variability and error in simulations of carbon dioxide in an urban region. *Atmospheric Environment*, 199: 55-69, 2019.

[96] T. Zheng, R. Nassar, M. Baxter. Estimating power plant CO2 emission using OCO-2 XCO2 and high resolution WRF-Chem simulations. *Environmental Research Letters*, 14(8), 2019.

[97] R. Lei, S. Feng, A. Danjou, G. Broquet, D. Wu, J. C. Lin, C. W. O'Dell, T. Lauvaux. Fossil fuel CO2 emissions over metropolitan areas from space: A multi-model analysis of OCO-2 data over Lahore, Pakistan. *Remote Sensing of Environment*, 264: 112625, 2021.

[98] McGuffie K., Henderson-Sellers A. Forty years of numerical climate modelling. *Int. J. Climatol.*, 21: 1067-1109, 2001.

[99] Flato, G., Gillett, N., Arora, V., Cannon, A., Anstey, J. Modelling Future Climate Change. *Chapter 3 in Canada's Changing Climate Report*, *Government of Canada, Ottawa, Ontario*, 74–111, 2019.

[100] Chiodo G., Polvani L.M., Marsh D.R., Stenke A., Ball W., Rozanov E., Muthers S., Tsigaridis K. The response of the ozone layer to quadrupled CO2 concentrations. *J Clim*., 32(22): 7629-7642, 2019.

[101] Sukhodolov, T., Egorova, T., Stenke, A., Ball, W. T., Brodowsky, C., Chiodo, G., Feinberg, A., Friedel, M., Karagodin-Doyennel, A., Peter, T., Sedlacek, J., Vattioni,

S., Rozanov, E. Atmosphere–ocean–aerosol–chemistry–climate model SOCOLv4.0: description and evaluation. *Geosci. Model Dev.*, 14: 5525–5560, 2021.

[102] Mauritsen, T., Bader, J., Becker, T., Behrens, J., Bittner, M., Brokopf, R., Brovkin, V., Claussen, M., Crueger, T., Esch, M., Fast, I., Fiedler, S., Fläschner, D., Gayler, V., Giorgetta, M., Goll, D. S., Haak, H., Hagemann, S., Hedemann, C., Hohenegger, C., Ilyina, T., Jahns, Th., Jimenéz-de-la-Cuesta, D., Jungclaus, J., Kleinen, Th., Kloster, S., Kracher, D., Kinne, S., Kleberg, D., Lasslop, G., Kornblueh, L., Marotzke, J., Matei, D., Meraner, K., Mikolajewicz, U., Modali, K., Möbis, B., Müller, W. A., Nabel, J. E. M. S., Nam, C. C. W., Notz, D., Nyawira, S.-S., Paulsen, H., Peters, K., Pincus, R., Pohlmann, H., Pongratz, J., Popp, M., Raddatz, Th. J., Rast, S., Redler, R., Reick, Ch. H., Rohrschneider, T., Schemann, V., Schmidt, H., Schnur, R., Schulzweida, U., Six, K. D., Stein, L., Stemmler, I., Stevens, B., von Storch, J.-S., Tian, F., Voigt, A., Vrese, Ph., Wieners, K.-H., Wilkenskjeld, S., Winkler, A., Roeckner, E. Developments in the MPI-M Earth System Model version 1.2 (MPI-ESM1.2) and its response to increasing CO2. *J. Adv. Model. Earth Sy.*, 11: 998–1038, 2019.

[103] Egorova, T., Rozanov, E., Zubov, V., Karol, I. Model for investigating ozone trends (MEZON). *Izvestiya, Atmos. Ocean. Phys.*, 39: 277–292, 2003.

[104] Weisenstein, D.K., Yue, G.K., Ko, M.K. W., Sze, N.-D., Rodriguez, J. M., Scott, C. J. A two-dimensional model of sulfur species and aerosols. *J. Geophys. Res.*, 102: 13019–13035, 1997.

[105] Skamarock, W. C., Klemp, J. B., Dudhia, J., Gill, D. O., Liu, Z., Berner, J., Wang, W., Powers, J.G., Duda, M.G., Barker, D., Huang, X. -yu. A Description of the Advanced Research WRF Model Version 4.1 (No. NCAR/TN-556+STR), P. 162, 2019, Web resource - [https://opensky.ucar.edu/islandora/object/technotes%3A576].

[106] Grell G.A., S.E. Peckham, R. Schmitz, S.A. McKeen, G. Frost, W.C. Skamarock, B. Eder. Fully coupled 'online' chemistry in the WRF model. *Atmos. Environ,* 39: 6957-6976, 2005.

[107] Beck, V., T. Koch, R. Kretschmer, J. Marshall, R. Ahmadov, C. Gerbig, D. Pillai, M. Heimann. The WRF Greenhouse Gas Model (WRF-GHG). *Technical Report No. 25*. *Max Planck Institute for Biogeochemistry, Jena, Germany,* P. 81, 2011.

[108] Oda, T., Maksyutov, S., and Andres, R. J. The Open-source Data Inventory for Anthropogenic CO2, version 2016 (ODIAC2016): a global monthly fossil fuel CO2 gridded emissions data product for tracer transport simulations and surface flux inversions. *Earth Syst. Sci. Data*, 10: 87–107, 2018.

[109] Bofeng Cai, Sai Liang, Jiong Zhou, Jinnan Wang, Libin Cao, Shen Qu, Ming Xu, Zhifeng Yang. China high resolution emission database (CHRED) with point emission sources, gridded emission data, and supplementary socioeconomic data. *Resources, Conservation and Recycling*, 129: 232-239, 2018.

[110] Liu Zhu, Bofeng Cai. High-resolution Carbon Emissions Data for Chinese Cities. *Paper, Environment and Natural Resources Program*, *Belfer Center*, 2018.

[111] Xinwanghao Xu, Hong Huo, Jingru Liu, Yuli Shan, Yuan Li, Heran Zheng, Dabo Guan, Zhiyun Ouyang, Patterns of CO2 emissions in 18 central Chinese cities from 2000 to 2014. *Journal of Cleaner Production*, 172: 529-540, 2018.

[112] Bergamaschi, P., A. Danila, R. F. Weiss, P. Ciais, R. L. Thompson, D. Brunner, I. Levin, Y. Meijer, F. Chevallier, G. Janssens-Maenhout, H. Bovensmann, D. Crisp, S. Basu, E. Dlugokencky, R. Engelen, C. Gerbig, D. Günther, S. Hammer, S. Henne, S. Houweling, U. Karstens, E. Kort, M. Maione, A. J. Manning, J. Miller, S. Montzka, S. Pandey, W. Peters, P. Peylin, B. Pinty, M. Ramonet, S. Reimann, T. Röckmann, M. Schmidt, M. Strogies, J. Sussams, O. Tarasova, J. van Aardenne, A. T. Vermeulen, F. Vogel. Atmospheric monitoring and inverse modelling for verification of greenhouse gas inventories. *EUR 29276 EN, Publications Office of the European Union, Luxembourg*, 2018.

[113] Super, I., Dellaert, S. N. C., Visschedijk, A. J. H., Denier van der Gon, H. A. C. Uncertainty analysis of a European high-resolution emission inventory of CO2 and CO to support inverse modelling and network design. *Atmos. Chem. Phys.*, 20: 1795–1816, 2020.

[114] M. Crippa, D. Guizzardi, E. Pisoni, E. Solazzo, A. Guion, M. Muntean, A. Florczyk, M. Schiavina, M. Melchiorri, A. Fuentes Hutfilte. Global anthropogenic emissions in urban areas: patterns, trends, and challenges. *Environ. Res. Lett.*, 16: 074033, 2021.

[115] Feng, L., Palmer, P. I., Yang, Y., Yantosca, R. M., Kawa, S. R., Paris, J.-D., Matsueda, H., Machida, T. Evaluating a 3-D transport model of atmospheric CO2 using ground-based, aircraft, and space-borne data. *Atmos. Chem. Phys.*, 11: 2789–2803, 2011.

[116] Hakkarainen J., Ialongo I., Tamminen J. Direct space-based observations of anthropogenic CO_2 emission areas from OCO-2. *Geophys. Res. Lett.,* 43: 11.400–11.406, 2016.

[117] Maksyutov, S., Oda, T., Saito, M., Janardanan, R., Belikov, D., Kaiser, J. W., Zhuravlev, R., Ganshin, A., Valsala, V. K., Andrews, A., Chmura, L., Dlugokencky, E., Haszpra, L., Langenfelds, R. L., Machida, T., Nakazawa, T., Ramonet, M., Sweeney, C., Worthy, D. Technical note: A high-resolution inverse modelling technique for estimating surface CO_2 fluxes based on the NIES-TM–FLEXPART coupled transport model and its adjoint. *Atmos. Chem. Phys.*, 21: 1245–1266, 2021.

[118] Monteil, G., Broquet, G., Scholze, M., Lang, M., Karstens, U., Gerbig, C., Koch, F.-T., Smith, N. E., Thompson, R. L., Luijkx, I. T., White, E., Meesters, A., Ciais, P., Ganesan, A. L., Manning, A., Mischurow, M., Peters, W., Peylin, P., Tarniewicz, J., Rigby, M., Rödenbeck, C., Vermeulen, A., Walton, E. M. The regional European atmospheric transport inversion comparison, EUROCOM: first results on European-wide terrestrial carbon fluxes for the period 2006–2015. *Atmos. Chem. Phys.*, 20: 12063–12091, 2020.

[119] Timofeyev Yu.M., Polyakov A.V. Mathematical aspects of ill-posed problems of atmospheric optics solution: study book. *SPb.: publisher S.-Peterb. un-ta*, P. 188, 2001 (in Russian).

[120] A. N. Tihonov. About regularization of ill-posed problems. Dokl. AN SSSR, 153(1): 49–52, 1963 (in Russian).

[121] Chandra, N., Patra, P. K., Niwa, Y., Ito, A., Iida, Y., Goto, D., Morimoto, S., Kondo, M., Takigawa, M., Hajima, T., Watanabe, M. Estimated regional CO2 flux and uncertainty based on an ensemble of atmospheric CO2 inversions. *Atmos. Chem. Phys.*, 22: 9215–9243, 2022.

[122] Menke W. Geophysical data analysis: discrete inverse theory. *San Diego:Academic Press*, P. 285, 1984.

[123] Houweling S., I. Aben, F.-M. Breon, F. Chevallier, N. Deutscher, R. Engelen, C. Gerbig, D. Griffith, K. Hungershoefer, R. Macatangay, J. Marshall, J. Notholt, W. Peters, S. Serrar. The importance of transport model uncertainties for the estimation of CO2 sources and sinks using satellite measurements. *Atmos. Chem. Phys.* 10: 9981–9992, 2010.

[124] Peylin, P., Law, R. M., Gurney, K. R., Chevallier, F., Jacobson, A. R., Maki, T., Niwa, Y., Patra, P. K., Peters, W., Rayner, P. J., Rödenbeck, C., van der Laan-Luijkx, I. T., Zhang, X. Global atmospheric carbon budget: results from an ensemble of atmospheric CO2 inversions. *Biogeosciences*, 10: 6699–6720, 2013.

[125] Jacob, Daniel J. Introduction to Atmospheric Chemistry. *Princeton: Princeton University Press*, P. 264, 1999.

[126] Velasco, E., Roth, M., Tan, S. H., Quak, M., Nabarro, S. D. A., Norford, L. The role of vegetation in the CO2 flux from a tropical urban neighbourhood. *Atmos. Chem. Phys.*, 13: 10185–10202, 2013.

[127] Chen, J., Viatte, C., Hedelius, J. K., Jones, T., Franklin, J. E., Parker, H., Gottlieb, E. W., Wennberg, P. O., Dubey, M. K., Wofsy, S. C. Differential column measurements using compact solar-tracking spectrometers. *Atmos. Chem. Phys.*, 16: 8479–8498, 2016.

[128] Viatte, C., Lauvaux, T., Hedelius, J. K., Parker, H., Chen, J., Jones, T., Franklin, J. E., Deng, A. J., Gaudet, B., Verhulst, K., Duren, R., Wunch, D., Roehl, C., Dubey, M. K., Wofsy, S., Wennberg, P. O. Methane emissions from dairies in the Los Angeles Basin. *Atmos. Chem. Phys.*, 17: 7509–7528, 2017.

[129] Dietrich F., Chen J., Voggenreiter B., Aigner P., Nachtigall N., Reger B. MUCCnet: Munich Urban Carbon Column network. *Atmos. Meas. Tech.*, 14: 1111–1126, 2021.

[130] Gisi, M., Hase, F., Dohe, S., Blumenstock, T., Simon, A., Keens, A. XCO2-measurements with a tabletop FTS using solar absorption spectroscopy. *Atmos. Meas. Tech.*, 5: 2969–2980, 2012.

[131] A. Font, Timothy B., I.S. Mudway, E. Purdie, C. Dunster, C.W. Fuller. Degradation in urban air quality from construction activity and increased traffic arising from a road widening scheme. *Science of The Total Environment*, 497–498: 123-132, 2014.

[132] Denzler, B., Bogdal, C., Kern, C., Tobler, A., Huo, J., Hungerbühler, K. Urban source term estimation for mercury using a boundary-layer budget method. *Atmos. Chem. Phys.*, 19: 3821–3831, 2019.

[133] Ionov D.V., A.V. Poberovsky. Integral emission of nitrogen oxides from the territory of St Petersburg according to mobile measurements and numerical modeling results. *Izv. RAN, PhAO*, 53(2): 232–241, 2017 (in Russian).

[134] Tomohiro O., Maksyutov S. ODIAC Fossil Fuel CO2 Emissions Dataset (Version name: ODIAC2020b). *Center for Global Environmental Research, National Institute for Environmental Studies,* 2015.

[135] Lin J.C., Gerbig C., Wofsy S.C., Andrews A.E., Daube B.C., Davis K.J., Grainger C.A. A near-field tool for simulating the upstream influence of atmospheric observations: The Stochastic Time-Inverted Lagrangian Transport (STILT) model. *J. Geophys. Res.*, 108: 4493, 2003.

[136] Callewaert, S., Brioude, J., Langerock, B., Duflot, V., Fonteyn, D., Müller, J.-F., Metzger, J.-M., Hermans, C., Kumps, N., Ramonet, M., Lopez, M., Mahieu, E., De Mazière, M. Analysis of CO2, CH4, and CO surface and column concentrations observed at Réunion Island by assessing WRF-Chem simulations. *Atmos. Chem. Phys.*, 22: 7763–7792, 2022.

[137] Nerobelov G., Timofeyev Y., Smyshlyaev S., Foka S., Mammarella I., Virolainen Y. Validation of WRF-Chem Model and CAMS Performance in Estimating

Near-Surface Atmospheric CO2 Mixing Ratio in the Area of Saint Petersburg (Russia). *Atmosphere*, 12(3): 387, 2021.

[138] Nerobelov G.M., Timofeyev Yu.M., Smyshlyaev S.P., Foka S.Ch., Imhasin H.H. Comparison of CO2 Content in the Atmosphere of St. Petersburg According to Numerical Modeling and Observations. *Izv. Atmos. Ocean. Phys.* 59: 275–286, 2023.

[139] Kempeneers, F. Sedano, L. Seebach, P. Strobl J. San-Miguel-Ayanz. Data Fusion of Different Spatial Resolution Remote Sensing Images Applied to Forest-Type Mapping. *IEEE Transactions on Geoscience and Remote Sensing*, 49(12): 4977-4986, 2011.

[140] Kilkki J., Aalto T., Hatakka J., Portin H., Laurila T. Atmospheric CO2 observations at Finnish urban and rural sites. *Boreal Env. Res.* 20: 227–242, 2015.

[141] A. Carlos, Q. Tu, F. Hase, M. V. Makarova, K. Gribanov, S.C. Foka, V. Zakharov, T. Blumenstock, M. Buchwitz, C. Diekmann, B. Ertl , M.M. Frey, H. Kh. Imhasin, D.V. Ionov, F. Khosrawi, S.I. Osipov, M. Reuter, M. Schneider, T. Warneke. Investigation of spaceborne trace gas products over St Petersburg and Yekaterinburg, Russia, by using COllaborative Column Carbon Observing Network (COCCON) observations. *Atmos. Meas. Tech*. 15: 2199–2229, 2022.

[142] Mlawer, E. J., Taubman, S. J., Brown, P. D., Iacono, M. J., Clough, S. A. Radiative transfer for inhomogeneous atmospheres: RRTM, a validated correlated-k model for the longwave. *J. Geophys. Res.*, 102(D14): 16663–16682, 1997.

[143] Dudhia, J. Numerical Study of Convection Observed during the Winter Monsoon Experiment Using a Mesoscale Two-Dimensional Model. *J. Atmos. Sci.*, 46: 3077–3107, 1989.

[144] Janjic Zavisa I. The Step–Mountain Eta Coordinate Model: Further developments of the convection, viscous sublayer, and turbulence closure schemes. *Mon. Wea. Rev.*, 122: 927–945, 1994.

[145] Monin A. S., A. M. Obukhov. Basic laws of turbulent mixing in the surface layer of the atmosphere. *Contrib Geophys Inst Acad Sci USSR*, 151:163–187, 1954.

[146] Janjic Zavisa I. The surface layer in the NCEP Eta Model. *Eleventh conference on numerical weather prediction. Norfolk, VA*, *19–23 August 1996*. *Amer Meteor Soc, Boston, MA*, 354–355, 1996.

[147] Chen F., J. Dudhia. Coupling an Advanced Land Surface-Hydrology Model with the Penn State-NCAR MM5 Modeling System. Part I: Model Implementation and Sensitivity. *Mon. Wea. Rev.*, 129: 569-585, 2001.

[148] Grell Georg A. Prognostic Evaluation of Assumptions Used by Cumulus Parameterizations. *Mon. Wea. Rev.*, 121: 764–787, 1993.

[149] Hong S.–Y., J.–O. J. Lim The WRF single–moment 6–class microphysics scheme (WSM6). *J. Korean Meteor. Soc.*, 42: 129–151, 2006.

[150] Salamanca, F., A. Martilli. A new building energy model coupled with an urban canopy parameterization for urban climate simulations—part II. Validation with one dimension off–line simulations. *Theor. Appl. Climatol.*, 99: 345–356, 2010.

[151] H. Hersbach, B. Bell, P. Berrisford, S. Hirahara, A. Horányi, J. Muñoz-Sabater, J. Nicolas, C. Peubey, R. Radu, D. Schepers, A. Simmons, C. Soci, S. Abdalla, X. Abellan, G. Balsamo, P. Bechtold, G. Biavati, J. Bidlot, M. Bonavita, G. De Chiara, P. Dahlgren, D. Dee, M. Diamantakis, R. Dragani, J. Flemming, R. Forbes, M. Fuentes, A. Geer, L. Haimberger, S. Healy, R.J. Hogan, E. Hólm, M. Janisková, S. Keeley, P. Laloyaux, P. Lopez, C. Lupu, G. Radnoti, P. de Rosnay, I. Rozum, F. Vamborg, S. Villaume, J.-N. Thépaut. The ERA5 global reanalysis. *Q J R Meteorol Soc.*, 146: 1999-2049, 2020.

[152] Hersbach, H., Bell, B., Berrisford, P., Biavati, G., Horányi, A., Muñoz Sabater, J., Nicolas, J., Peubey, C., Radu, R., Rozum, I., Schepers, D., Simmons, A., Soci, C., Dee, D., Thépaut, J-N. ERA5 hourly data on single levels from 1959 to present. *Copernicus Climate Change Service (C3S) Climate Data Store (CDS)*, 2018.

[153] A. R. Jacobson, K. N. Schuldt, J. B. Miller, P. Tans, A. Andrews, J. Mund, T. Aalto, P. Bakwin, P. Bergamaschi, S. C. Biraud, H. Chen, A. Colomb, S. Conil, P. Cristofanelli, K. Davis, M. Delmotte, J. P. DiGangi, E. Dlugokencky, L. Emmenegger, M. L. Fischer, J. Hatakka, M. Heliasz, O. Hermanssen, J. Holst, D. Jaffe, A. Karion, P. Keronen, K. Kominkova, D. Kubistin, O. Laurent, T. Laurila, J.

Lee, I. Lehner, M. Leuenberger, M. Lindauer, M. O. Löfvenius, M. Lopez, I. Mammarella, G. Manca, M. V. Marek, P. Marklund, M. Y. Martin, K. McKain, C. E. Miller, M. Mölder, C. L. Myhre, J. M. Pichon, C. Plass-Dölmer, M. Ramonet, B. Scheeren, M. Schumacher, C. D. Sloop, M. Steinbacher, C. Sweeney, K. Thoning, K. Tørseth, J. Turnbull, B. Viner, G. Vitkova, S. D. Wekker, D. Weyrauch, D. Worthy. CarbonTracker Near-Real Time, CT-NRT.v2020-1. *NOAA Earth System Research Laboratory, Global Monitoring Division,* 2020.

[154] Böttcher K., Markkanen T., Thum T., Aalto T., Aurela M., Reick C.H., Kolari P., Arslan A.N., Pulliainen J. Evaluating Biosphere Model Estimates of the Start of the Vegetation Active Season in Boreal Forests by Satellite Observations. *Remote Sensing*, 8(7): 580, 2016.

[155] Mahadevan, P., S. C. Wofsy, D. M. Matross, X. Xiao, A. L. Dunn, J. C. Lin, C. Gerbig, J. W. Munger, V. Y. Chow, E. W. Gottlieb. A satellite-based biosphere parameterization for net ecosystem CO2 exchange: Vegetation Photosynthesis and Respiration Model (VPRM). *Global Biogeochem. Cycles*, 22: GB2005, 2008.

[156] K. Wesslander, A. O., B. Schneider. Inter-annual and seasonal variations in the air–sea CO2 balance in the central Baltic Sea and the Kattegat. *Continental Shelf Research*, 30(14): 1511-1521, 2010.

[157] Wesslander K. The Carbon Dioxide System in the Baltic Sea Surface Waters. *Doctoral thesis. University of Gothenburg, Department of Earth Sciences*, P. 36, 2011.

[158] Humborg Ch., Geibel M.C., Sun X., McCrackin M., Mörth C.M., Stranne Ch., Jakobsson M., Gustafsson B., Sokolov A., Norkko A., Norkko J. High emissions of carbon dioxide and methane from the coastal Baltic Sea at the end of a summer heat wave. *Front. Mar. Sci.*, 6: 493, 2019.

[159] Wanninkhof R. Relationship between wind speed and gas exchange over the ocean revisited. *Limnol. Oceanogr. Methods,* 12: 351–362, 2014.

[160] Nerobelov, G.M., Timofeyev, Y.M. Estimates of CO2 Emissions and Uptake by the Water Surface near St. Petersburg Megalopolis. *Atmos Ocean Opt.*, 34: 422–427, 2021.

[161] Nikitenko A.A., G.M. Nerobelov, Yu.M. Timofeyev, A.V. Poberovskii. Analysis of ground-based spectroscopic measurements of CO2 in Peterhof. *Sovremennye problemy distantsionnogo zondirovaniya Zemli iz kosmosa*, 18(6): 265–272, 2021. (in Russian)

[162] F. Chevallier, P. Ciais, T. J. Conway, T. Aalto, B. E. Anderson, P. Bousquet, E. G. Brunke, L. Ciattaglia, Y. Esaki, M. Fröhlich, A. Gomez, A. J. Gomez-Pelaez, L. Haszpra, P. B. Krummel, R. L. Langenfelds, M. Leuenberger, T. Machida, F. Maignan, H. Matsueda, J. A. Morguí, H. Mukai, T. Nakazawa, P. Peylin, M. Ramonet, L. Rivier, Y. Sawa, M. Schmidt, L. P. Steele, S. A. Vay, A. T. Vermeulen, S. Wofsy, D. Worthy. CO2 surface fluxes at grid point scale estimated from a global 21 year reanalysis of atmospheric measurements. *J. Geophys. Res.*, 115: D21307, 2010.

[163] Mues, A., Lauer, A., Lupascu, A., Rupakheti, M., Kuik, F., and Lawrence, M. G. WRF and WRF-Chem v3.5.1 simulations of meteorology and black carbon concentrations in the Kathmandu Valley. *Geosci. Model Dev*. 11: 2067–2091, 2018.

[164] H.D. Li, B. Claremar, L.C. Wu, C. Hallgren, H. Körnich, S. Ivanell, E. Sahlée A sensitivity study of the WRF model in offshore wind modeling over the Baltic Sea. *Geosci. Front*., 12: 101229, 2021.

[165] Miller, S. T. K., Keim, B. D., Talbot, R. W., Mao, H. Sea breeze: Structure, forecasting, and impacts. *Rev. Geophys*., 41: 1011, 2003.

[166] Lauvaux, T., Miles, N. L., Richardson, S. J., Deng, A., Stauffer, D. R., Davis, K. J., Jacobson, G., Rella, C., Calonder, G.-P., DeCola, P. L. Urban Emissions of CO_2 from Davos, Switzerland: The First Real-Time Monitoring System Using an Atmospheric Inversion Technique. J*ournal of Applied Meteorology and Climatology*, 52(12): 2654–2668, 2013.

[167] Dekking, F. M.; Kraaikamp, C.; Lopuhaä, H. P.; Meester, L. E. A Modern Introduction to Probability and Statistics. *Springer Texts in Statistics*, *Springer London*, P. 488, 2005.

[168] Nerobelov G.M., Y. Timofeyev, S. Smyshlyaev, Y. Virolainen, M. Makarova, S. Foka. Comparison of CAMS Data on CO2 with Measurements in Peterhof. *Atmos Ocean Opt*, 34: 689–694, 2021.

[169] Nerobelov G., Timofeyev Y., Foka S., Smyshlyaev S., Poberovskiy A., Sedeeva M. Complex Validation of Weather Research and Forecasting—Chemistry Modelling of Atmospheric CO2 in the Coastal Cities of the Gulf of Finland. *Remote Sens*, 15: 1-30, 2023.

[170] Serebritsky I.A. (Ed.) The Report on Environmental Conditions in St. Petersburg for 2017. Web resource - [https://www.gov.spb.ru/static/writable/ckeditor/uploads/2018/06/29/Doklad_EKOLOGIA2018.pdf]

Appendix A

Measurements of CO_2 uptake and release by vegetation at SMEAR stations

To optimize and validate the VPRM model, air temperature, GPP (Gross Primary Product; CO2 absorbed by vegetation) and NEE (Net Ecosystem Exchange; difference between GPP and Resp) measurements from the "SMEAR II Hyytiälä forest" station are used in the study. The parameter Resp (Respiration; CO_2 emitted by vegetation) is calculated as the sum of NEE and GPP. At the Hyytiälä station, NEE and GPP measurements are carried out at a height of about 23-25 m (https://wiki.helsinki.fi/display/SMEAR/Eddy233). The assessment of GPP, Resp and NEE is based on a simple empirical model [155] and measurements of biogenic CO_2 fluxes using a set of instruments consisting of a Gill HS-50 ultrasonic anemometer measuring wind speed and temperature and a Li-7200 gas analyzer measuring CO_2 and water vapor content. The data is available at https://smear.avaa.csc.fi/download.

At Hyytiälä station, mast measurements are available at several heights of about 10, 20 m and above. We used air temperature data closest to the Earth's surface due to the fact that CO_2 emissions from vegetation in the VPRM model are calculated based on linear regression with air temperature. In addition, the analysis showed that the air temperature at an altitude of about 27 m, based on measurements at the Hyytiala station, differs from the temperature at an altitude of 1.5 m by an average of ~3% and has a correlation of ~0.99. GPP, Resp and NEE are obtained using the turbulent pulsation method.

Table A1: Parameters a and b for the calculation of Resp by VPRM before and after correction

Parameters	Before correction	After correction
a	0.1797	0.1816
b	0.8800	1.4650

Appendix B

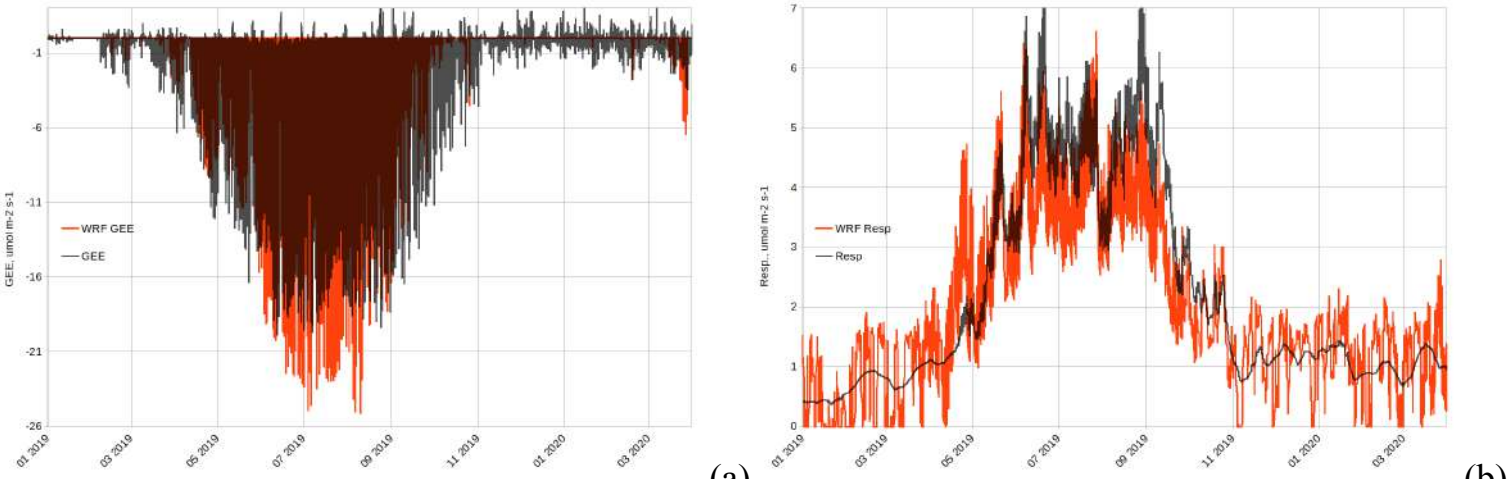

(a) (b)

Figure B1: Time series of GEE (a) and Resp (b) according to WRF-Chem modeling and measurements at the "SMEAR II Hyytiälä forest" station in Finland for Jan 2019 - Mar 2020.